

## STELLINGEN

behorende bij het proefschrift

"Improvement of Speech Intelligibility in Noise"

1. In situaties met achtergrondlawaai bereikt een slechthorende, die gebruik maakt van een microfoon-array, een zelfde spraakverstaanbaarheid als een normaalhorende. (Dit proefschrift, pagina 146).
2. Een adaptieve array-techniek is vanuit wetenschappelijk oogpunt interessant maar is nauwelijks geschikt om praktisch toegepast te worden.
3. De makers van de ouderwetse akoestische hoorn hebben goed aangevoeld dat richtinggevoeligheid en versterking belangrijk zijn om beter spraak te verstaan.
4. Een hoortoestel-aanpasser die toegeeft aan de klacht van een cliënt dat het hoortoestel onaangenaam scherp klinkt bewijst zijn cliënt een slechte dienst.
5. Er dient overwogen te worden om multi-functionele zalen te ontwerpen met een optimale akoestiek voor spraak en aan te vullen met de nieuwste mogelijkheden op het gebied van de elektro-akoestiek. Dit vergroot niet alleen de multi-functionaliteit van de zaal door een goede spraakverstaanbaarheid en een variabele akoestiek voor muziek maar is ook vanuit financieel en architectonisch oogpunt zeer interessant.
6. De brede wetenschappelijke kennis van een promovendus kan niet vastgesteld worden aan de hand van de stellingen bij een proefschrift (Promotiereglement TU-Delft).
7. Na het geloof in wetenschap en techniek in de jaren zestig en een onbegrensd vertrouwen in automatisering in de jaren tachtig wordt het nu tijd om in te zien dat de maakbaarheid van de samenleving vooral bepaald wordt door de mensen die daarin bezig zijn.
8. De tijd- en geldinvestering die nodig is om elke middelbare scholier typen te leren wordt in deze tijd van tekstverwerking en automatisering ruimschoots terugverdiend.

9. De betrokkenheid van de oudere mens bij de samenleving wordt bepaald door de individuele communicatie mogelijkheden.
10. De actie van de Bedrijfsvereniging Voor de Gezondheidszorg om door middel van premieaanslagen te komen tot een betere regeling van de arbeidsomstandigheden binnen de fysiotherapie heeft ertoe geleid dat vele maatschappen met matige contracten en een verslechterde positie voor jonge fysiotherapeuten zijn ontstaan.
11. Kerkelijke gemeenschappen die om financiële redenen geen Regeling voor Kerkmusici willen treffen onderschatten de eigen taal van kerk- en orgelmuziek als bijdrage tot de geloofsbeleving in vergelijking tot het gesproken Woord.
12. Een goed filosoof ziet in dat carpoolen het wachten in een file veraangenaamt.

Delft, 12 november 1990

Wim Soede

522 920 / 2180492  
TR diss 1862

**TR diss  
1862**

## IMPROVEMENT OF SPEECH INTELLIGIBILITY IN NOISE

Development and Evaluation of

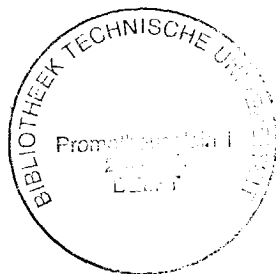
a New Directional Hearing Instrument

Based on Array Technology

**IMPROVEMENT OF SPEECH INTELLIGIBILITY IN NOISE**  
**Development and Evaluation of**  
**a New Directional Hearing Instrument**  
**Based on Array Technology**

**PROEFSCHRIFT**

ter verkrijging van de graad van doctor  
aan de Technische Universiteit Delft,  
op gezag van de Rector Magnificus,  
prof. drs. P.A. Schenck,  
in het openbaar te verdedigen  
ten overstaan van een commissie,  
aangewezen door het College van Dekanen  
op maandag 12 november 1990 te 16.00 uur door



**WILLEM SOEDE**

geboren te de Bilt  
natuurkundig ingenieur

Gebotekst Zoetermeer / 1990

Dit proefschrift is goedgekeurd door de promotoren:

prof. dr. ir. A.J. Berkhout en prof. dr. ir. F.A. Bilsen.

Copyright © 1990, by Delft University of Technology, Delft, The Netherlands.

All rights reserved. No part of this publication may be reproduced, stored in a retrieval system or transmitted in any form or by any means, electronic, mechanical, photocopying, recording or otherwise, without the prior written permission of the author, W. Soede, Delft University of Technology, Faculty of Applied Physics, P.O. Box 5046, 2600 GA Delft, The Netherlands.

CIP-DATA KONINKLIJKE BIBLIOTHEEK, DEN HAAG

Soede, Willem

Improvement of speech intelligibility in noise :  
development and evaluation of a new directional hearing  
instrument based on array technology / Willem Soede

[S.L. : s.n.] (Zoetermeer : Gebotekst). - III.

Thesis Delft. - With ref. - With summary in Dutch

ISBN 90-9003763-2

SISO 605.4 UDC 681.88.02(043.3)

Subject headings: hearing instrument / array technology.

#### SUPPORT

The research for this thesis was financially supported by the Dutch foundation for Fundamental Research on Matter (FOM) and the Dutch foundation for Technology (STW); (DTN 44.0758).

printed in The Netherlands by: N.K.B. Offset bv, Bleiswijk

Voor mensen die  
naar andere mensen  
*willen luisteren*

---

## PREFACE

The research reported on in this thesis is certainly not the result of a study on one specific topic within acoustics. The knowledge and expertise of several people was indispensable to achieve the goal: a new directional hearing instrument based on array technology.

The research project was mainly carried out within the group of acoustics of Delft University of Technology under supervision of Professor Berkhout and Professor Bilsen. I would like to thank Professor Berkhout for his enthusiasm and 'broadside' view. I would also like to thank Professor Bilsen for his ever stimulating support: his door was always open for questions and help. Furthermore I would like to thank the staff and colleagues of the sections Perceptual Acoustics and Seismics and Acoustics respectively. I want to mention especially Rinus, Niels, Henk, Gerrit, Eric and Hanneke, you were fine companions.

A very important part of the project was the assessment of the developed microphone arrays in tests with hearing impaired people. Therefore, I thank Hans Verschuure and the members of the ENT-department of the University Hospital Rotterdam for their hospitality and co-operation. Your help and audiological knowledge made the listening tests successful! The contribution of Patrick Pellen, who carried out a large number of listening tests, must also be mentioned.

Finally, I would like to mention Roland, Gea and my parents. Roland, you became a fine friend and did a terrific job following your own law: fast and reliable. Gea, mum and dad, I appreciate you were always a point of support.

---

# CONTENTS

## Page

---

### 1 INTRODUCTION

1	1.1 Problem Description
2	1.2 The Ear, Hearing-Impairment and Hearing Aids
11	1.3 Improvement of Speech to Noise Ratio
15	1.4 A Review of Microphone Array Techniques
21	1.5 Preliminary Choices
23	1.6 Outline of this Thesis

### 2 THEORETICAL ASPECTS

25	2.1 Introduction
26	2.2 Wave Theoretical Aspects
33	2.3 Directivity Patterns of Receiver Arrays
40	2.4 Properties of Discrete Microphone Arrays: Broadside, Endfire and Jacobi Arrays



---

## CONTENTS (Continued)

### 3 OPTIMIZATION AND STABILITY

57	3.1 Introduction
58	3.2 Endfire Solution with the Hansen-Woodyard Condition
62	3.3 Numerical Approach to Optimization
68	3.4 Stability
74	3.5 Comparison and Choices

### 4 ARRAY MEASUREMENTS

83	4.1 Introduction
84	4.2 Set-up of Directivity Measurements
85	4.3 Free Field Directivity Measurements
98	4.4 Directivity Measurements with an Artificial Head
104	4.5 Portable Array Microphones: Development and Measurements

### 5 TECHNICAL ASSESSMENT IN NOISE FIELDS

111	5.1 Introduction
112	5.2 Experimental Set-up with an Artificial Diffuse Noise Field
121	5.3 KEMAR Measurements in Artificial Diffuse Noise Field
124	5.4 Free Field Measurement in Natural Diffuse Noise Field

### 6 LISTENING TESTS

127	6.1 Introduction
128	6.2 Description of the Listening Test
134	6.3 Monaural Listening Tests
139	6.4 Binaural Listening Tests

### 143 7 CONCLUSIONS AND EVALUATION

151	REFERENCES
155	SUMMARY
157	SAMENVATTING
159	CURRICULUM VITAE



---

# INTRODUCTION

## Chapter 1

### 1.1 Problem Description

Communication	<p>Many people have great difficulty in understanding speech in surroundings with background noise and/or reverberation. This is especially a problem for the increasing number of elderly people. A serious consequence is that they may get easily isolated by the lack of communication with people in their immediate surroundings. This is particularly true in situations such as informal get togethers, parties and meetings, where the background noise level may become very high.</p> <p>Hearing impairment may be due to several causes either external or pathological but is frequently the result of aging of the auditory organ itself. Hence, rehabilitation by means of surgery cannot be done; the great majority of hearing impairments due to aging are sensorineural and,</p>
Sensorineural hearing impairment	<p>therefore, inoperable. A sensorineural hearing impairment resulting in a hearing loss for speech can be regarded as the sum of <i>attenuation</i> of sounds and of <i>distortion</i> of sounds (Plomp,1978). The distortion of sounds results in a worse speech intelligibility in noise. Consequently, it will</p>

Solution	be clear that this cannot be compensated by amplification alone, but requires another solution. This solution must compensate the reduced sound discrimination (selective hearing) and must be based on the attenuation of the aforementioned background sounds relative to the desired speech signals.
Speech intelligibility in noise	Several investigations on speech intelligibility in noisy situations have demonstrated that subjects with sensorineural hearing loss may need a 5 to 15 dB higher signal-to-noise ratios than normal hearing subjects. Every 4–5 dB improvement of the signal-to-noise ratio may raise the speech intelligibility by about 50 % (Groen, 1969; Plomp, 1977, 1979b). Therefore, attention should be paid to the acoustical environment. This means, for example, that rooms used for social gatherings should generally be sound-absorbent creating a reverberation noise level that is low enough for satisfactory communication. However, this may be not sufficient in typical cocktail party situations where the direct noise level due to the voice babble of all competing talkers can be very near to the limit understanding (Plomp, 1977).
Directional Hearing Aid	A directional hearing aid may reduce background noise relative to the desired speech signal. Until now, directional hearing aids consisted of a conventional hearing aid with a single directional (cardioid) microphone. In practice the reduction of background noise with this type of microphone is not yet sufficient because owing to the low directivity a maximum improvement can be reached of only about 2 dB. Therefore a research project has been started to develop a directional microphone that reduces the background noise by at least 5 dB (corresponding with an improvement of the speech intelligibility of about 50% in those difficult situations). In this thesis the results of this research project will be presented.

## 1.2 The Ear, Hearing Impairment and Hearing Aids

### THE EAR

The human auditory organ, seen in figure 1.1, can be divided into three functional subsystems (e.g. Dallos, 1973): the external ear, the middle ear and the inner ear.

External ear	The <i>external ear</i> consists of the auricle (pinna) and the auditory canal (meatus) and has its boundaries at the tympanic membrane.
--------------	--

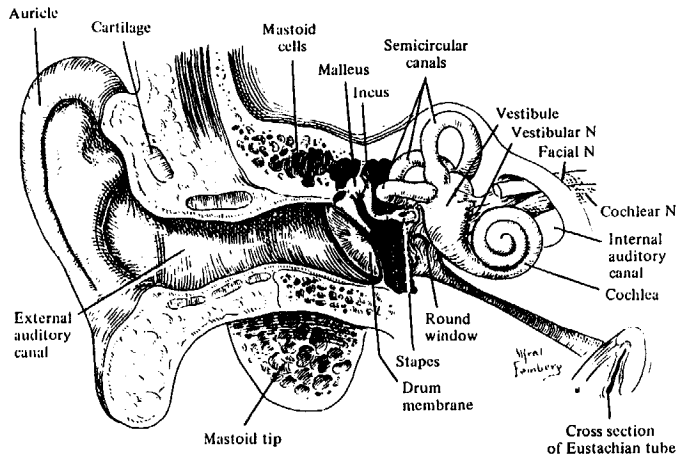


Figure 1.1 Review of the human auditory organ (after Feinberg, Davis, 1970). The auditory organ can be divided into 3 parts: external, middle, and inner ear. The external ear, consisting of the auricle and the external auditory canal, ends at the tympanic membrane (drum membrane). The middle ear, an air-filled cavity with the middle ear ossicles, is connected by the Eustachian tube (tuba auditiva, auditory tube) with the nasopharyngeal cavity. The inner ear consists of the cochlea and the vestibular organs.

The auricle and the auditory canal have two functions, viz. the protection of the tympanic membrane from mechanical damage and guiding of the sound waves to the tympanic membrane. The tympanic membrane defines the border between the external ear and the middle ear.

#### Middle ear

The *middle ear* is an air-filled cavity which contains the middle ear ossicles. This cavity is connected with the nasopharyngeal cavity (nose, throat) by the Eustachian tube (tuba auditiva). The cavity is lined with mucous membrane providing constant temperature and humidity. By means of the middle ear ossicles, the hammer (malleus), anvil (incus) and stirrup (stapes), the vibrations of the tympanic membrane are conducted to the oval window at the entrance of the cochlea. The Eustachian tube permits air to get into the middle ear to provide pressure equalization between pressure inside and outside at the tympanic membrane, drainage of mucous fluids and aeration of the mucous membrane. This tube opens during swallowing, chewing or yawning.

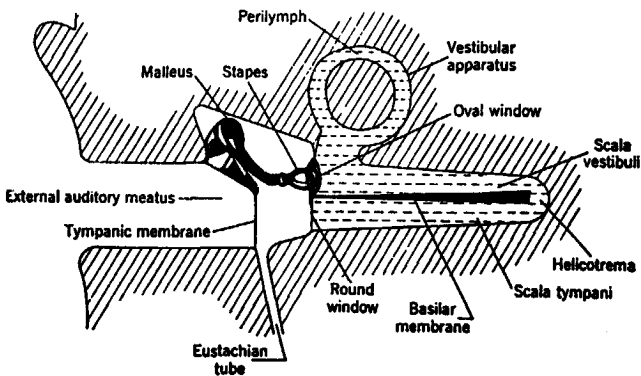
#### Inner ear

The *inner ear* is a system of cavities within the temporal bone. These interconnecting cavities, filled with lymph fluid, form the bony labyrinth within which the organs of equilibrium and hearing are in intimate contact.

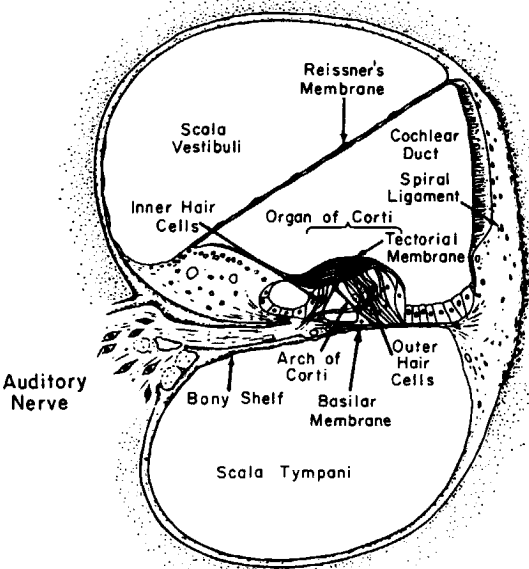
The vestibular portion forms the organ of equilibrium with three semicircular canals, the utricle and the saccule.

The *cochlea* is a snail-shell shaped canal that contains the organ of Corti, the actual sensory receptor of the auditory organ (figure 1.2). The canal is divided into an upper compartment (scala vestibuli) and

1.2



a. Uncoiled Cochlea.



b. Transverse section.

Figure 1.2 Drawing of the auditory organ with uncoiled cochlea (a) and a transverse section of the cochlea (b) (a: Möller, 1974; b: Levitt, 1980). The cochlear duct is formed by the Reissner membrane and basilar membrane and divides the cochlear canal into the the scalae tympani and vestibuli. The organ of Corti is the actual sensory receptor of the auditory organ. The mechanical vibrations of the basilar membrane are detected by the hair cells of the organ of Corti and translated into nervous action potentials that are sent to the brain by the auditory nerve.

lower compartment (scala tympani) by the osseous spiral lamina and the cochlear duct (scala media). The cochlear duct is formed by the basilar membrane and the Reissner membrane and terminates prior to the termination of the cochlear canal at the top of the spiral (apex) making possible communication between scalae vestibuli and tympani through an opening, the helicotrema. The scala vestibuli is also connected with the three semicircular canals of the vestibular organ and communicates at the base of the cochlea with the middle ear through the oval window. The scala tympani at the base of the cochlea is in communication with the middle ear cavity through the round window.

**Frequency tuning**      The basilar membrane vibrates if a pressure wave is caused in the cochlea by the piston-like excursions of the stapes at the oval window. A gradual variation in the mechanical properties of the basilar membrane results in frequency tuning. High frequencies will generate mechanical vibrations near the basal turn of the cochlea. Low frequencies generate vibrations near the top end of the snail-shell. The mechanical vibrations are detected by the hair cells of the organ of Corti and translated into nervous action potentials that are sent to the brain by the auditory nerve.

**Dynamic range**      A properly functioning ear can transduce a wide range of sound levels. Figure 1.3 gives the level of some well-known sounds expressed in decibels sound pressure (dB SPL). The decibelscale is a logarithmic scale used to express sound pressure. The reference sound pressure is 20  $\mu$ Pa. A properly functioning ear has a range of about 120 dB,

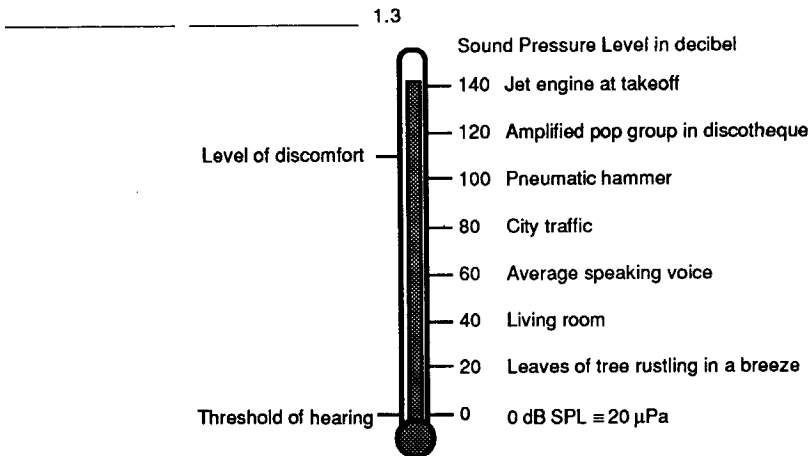


Figure 1.3 The Sound Pressure Level of some well-known sounds expressed in decibels relative to the reference of 20  $\mu$ Pa.

while a hearing impaired person may have a smaller range depending on the pathological cause. Above about 110 dB, sounds generally have an uncomfortable loudness.

**Frequency range** When a complex sound, like speech or music reaches the cochlea it is analyzed by splitting it up in frequency components. A normal young ear can hear sounds ranging in frequency from 30 Hz to 20.000 Hz approximately. With age this frequency range decreases to 50-8000 Hz approximately. Although it seems a substantial reduction, it causes no problems with regard to understanding speech, because speech frequencies range from about 200 Hz to 5000 Hz. Some consonants like f,s and t have frequency components up to 8000 Hz.

In practice, sufficient speech-intelligibility is found if the inner ear is able to analyze sounds ranging in frequency from about 200 Hz to about 5000 Hz. Within this range the frequencies from 1500 to 4000 Hz are most important for vowel and consonant discrimination.

#### HEARING IMPAIRMENT

**Pathology** A normal young ear can perceive sounds ranging in frequency from 30 Hz and 20000 Hz and in level between 0 dB SPL and 120 dB SPL. Disease causing a hearing impairment can occur at several places in the human auditory organ: the outer, middle and inner ear or the central nervous system (retro-cochlear). Furthermore, disease may give rise to a combination of problems like hearing loss, recruitment, poor frequency and impaired time resolution, dizziness and headaches (e.g. disease of Menière and neurinoma acusticus, Katz et al., 1978).

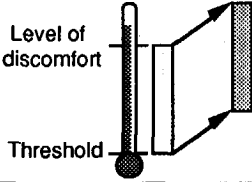
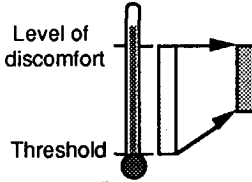
In this section we will summarize two different types of hearing impairment: a conductive hearing loss with pathology located in the outer or middle ear and a perceptive or sensorineural loss with pathology located in the inner-ear (table 1.1).

**Conductive loss** A *conductive loss* occurs when *the outer ear canal* is obstructed by e.g. cerumen, malformation or otitis externa. In most cases this can be treated by an otologist. A larger loss, up to 50 dB, can occur when the tympanic membrane is missing or has substantial perforations.

**Otitis Media** A common cause of middle ear disease is *otitis media*. It includes many different varieties with or without effusion, with or without infection, some resulting in mild, others in severe losses. Otitis media with effusion is often caused by a dys-functioning of the Eustachian tube. The accumulation of fluid in the middle ear impedes the movements of the tympanic membrane and the ossicles, thus causing a conductive hearing loss.



Table 1.1 Review of conductive and perceptive, sensorineural hearing loss.

Hearing Loss	Conductive	Perceptive , Sensorineural
Localisation Disease Impairment	Outer ear , Middle ear Otitis Media, Otosclerosis Loss: 30-50 dB	Inner ear Presbycusis, Noise induced Hearing Loss Loss: Frequency dependent 20-120 dB Frequency / Time resolution
Dynamic Range		

1.1

#### Otosclerosis

Other causes of a considerable conductive loss are: interruption in the ossicular chain, growth of cholesteatomas (formed by epithelial cells and cholestrine crystals), or otosclerosis. Otosclerosis is a disease in which the normal bone is resorbed and replaced by irregular richly vascularized bone. It often starts at the oval window but can also occur around the cochlea. In the process toxic substances are formed that can cause cochlear loss. When sufficient medical treatment is not possible or not wanted a conventional hearing-aid can give adequate results to compensate the hearing loss. A conductive hearing loss is mainly an elevation of the threshold of hearing resulting in a shift of the dynamic range to higher sound levels which is depicted table 1.1.

#### Perceptive loss

A *perceptive or sensorineural loss* is caused by the inner ear pathology. The main explanation can be atrophy, destruction or disappearance of the hair cells of the organ of Corti, in the cochlea. The deterioration of the hair cells does not only give a threshold elevation but also an impairment of the possibility to discriminate between different sounds due to a diminishing temporal and frequency resolution (Festen 1983; Helle 1986). A mere amplification of sounds with a hearing aid will not be adequate mainly because of the diminished resolution but also due to the smaller dynamic range. The picture of table 1.1 shows that the threshold of hearing is higher whereas the level of discomfort is the same as for normal hearing or even lower.

#### Presbycusis

Most common forms of perceptive loss are *presbycusis* and *noise-induced hearing loss*. Presbycusis comes with age and more than 24% of the people of 65 and older have serious problems with hearing (Plomp, 1986).

Noise exposure      A similar perceptive loss can be caused by noise exposure. Machinery, jet engines, but also live music and music reproducing equipment can produce noise levels that may damage the hair cells of the organ of Corti. The extent of damage depends on frequency content, noise intensity and duration of exposure. Protection against the noise exposure is the only way to prevent permanent hearing loss.

#### HEARING AIDS

Tapered horn      A variety of devices has been introduced in the past to amplify sounds for the hearing impaired, often shaped as a tapered horn (trumpet-like). Figure 1.4 shows two hearing aids designed at the beginning of this century. The sound energy at the large opening is concentrated towards a small opening at the side of the ear. Actually, this is an acoustic impedance matching and use of directivity. Measurements carried out with the two old hearing aids in an anechoic room show a higher directivity between 3000 and 5000 Hz than the electronic directional hearing aid microphones.

Electrical hearing aid      The main purpose of the modern electrical hearing aid is sound amplification in order to compensate for the threshold shift. It must be noted that amplification alone is usually insufficient because the hearing impairment also results in a poor temporal and frequency resolution, as was mentioned above. Furthermore, not only the desired sound but also noise is amplified. In principle, an electrical hearing aid consists of an electret microphone, an electronic amplifier, a telephone (earphone) and a battery. The telephone is replaced by a bone-conductor placed on the mastoid behind-the-ear in some cases of conductive hearing loss. The larger hearing aids are generally supplied with a pick-up coil for listening via an induction loop-system e.g. in churches or cinemas. The actual hearing aids can be classified as body worn, behind-the-ear and in-the-ear hearing aids. Figure 1.5 shows the different types.

Body worn aid      The body worn hearing aid is worn on the chest and its main advantage is high amplification without acoustical feedback and easy operation (Dreschler, 1988). The telephone, connected with a cable, is placed in an earmould in the auricle of the ear. The main disadvantages are the unnatural place of the microphone, cable-break, clothing noise and size.

Behind-the-ear aid      The most used hearing instrument is the behind-the-ear type. The advantages of this type are the rather high amplification without acoustical feedback, the possibility of binaural fitting and the acceptable size from a cosmetic point of view. A main disadvantage is wind noise.

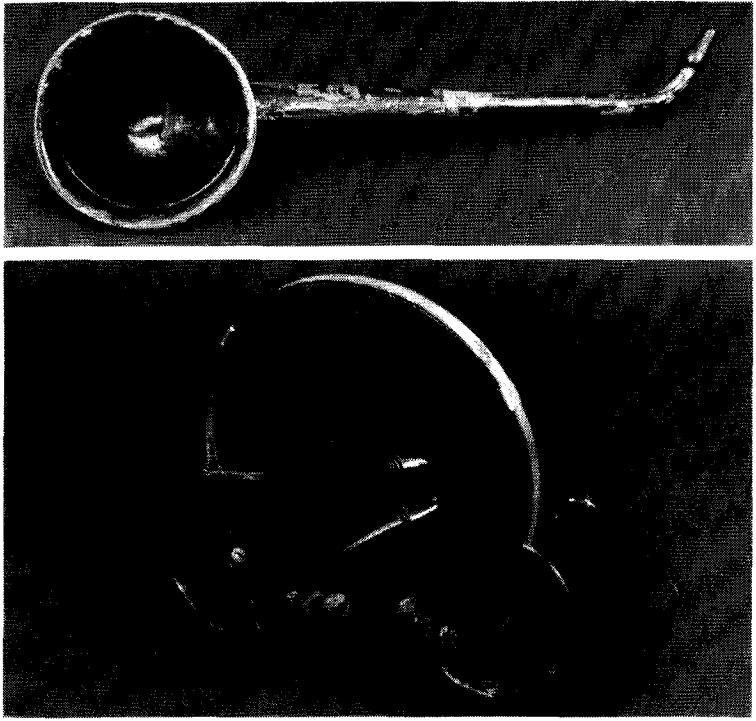


Figure 1.4 Photos of horn-like hearing-aids built in the beginning of this century.  
(Collection of Veenhuis BV., Medical Audio, Gouda, The Netherlands)

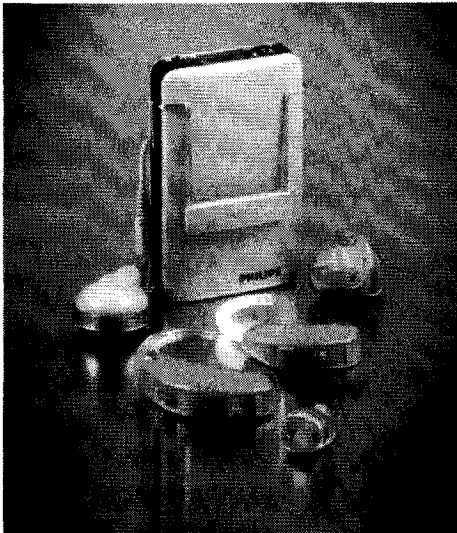


Figure 1.5 Photo of some frequently used hearing aids.



Figure 1.6 A behind-the-ear hearing aid connected to an earmould.

The sound of the telephone is directed to the tympanic membrane through a tube and an individually fitted earmould. Figure 1.6 shows a hearing aid with an earmould.

Lybarger (1978) and Libby (1979) have shown that the internal size of the connecting tube and a correct bore of the canal in the earmould are very important for a good transmission of all required frequencies.

#### In-the-ear aid

The in-the-ear hearing aids have their main advantages in the size and the natural placement of the microphone. The disadvantages are the rather small amplification, wind noise, the absence of a pick-up coil and of fine tuning possibilities to the specific hearing loss. The individual fitting of the in-the-ear hearing aid in the ear canal needs to be done carefully to prevent a leakage which will give acoustical feedback.

#### Signal processing

Linear amplification of all sound levels is unpleasant for a person with a sensorineural impairment because the level of discomfort is the same as for a normal-hearing person or even lower. The dynamic range of daily sounds should be compressed into the small dynamic range of the hearing impaired person (see table 1.1). Therefore, some types of hearing aids are equipped with an automatic gain control, a limiter for clipping high sound levels, or a compression/ expansion circuitry.

It is a matter of research to decide whether these different types of signal processing are beneficial or not for speech intelligibility. Until now, the influence of this type of signal processing to speech intelligibility is obscure (Maré, 1989; Dreschler 1989). Further, spatial signal processing can be carried out with a directional hearing aid; it will be discussed in the next section.

### 1.3 Improvement of Speech to Noise Ratio

The need for improvement in speech to noise ratio in cases of background noise especially for hearing impaired persons with a perceptive loss was discussed in the previous sections. In normal hearing an improvement of the signal-to-noise ratio is achieved by binaural interaction

Localization and by some properties of monaural hearing. In this context, two aspects are important, viz. *directional hearing (localization)* and *noise suppression*. Localization is important for detecting the position of the sound source, e.g. for detecting danger or for drawing attention. Binaural noise suppression is important for speech intelligibility. Listening with one or two ears will affect both localization as well as noise suppression. In this section we focus on noise suppression and its dependence on listening with one or two ears, and consequently on hearing with one or two conventional hearing aids respectively. Finally the possibility of noise suppression by signal processing will be discussed.

#### HEARING AND NOISE SUPPRESSION

Monaural hearing With one ear (monaural hearing) localization and noise suppression are possible because the transfer function at the tympanic membrane is dependent on the angle of incidence as a result of diffraction and reflection around the body, the head and the auricle. Also reflections in the small cavities of the auricle play a role in localization. Improvement of the signal-to-noise ratio can be obtained by the effect of head shadow.

Speech in noise Binaural hearing contributes significantly to noise suppression when the desired signal and the undesired signal(s) are spatially separated. The speech intelligibility in noise is enhanced by the following aspects: inter-aural phase and head shadow. The inter-aural phase differences of signal and noise contribute to a different psycho-physical masking level (Binaural Masking Level Difference, BMLD), while the head shadow effect may give a maximum level difference of 13 dB. Several investigations have shown that the binaural processing in the brain of the different audio-signals in the brain may improve speech intelligibility in noise by 3-9 dB (figure 1.7). (e.g. Plomp 1976, Bronkhorst, 1988).

Speech intelligibility Markides (1977) found binaural hearing to improve the speech intelligibility in quiet by internal summation of the sound signals at both ears resulting in a simple amplification of 3 dB which can be very important for hearing impaired people listening to speech at threshold level.

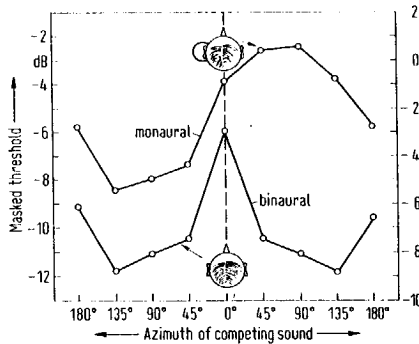


Figure 1.7 Binaural and monaural masked threshold of intelligibility of connected discourse with 0° azimuth relative to the SPL of a competing sound source as a function of its azimuth with reverberation time  $T = 0$  s (Plomp, 1976). Left-hand-scale: connected discourse; Right-hand scale: noise as the competing sound.

#### Binaural hearing

It should be noted, however, that binaural hearing is not a simple summation of the two audio signals coming from the two ears. Bilsen (1977) and Raatgever and Bilsen (1986) showed that the binaural processing of the audio signals in the auditory pathway can be described by a central spectrum model based on peripheral frequency analysis, a Jeffress-type of internal delay network, power summation and spectral pattern recognition. For a review of psychophysical data and binaural interaction models we refer to Blauert (1983).

#### HEARING AIDS AND NOISE SUPPRESSION

The speech-to-noise ratio necessary to understand speech for hearing impaired persons depends mainly on the hearing loss, the hearing aid type, the built-in directional or omni-directional microphone and whether the fitting was done monaurally or binaurally. It must be noted that the choice of a specific hearing aid type, including monaural or binaural fitting and microphone type, influences localization as well as speech intelligibility in noise.

#### Hearing aid type

The effect of the hearing aid type on localization is greatly determined by the position of the microphone. For a behind-the-ear and an in-the-ear hearing aid the microphone is placed just near the top of the auricle or near the ear canal entrance respectively. These positions are better than in body worn hearing aids because the sound is picked up near the entrance of the ear canal, enabling the hearing impaired person to use head movements for sound localization. The best monaural localization can be achieved with a

microphone near the ear canal entrance (e.g. Türk, 1987). Some spatial noise suppression can only be obtained with head shadow for behind-the-ear and in-the-ear hearing aids and body shadow for body worn hearing aids.

**Binaural hearing aids** The fitting of two hearing aids can provide a substantial improvement of localization and speech intelligibility in noise. Markides (1977) reported that hearing impaired subjects with a symmetrical impairment (difference < 20 dB) with a hearing aid at both ears showed significant improvements in localization and speech intelligibility in noise. Nowadays, binaural hearing aid prescription is widely accepted as an important contribution to speech intelligibility in noise. However, in general, the speech to noise ratio obtained with binaural hearing aids is not yet sufficient.

**Microphone type** The behind-the-ear hearing aid with a built-in directional microphone<sup>1</sup> was introduced twenty years ago. It is more sensitive to sounds coming from the front than to sounds from any other directions. It is assumed that the interesting sound comes from the front (where the person is looking), and hence, the hearing aid has the potential to improve speech intelligibility in noise in comparison to an omni-directional microphone.

The actual improvement of the signal-to-noise ratio of a directional microphone depends on the directivity pattern of the microphone and the spatial separation of the signal and the noise.

**Directivity Index** A suitable measure of the directional effect of a microphone is the *directivity index*<sup>2</sup>. It indicates in decibels the amount to which a directional microphone attenuates sounds in a diffuse sound field as compared with an omni-directional microphone. According to the definition the directivity index of an omni-directional microphone will be 0 dB whereas a directional microphone as used in a behind-the-ear hearing aid, has a theoretical value of 4.7 dB.

In practice (Dillon 1986 and Helle 1986), this value is only achieved for the frequency bands up to 2000 Hz. For higher frequencies, in the range 2000 to 5000 Hz, the directivity index goes down to 1 or 2 dB. The low directivity for the higher frequencies will result in a poor speech intelligibility for consonants, which hearing impaired people tend to perceive poorly.

Although Mueller (1981) and Hillman (1981) published on studies showing a preference for a hearing aid with a directional microphone, the directional hearing aid has not yet enjoyed the widespread clinical acceptance that

---

<sup>1</sup>For a description of a directional microphone see also section 2.4.

<sup>2</sup>The Directivity Index is defined as the ratio, expressed in decibels, of the sensitivity for a plane wave in the main direction and the average sensitivity in a diffuse sound field. (see also section 2.4)

would be expected on theoretical grounds. The main reason seems to be the low directivity in the higher frequency range of the current solutions which explains the rather small practical improvement in speech intelligibility. It is therefore important to look for methods to improve the directivity especially in the higher frequencies with a probable better speech intelligibility in noise.

#### NOISE SUPPRESSION BY SIGNAL PROCESSING

Noise suppression by signal processing can be divided in one-dimensional processing strategies in case of a single input-signal, and more-dimensional processing strategies when several, different, input-signals are available. Here we will only describe one-dimensional signal processing strategies. More-dimensional processing strategies will be described in the next section.

One dimensional signal processing in the frequency domain assumes a difference between the spectrum of the background noise and the desired speech signal. For example, the spectrum of the noise contains a lot of energy in the low frequencies, which is sometimes the case with machine or traffic noise, while the speech spectrum contains energy in the higher frequencies. In such a case the noise can be suppressed with a high-pass filter which cuts off the frequencies below e.g. 500 Hz. This type of noise suppression can easily and successfully be realized in a conventional hearing aid by setting the slope of a high-pass filter (figure 1.8). Other types of signal processing as discussed in the preceding section are mainly used for gain control, peak clipping and compression or expansion.

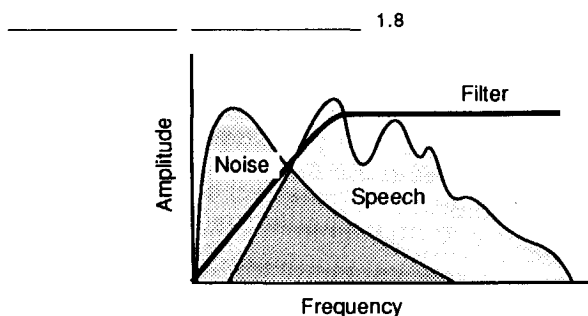


Figure 1.8 Spectrum of speech and background noise. The noise is filtered by a high-pass filter



It is expected that, in the near future, digital hearing aids will become available with an automatic adaptation of the gain in different frequency bands. The advantage of automatic adaptation is the possibility to suppress stationary noise sources in the lower frequency bands and also to adapt the gain to the overall sound level (Festen, 1990).

It is obvious that this one-dimensional noise suppression cannot suppress noises with similar spectra as speech (see also figure 1.8). This, however is the typical problem at public meetings.

## 1.4 A Review of Microphone Array Techniques

In the previous sections it was discussed that hearing impaired persons have great difficulty in understanding speech in environments with background noise. A hearing aid with a directional microphone may reduce background noise relative to the desired speech signal. In section 1.3 we have also seen that the existing behind-the-ear hearing aid with a directional microphone may improve the signal-to-noise ratio by only 1 or 2 dB due to a low directivity for the higher frequencies. It was mentioned that we may expect a better speech intelligibility if a solution can be found with strong directional characteristics up to 5000 Hz.

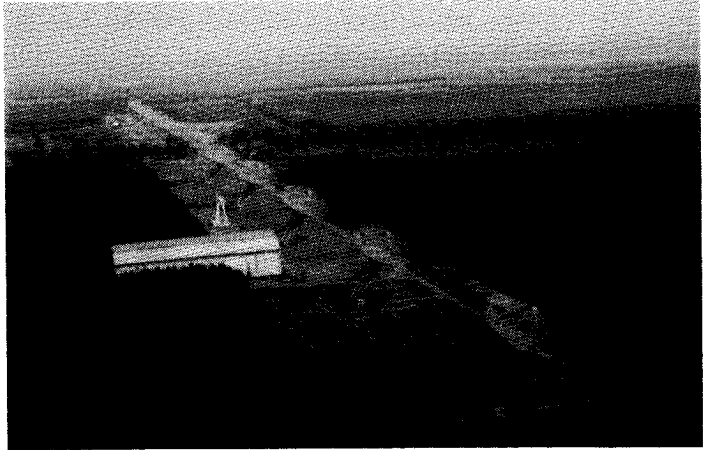
### ARRAY TECHNIQUES

Directional characteristics can be improved using a spatial distribution of microphones. A substantial directivity can only be obtained with a spatial distribution larger than the minimum relevant wavelength. Such techniques are used in many other fields like astronomy, sonar, radar and seismology. Because the sensors, and in some applications, also the sources are often put in a straight line the method is referred to as *Array-techniques* or *Array-processing*.

### Examples

Figure 1.9 shows some arbitrary examples of the application of array-techniques for directional signal reception or generation. Figure 1.9a shows a picture of the Westerbork Synthetic Radio Telescope used for astronomic purposes. In seismology array-techniques are used not only for detection but also for the generation of seismic waves. Figure 1.9b shows a picture of three vibroseis trucks where a seismic wave is generated with vibrating base plates. Finally, in figure 1.9c a picture is shown of a synthetic acoustic antenna for highly directional sound measurements (Boone, 1987).

a. Westerbork  
Synthetic Radio  
Telescope (WSRT).  
(Photo, Aerophoto,  
Eelde, The  
Netherlands).



b. Seismic wave field  
generation with an  
array of  
vibroseis-trucks.  
(Photo, Delft  
Geophysical, The  
Netherlands).



c. Synthetic  
acoustic antenna  
for highly  
directional sound  
measurements.  
(Photo, R. Boone,  
Zoetermeer, The  
Netherlands).

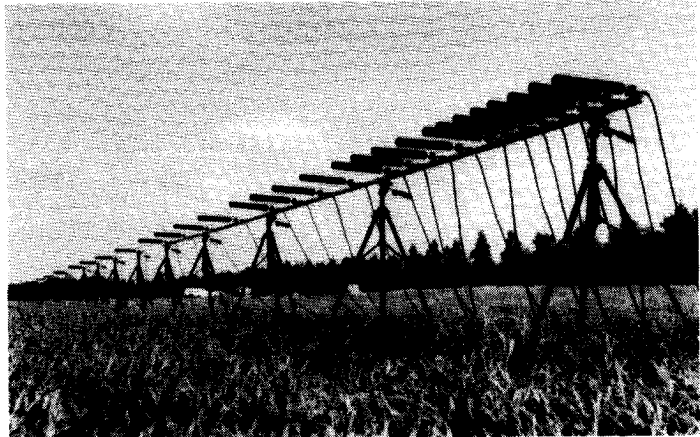


Figure 1.9 Examples of array-techniques.

Array-processing techniques can be subdivided, depending on the application, in 'real-time' techniques (sonar, radar, acoustic control and audio-applications) and 'off-line' techniques (astronomy, seismology) where signal-processing like correlation and inversion are very important to obtain a high signal-to-noise ratio and a high resolution.

Real-time  
processing in  
hearing aids

The processing of the audio signal within a hearing aid must evidently be done in real-time and also over a wide frequency range of at least 200 Hz up to 5000 Hz.

Conventional hearing aids so far have been built using analogue electronics, but in the near future simple digital audio processors will become available with real-time signal processing capabilities. Although digital audio processors will offer more possibilities and flexibility, it is better at the moment to choose an array technique which can be carried out with analogue electronics because we will need more than two input channels. In the future, the array signal processing may be implemented digitally when processors will be very small, have more than two input channels and have a low power consumption. With respect to real-time techniques a further division can be made in *fixed array processing* and *adaptive array processing*.

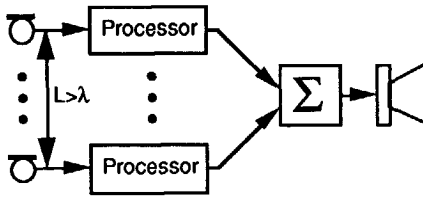
Fixed array  
processing

In *fixed array processing* techniques, the transfer functions of the microphone signals of an array are kept constant to achieve a *fixed* directional pattern. The fixed directional pattern can be designed in such a way that the desired speech signal in front of the listener will be transmitted optimally. The background noise and reflections by walls etc. coming from other directions will be suppressed as much as possible. Figure 1.10 shows a scheme of fixed array processing and a sketch of the resulting directivity pattern. The signal of each microphone is processed optionally while the signal processing may consist of e.g. filtering, amplitude weighting and time delay. The output signal is a summation of each processed microphone signal and can be used as an input signal for further processing or reproduction.

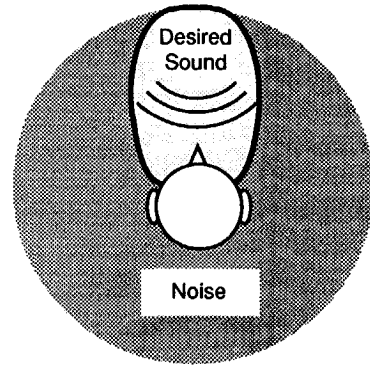
A directivity pattern, as sketched in figure 1.10 b, with a beam pointing towards the desired sound source is an ideal pattern. The undesired background noise, coming from directions in the shaded area, is suppressed.

adaptive array  
processing

In adaptive array processing, the processing of the microphone signals of an array is continuously adjusted according to properties of the received sound signals.

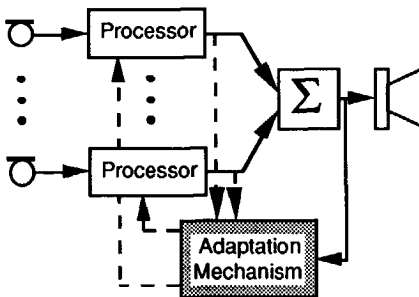


a. Scheme of fixed array processing

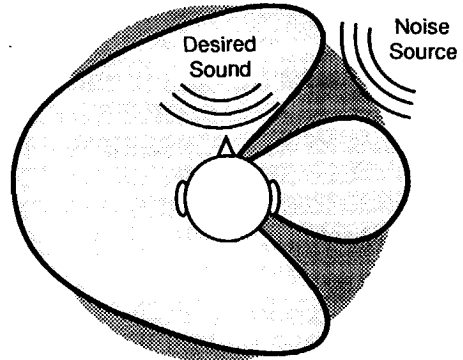


b. Sketch of directivity pattern

Figure 1.10 Scheme (a) and resulting directivity pattern (b) of fixed array processing. The length of the microphone array must be larger than the wavelength. The signal processor may consist of filtering, amplitude weighting and time delay.



a. Scheme of adaptive array processing



b. Sketch of directivity pattern

Figure 1.11 Scheme (a) and resulting directivity pattern (b) of adaptive array processing. The adaptive microphone signal processor may consist of e.g. filtering, amplitude weighting and time delay. The adaption mechanism controls the processors based on the output signal and some programmed constraints.

In figure 1.11 a scheme of adaptive array processing and a sketch of the resulting directivity pattern is given. The processing of the microphone signals is now controlled by an adaptation mechanism which can be implemented on a signal processor. The control signal is computed by an implemented algorithm and depends on the summed output signal or separate microphone signals.

The adaptation mechanism can create a directivity pattern, as sketched in figure 1.11 b, to suppress a specific noise source. The noise source is suppressed fully by creating the low sensitivity in that particular direction. Background noise, coming from other directions, will now hardly be suppressed in comparison with the desired sound signal. In an ideal situation the adaption algorithm with the aid of a sufficient number of microphones will be able to suppress more undesired noise sources

## RESEARCH ON OTHER SOLUTIONS

Improvement of speech to noise ratio using directivity is a research subject at some other laboratories. We will give a summary of research projects at three laboratories focussing on hearing impaired listeners; one research project with a fixed solution and two research projects with an adaptive solution.

Two directional  
microphones

In 1986 Helle reported on an arrangement of two pairs of microphones placed in both legs of a pair of spectacles developed for the Siemens Medical Engineering Group, Erlangen and patented by Zwicker (1986, 1987). Each pair of microphones forms a directional microphone with a so-called hyper-cardioid directivity pattern. The signals of both pairs are summed, giving a better directivity pattern and higher directivity index than for one single directional microphone (figure 1.12). Until now no listening test results have been published, and no hearing aid, based on this arrangement has been introduced.

Comments

The arrangement of the two pairs of microphones gives a directivity index of 6 dB approximately. It might be expected that this arrangement will give an improved speech intelligibility in noise.

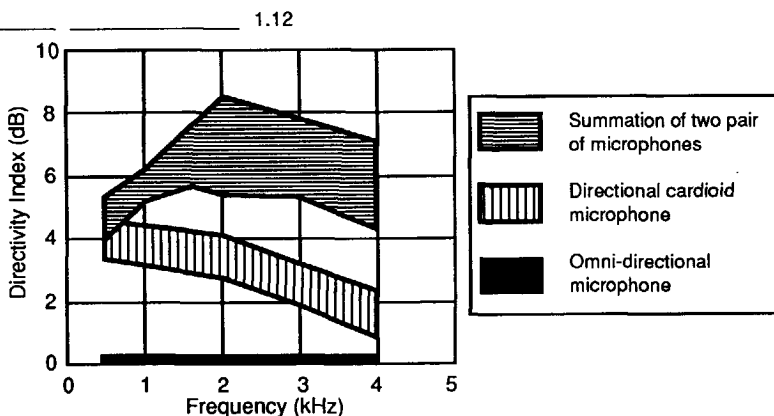


Figure 1.12 Directivity Index of solution of Helle compared with a directional and omni-directional microphone (Helle, 1986).

In practice, however, the improvement will be less and insufficient as a result of diffraction and reflections of the head. Furthermore, we can expect that series production needs to be done carefully. The hyper-cardioid directivity pattern of one pair of microphones is obtained by summation of the two microphone signals in counter-phase and thus depends strongly on variations in microphone characteristics and variations in electronics.

Adaptive beam forming	<p>Peterson et al. (1987) reported on multi-microphone adaptive beam forming for interference reduction in hearing aids. Listening tests were done for a computer simulated adaptive beam-former consisting of two microphones. The function of the adaptation mechanism is the preservation of signals arriving from straight-ahead while minimizing output power from off-axis interfering sources.</p> <p>Listening tests were done for on-axis speech and one noise source consisting of an interfering speech babble at 45°. The results of the listening tests with normal-hearing subjects show a significant gain of 30 dB and 14 dB for simulated anechoic and living-room conditions respectively. For simulated conference-room conditions, with a reverberation time of 480 ms, the gain drops to 0 dB.</p>
Comments	<p>In their own comments the authors expect that the improvement will decrease dramatically when multiple sources are introduced. Therefore, it is concluded that further study need to be made on the influence of different reverberant conditions and the processing of more microphone signals to suppress multiple noise sources. Moreover, the adaptation mechanism needs to be investigated and the implications for a practical hearing aid where the influence of head shadow, transducer directivity and adaptation time to changing environments will also be taken into account.</p> <p>Following the comments of the authors we can expect that it will be a problem to find a stable adaptive noise suppression system in situations with multiple noise sources and/or reverberation.</p>
Adaptive noise canceller	<p>Weiss (1987) reported on an adaptive noise canceller as an input preprocessor for a hearing aid based on two microphones. One omni-directional microphone and one directional microphone pointing backward are placed on an artificial head. The signal of the directional microphone is used to cancel the noise picked up with the omni-directional microphone. In an anechoic room an improvement of the signal-to-noise ratio was found to be more than 10 dB for a noise source just behind the artificial head.</p>

In conditions with a reverberation time of 380 ms for noise sources the improvement decreased to a few decibels.

Comments

The results of Weiss show that an adaptive noise canceller can give a significant reduction in a situation with one noise source and without reverberation. The noise canceller fails in a situation with more noise sources and some reverberation. We can conclude that in a realistic situation the adaptive noise canceller will fail and that nearly the same results can be obtained with the directional microphone pointing to the desired signal.

Schwander and Levitt (1987) used the same adaptive noise canceller for a study on the effect of head movements on this system. Listening tests were done with 5 normal-hearing subjects for one single situation with a reverberation time of 410 ms. The speech source was placed at 0° and only one noise source at 180°. Without head movements the speech intelligibility for words increased from 33% to 73%, while head movements reduced the speech intelligibility to 62%, still a significant gain.

Comments

The results of the listening tests show that with and without head movements a significant improvement of the speech intelligibility can be obtained for a situation of maximal spatial separation of the speech and the noise source. On the evaluation by Weiss, we may expect that the improvement of the speech intelligibility will diminish when more noise sources are used and head movements are allowed. We may conclude that adaptive noise reduction will be beneficial in situations with only one noise source and moderate reverberation and will fail in realistic situations with multiple noise sources (e.g. cocktail party) and a diffuse noise sound field. Furthermore, adaptive methods have problems in adapting to head movements and changing environments.

## 1.5 Preliminary Choices

In the preceding section a short review was given of multi-microphone techniques that have been proposed to improve the speech intelligibility in environments with undesired background noise. At the start of our research project in 1986 we planned to develop a hearing aid with strong directional characteristics using microphone array techniques.

Before the results of our project are presented in the next chapters we will summarize the preliminary choices and assumptions made during the project.

Table 1.2 Review of advantages and disadvantages of fixed and adaptive techniques to be applied as an audiological aid.

	Advantage	Disadvantage
Fixed Array Techniques	<ul style="list-style-type: none"> <li>- Optimum diffuse noise suppression</li> <li>- Simple / Robust</li> <li>- Localisation</li> <li>- Listening direction is view direction</li> </ul>	<ul style="list-style-type: none"> <li>- Array dimension</li> <li>- Cosmetic Aspects</li> </ul>
Adaptive Techniques	<ul style="list-style-type: none"> <li>- Efficient suppression of specific noise sources</li> <li>- Array dimension</li> </ul>	<ul style="list-style-type: none"> <li>- No suppression additional noise sources and diffuse soundfield</li> <li>- Adaptation to head movements</li> <li>- No localisation</li> <li>- Digital electronics for adaption mechanism</li> </ul>

## 1.2

### Comparison

A review of the pros and cons of a fixed array technique and adaptive multi-microphone techniques with respect to our application is given in table 1.2.

A *fixed array technique* offers the possibility of sufficient suppression of diffuse background noise while the desired speech signal in front of the user is transmitted undistorted. A high and robust directivity can be obtained when the length of the array is larger than the wavelength. The signal processing can be done with relatively simple analogue electronics. Furthermore, the user will be able to locate sound sources after a practice period, although this is not the main purpose of the application.

A desired sound source can be chosen by moving the head and body towards the source. An important cosmetic disadvantage of a fixed array technique is the array length determining the width of the main beam.

The main advantage of an *adaptive multi microphone technique* is the possibility to suppress one single noise source with few microphones as was shown by Peterson (1987) and Weiss (1987). A major disadvantage however is the impossibility to suppress more additional noise sources or a diffuse sound field. Furthermore, the technique can be expected to have problems with head movements and moving noise sources and it can also be expected that the user will have problems with localization due to the continuously changing directivity pattern. Finally, an important disadvantage is the use of digital techniques for the adaptation mechanism. This is especially disadvantageous when more microphones are used to suppress multiple noise sources: a small, wearable, audio processor with more input channels and low power consumption must be developed.



Choice	Regarding the (dis-)advantages of the fixed and adaptive techniques, it was decided to focus our attention on a fixed array technique: a sufficient directivity should be achieved with a stable configuration, with acceptable array dimensions and with simple analogue electronic circuitry. Our goal was a significant improvement of the signal-to-noise ratio with at least 5 dB which is equivalent to a directivity index of 5 dB and an improvement of speech intelligibility by 50%.
Directivity Index	The directivity index was accepted as a measure to differentiate between possible solutions. It was decided to optimize the directivity index within a frequency range of 500 Hz to 4000 Hz. The shape of the directivity pattern was considered to be of minor importance.
Monaural	The new directional microphone should be used monaurally. Profits of binaural fitting should be added by simply using two devices.
On-off switch	In some situations a high directivity index is not necessary, or can be undesirable or even dangerous. Therefore the user must be able to switch off the directionality of the microphone choosing between a directional and an omni-directional position in case of e.g. less background noise and participation in traffic.
Cosmetic aspects	The use of any kind of array technique has an important cosmetic drawback because the microphones have to be placed in a spatial configuration ( $L > \lambda$ ). This drawback of the application of array techniques to hearing aids must not be underestimated. A lot of attention must therefore be paid to the final design of the concept, including good portability and an aesthetical modern design.
Pair of spectacles	At the beginning of the project it was postulated that the microphone array should be connected to, or built in, a pair of spectacles and should be used in combination with a conventional hearing aid.

## 1.6 Outline of this Thesis

This thesis can be divided into two parts: development of directional microphone arrays in chapters 2,3 and 4, and the assessment of the microphone arrays in chapters 5 and 6.

In chapter 2, the theoretical aspects of fixed array techniques are given. Chapter 3 shows the results of a study on optimization of stability for various array-types with the aid of simulation and optimization software. The choices for a suitable microphone array for a new hearing instrument are made.

In chapter 4 measurements with a laboratory array model are given. Measurements have been carried out in an anechoic room where the

directivity is measured in a free-field situation and in combination with an acoustic manikin. Based on these measurements portable microphone arrays were made.

In chapter 5 the experimental set-up of for the assessment of the developed portable microphone arrays is presented. Measurements were done in this set-up and in a natural diffuse noise field. The results of the listening tests with the experimental set-up are presented in chapter 6.

The conclusions and an evaluation of the research project are given in chapter 7.

---

# THEORETICAL ASPECTS

## Chapter 2

### 2.1. Introduction

Array techniques are used in many fields e.g. astronomy, radar, acoustics and seismology. This means that for applications in these fields a lot of knowledge is available in the form of mathematical models and design techniques.

In this chapter we will largely follow Berkhout, 1987, chapters III, V, VIII and IX. We start with the acoustic wave equation, derive the spherical wave field of a point source and show that the Rayleigh integral can be rewritten in terms of a spatial Fourier integral in the "Fraunhofer area" (section 2.2). Next, in section 2.3 the directivity patterns of different receiver arrays will be presented with the use of the spatial Fourier integral. Finally, in section 2.4 the results will be used to examine the properties of discrete microphone arrays, suitable for our purpose. We will distinguish *broadside* microphone arrays, *endfire* and *jacobi* microphone arrays.

## 2.2. Wave Theoretical Aspects

In this section we describe the spherical acoustic wave field of a point source as a solution of the acoustic wave equation. Next, it will be shown that the response of a receiver array in the Fraunhofer area can be described with the aid of a spatial Fourier integral. The discrete spatial Fourier transform will be used to examine the basic properties of different receiver configurations.

### WAVE FIELD OF A POINT SOURCE

Consider a point source with a wave field that depends on the distance to the position of the source only ( isotropic point source or monopole) with

$$p = p(r) , \quad (2.1a)$$

$$\mathbf{v} = v(r) \mathbf{e}_r , \quad (2.1b)$$

where  $p$  represents the acoustic pressure,  $r$  the distance to the source,  $v$  the particle velocity and  $\mathbf{e}_r$  the unit vector in radial direction (figure 2.1).

2.1

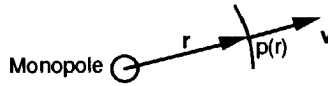


Figure 2.1 The wave field of a monopole is spherical symmetric.

For a medium without losses, the linearized equation of motion and the linearized equation of continuity are given by

$$\nabla p = -\rho \frac{\partial \mathbf{v}}{\partial t} \quad (2.2)$$

and

$$\nabla \cdot \mathbf{v} = -\frac{1}{K} \frac{\partial p}{\partial t} \quad (2.3)$$

respectively. Here  $\rho$  represents the mass density,  $K$  represents the adiabatic compression modulus and  $t$  represents the time. The gradient of the spherical symmetric scalar pressure field  $p$  (2.1) can be written as

$$\nabla p = \frac{\partial p}{\partial r} \mathbf{e}_r . \quad (2.4)$$

For a vector field with spherical symmetry it can be derived that the divergence equals

$$\nabla \cdot \mathbf{v} = \frac{1}{r^2} \frac{\partial(r^2 \mathbf{v})}{\partial r} = \frac{\partial \mathbf{v}}{\partial r} + \frac{2}{r} \mathbf{v} \quad (2.5)$$

Hence, substitution of (2.4) and (2.5) into (2.2) and (2.3) respectively gives the two basic equations

$$\frac{\partial p}{\partial r} = -\rho \frac{\partial v}{\partial t} \quad (2.6)$$

and

$$\frac{\partial v}{\partial r} + \frac{2v}{r} = -\frac{1}{K} \frac{\partial p}{\partial t} \quad (2.7)$$

If we differentiate equation (2.7) with respect to time, interchange the temporal and spatial differentiation and substitute equation (2.6) in the result, the particle velocity can be eliminated and, assuming a constant density  $\rho$ , the wave equation for the pressure field of an isotropic point source is obtained ( $r \neq 0$ ):

$$\text{Wave equation} \quad \frac{\partial^2 p}{\partial r^2} + \frac{2}{r} \frac{\partial p}{\partial r} = \frac{1}{c^2} \frac{\partial^2 p}{\partial t^2} \quad (2.8)$$

where  $c = \sqrt{K/\rho}$  represents the wave propagation velocity. The term  $(2/r) (\partial p / \partial r)$  makes the equation different from the well-known linear wave equation for plane waves. Hence, we may expect that for large values of  $r$  the spherical wave may be locally considered to be a plane wave.

Fourier Transform Fourier transformation<sup>1</sup> of equation (2.8) to the frequency domain gives

$$\frac{\partial^2 P}{\partial r^2} + \frac{2}{r} \frac{\partial P}{\partial r} + k^2 P = 0 \quad (2.9)$$

where  $k = \omega/c$  represents the wave number. Equation (2.9) represents a normal, linear, homogeneous, second-order differential equation. The solution of the differential equation is given by

$$P(r, \omega) = S(\omega) \frac{e^{-jkr}}{r} = S(\omega) \frac{e^{-j\omega(\frac{r}{c})}}{r} \quad (2.10)$$

---

<sup>1</sup>Forward temporal Fourier transform  $P(r, \omega) = \int_{-\infty}^{\infty} p(r, t) e^{-j\omega t} dt$

with  $S(\omega)$  being a source dependent constant. A second solution obtained by replacement of  $k$  with  $-k$  is deleted on practical grounds.

The time domain solution is obtained by applying the inverse Fourier transform to equation (2.10):

$$p(r,t) = \frac{s(t - \frac{r}{c})}{r} \quad (2.11)$$

Equation (2.11) shows that moving away from a monopole has two effects on the sound pressure: attenuation of the pressure of 6 dB per distance doubling and delay by  $r/c$ .

Particle velocity

The particle velocity of the monopole can be computed by using the Fourier transformed version of equation (2.6):

$$V(r,\omega) = -\frac{1}{j\omega\rho} \frac{\partial P(r,\omega)}{\partial r} \quad (2.12)$$

and equation (2.10) giving:

$$V(r,\omega) = \frac{S(\omega)}{\rho c} \left[ \frac{1+jkr}{jkr} \right] \frac{e^{-jkr}}{r} \quad (2.13)$$

Far-field

In the *far-field* equation (2.13) can be approximated with

$$V(r,\omega) \approx \frac{S(\omega)}{\rho c} \frac{e^{-j\omega(r/c)}}{r} \quad \text{for } r \gg \frac{\lambda}{2\pi} \quad (2.14)$$

Near-field

and in the *near-field*

$$V(r,\omega) \approx \frac{1}{jk} \frac{S(\omega)}{\rho c} \frac{e^{-j\omega(r/c)}}{r^2} \quad \text{for } r \ll \frac{\lambda}{2\pi} \quad (2.15)$$

Flux

The term  $S(\omega)$  can now be evaluated by considering the modulus of the total flux of a monopole in the near-field:

$$\begin{aligned} F(\omega) &= \oint_S \mathbf{V} \cdot \mathbf{n} \, dS \\ &= 4\pi r^2 V(r,\omega) = 4\pi \frac{S(\omega)}{j\omega\rho} \end{aligned}$$

where  $S$  represents a spherical surface with radius  $r \rightarrow 0$ . Hence,

$$S(\omega) = j\omega \frac{\rho F(\omega)}{4\pi} \quad \text{or} \quad s(t) = \frac{\rho}{4\pi} \frac{\partial}{\partial t} f(t) \quad (2.16)$$

The term  $\rho F(\omega)$  indicates the total mass flow per unit time (mass flux) and  $F(\omega)$  may be considered as a representation for the strength of a monopole.

## RESPONSE OF A RECEIVER IN THE FRAUNHOFER AREA

The response of a receiver array, placed in a wave field, depends on the frequency content of the wave field, the spatial characteristics of the receiver array and the properties of each receiver element. In general, receiver arrays with dimensions larger than the wavelength will show spatial directivity. Hence, directivity is a frequency dependent property that increases with raising frequencies. Quantification of the directivity of receiver arrays always occurs in the far field using the so-called Fraunhofer approximation. In the "Fraunhofer area" the spherical source wave field may be considered as a scaled local plane wave along the receiver array, the scaling factor being dependent on the distance to the source.

The response of a planar receiver placed in a spherical wave field can be written in the form of a Rayleigh integral using reciprocity. It will be shown that in the Fraunhofer area this reciprocal Rayleigh integral can be written as a Fourier integral. The "directivity pattern" will be discussed in the next section showing the response of a receiver plane to a plane wave as a function of the directional angles  $\phi$  and  $\theta$  for a given frequency.

### Rayleigh I

Consider the well-known Rayleigh integral of the first kind. It describes an acoustic wave field in a homogeneous half space when the wave field is known on the bounding surface  $S_0$ :

$$P_A = \frac{jk}{4\pi} \int_{S_0} 2\rho c V_n \frac{e^{-jkr}}{r} dS_0 \quad (2.17)$$

The Rayleigh I integral states that the pressure field in point A may be computed when the normal component of the particle velocity is known on the surface  $S_0$  or also that the pressure field in A above  $S_0$  can be synthesized by means of a secondary monopole distribution on the plane  $S_0$  with radiated flux per unit area  $F(\omega)=2V_n$  (Figure 2.2).

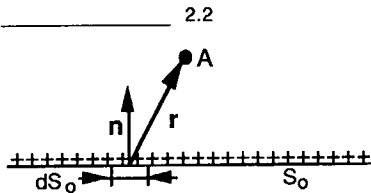


Figure 2.2 A pressure field in point A can be synthesized from the wave fields of a secondary monopole distribution on plane surface  $S_0$ .

This means that any pressure field in a point A can be decomposed into spherical waves generated by a distribution of monopoles on surface  $S_0$ .

Using reciprocity, the Rayleigh I integral can be rewritten for the monopole response of a receiver array with omni-directional receivers in a limited area  $\Delta M_0$  of a plane  $M_0$  at  $z=0$  :

$$U_M(\omega) = S(\omega) \int_{-\infty}^{\infty} \int_{-\infty}^{\infty} M(x,y,\omega) \frac{e^{-jkr}}{r} dx dy , \quad (2.18)$$

where  $M(x,y,\omega)$  represents the frequency dependent receiver with  $M(x,y,\omega) = 0$  outside  $\Delta M_0$  and  $U_M(\omega)$  equals the frequency dependent output signal of the receiver array. If the centre of  $\Delta M$  is placed in the origin of a cartesian coordinate system then for a monopole source in a point B (figure 2.3)

$$r_B = r(x_B, y_B, z_B) = \sqrt{x_B^2 + y_B^2 + z_B^2} \quad (2.19a)$$

and

$$\mathbf{r}_B = \begin{bmatrix} r_B \cos \phi_B \sin \theta_B \\ r_B \sin \phi_B \sin \theta_B \\ r_B \cos \theta_B \end{bmatrix} . \quad (2.19b)$$

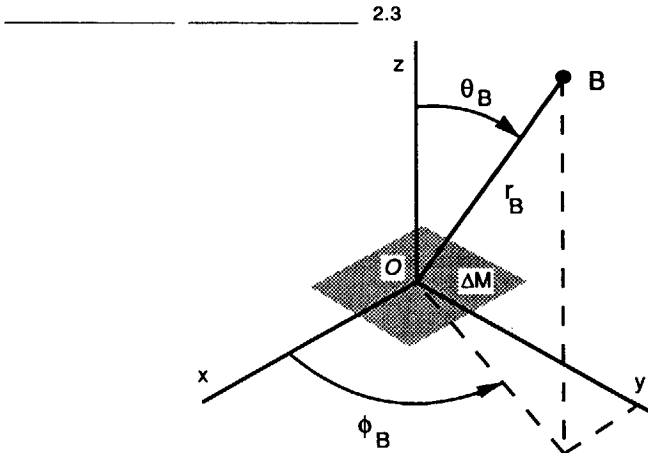


Figure 2.3 A planar receiver in the origin of a cartesian coordinate system with a monopole source in point B.



The distance  $r$  between B and a point in the plane  $M_O$  is given by

$$r = r(x, y, z=0) = \sqrt{(x_B - x)^2 + (y_B - y)^2 + z_B^2} . \quad (2.20)$$

For small  $x$  and  $y$  values around the origin we may linearize the phase of (2.18):

$$kr = k \left[ r_B + \frac{\partial r}{\partial x_O} x + \frac{\partial r}{\partial y_O} y \right] . \quad (2.21)$$

The partial derivatives can be computed from (2.20) (omitting subscripts)

$$\frac{\partial r}{\partial x_O} = \left[ \frac{-1}{2r} \quad 2(x_B - x) \right]_O = \frac{-x_B}{r_B} \stackrel{(2.19b)}{=} -\cos \phi \sin \theta \quad (2.22a)$$

$$\frac{\partial r}{\partial y_O} = \left[ \frac{-1}{2r} \quad 2(y_B - y) \right]_O = \frac{-y_B}{r_B} \stackrel{(2.19b)}{=} -\sin \phi \sin \theta . \quad (2.22b)$$

Substitution of the partial derivatives in expression (2.21) yields

$$kr = kr_B - (k \cos \phi \sin \theta x + k \sin \phi \sin \theta y) \quad (2.23a)$$

or

$$kr = kr_B - (k_x x + k_y y) , \quad (2.23b)$$

where  $k_x = k \cos \phi \sin \theta$  and  $k_y = k \sin \phi \sin \theta$ .

Substitution of (2.23) in (2.18) with  $r \sim r_B$  (amplitude) gives

$$U_M(\omega) = S(\omega) \frac{e^{-jkr_B}}{r_B} \int_{-\infty}^{\infty} \int_{-\infty}^{\infty} M(x, y, \omega) e^{j(k_x x + k_y y)} dx dy \quad (2.24a)$$

or

$$U_M(\theta, \phi, r_B, \omega) = S(\omega) \frac{e^{-jkr_B}}{r_B} F \{ M(x, y, \omega) \} , \quad (2.24b)$$

where  $F \{ M(x, y, \omega) \}$  denotes the Fourier Transform with respect to  $x$  and  $y$ . The response of the receiver array can now be considered as the response to a point source in B of an omni-directional receiver in the center of the array multiplied with the spatial Fourier Transform of the receiver array sensitivity, denoting the directivity of the receiver array.

Fraunhofer  
approximation

Expressions (2.24) equal the Fraunhofer approximation of the Rayleigh integral. It formulates that at the Fraunhofer area a *Rayleigh* integral may be approximated by a *Fourier* integral.

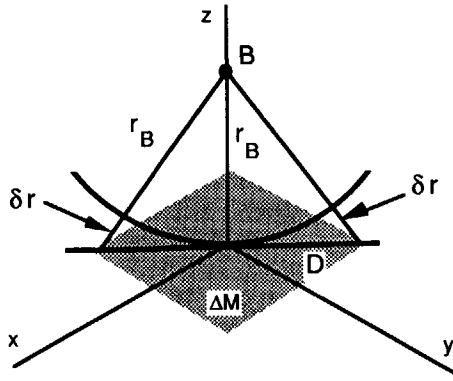


Figure 2.4 Error  $\delta r$  due to linearization of a spherical wave field into a plane wave field for a point source on the z-axis ( $\phi=0$ ,  $\theta=0$ ).

The Fraunhofer approximation of the Rayleigh integral is only valid when the phase may be linearized along the array. Hence, if a point source is located in a point B, the Fraunhofer approximation may only be applied if the wave field on  $\Delta M_0$  may be considered to be a plane wave.

Figure 2.4 shows the error  $\delta r$  due to linearization of a spherical wave field into a plane wave field for a point source on the z-axis. Using Pythagoras  $\delta r$  can be easily approximated:

$$\delta r = \sqrt{r_B^2 + \left(\frac{D}{2}\right)^2} - r_B \approx \frac{D^2}{8 r_B} \quad (2.25)$$

with D being the diameter of the area  $\Delta M_0$ . The Fraunhofer approximation is allowed when the phase error

$$k \delta r \ll \pi/2 \quad \text{or} \quad r_B \gg \frac{D^2}{2\lambda} \quad (2.26)$$

Now, in the Fraunhofer area the spherical wave fields of the monopoles may be considered to be a plane wave along the receiver array. Therefore we may conclude that any wave field in the receiver plane due to any source distribution can be considered as a sum of monochromatic three dimensional plane waves. In conclusion, the response of a receiver array in the Fraunhofer area can be described with equations (2.24).

The total output  $U_M$  to multiple sources can be described with:

$$U_M(\omega) = \sum_b S_b(\omega) \frac{e^{-jkr_b}}{r_b} \int_{-\infty}^{\infty} \int_{-\infty}^{\infty} M(x,y,\omega) e^{j(k_{xb}x + k_{yb}y)} dx dy \quad (2.27)$$

with  $k_{xb} = k \cos \phi_b \sin \theta_b$  and  $k_{yb} = k \sin \phi_b \sin \theta_b$ . The output depends on the positions of the sources with respect to the receiver array, the source characteristics  $S_b(\omega)$  and the geometrical properties of the receiver array.

3-Dimensional

For a three-dimensional receiver we can extend equation (2.27):

$$U_M(\omega) = \sum_b S_b(\omega) \frac{e^{-jkr_b}}{r_b} \iiint_{-\infty}^{\infty} M(x,y,z,\omega) e^{j(k_{xb}x + k_{yb}y + k_{zb}z)} dx dy dz \quad (2.28)$$

where  $k_z = k \cos \theta$  and assuming the validity of the Fraunhofer approximation.

## 2.3 Directivity Patterns of Receiver Arrays

Definition

We will now define the directivity pattern  $Q(\phi, \theta, \omega)$  of a receiver by dividing equation (2.28) into a source dependent and a receiver dependent part respectively:

$$U_M = \sum_b S_b(\omega) \frac{e^{-jkr_b}}{r_b} Q(\phi, \theta, \omega) \quad \text{with}$$

$$Q(\theta, \phi, \omega) = \iiint_{-\infty}^{\infty} M(x,y,z,\omega) e^{+jk[(\cos \phi \sin \theta)x + (\sin \phi \sin \theta)y + (\cos \theta)z]} dx dy dz. \quad (2.29)$$

The definition of the directivity pattern allows us to examine the directional behaviour of a receiver independent of the incident wave field. Using equation (2.29), it must be noted that this examination is done in the Fraunhofer area which enables us to obtain the directivity pattern by a Fourier transformation of the function  $M(x,y,z,\omega)$  to the spatial Fourier domain!

We will start the examination of the directivity pattern for a line receiver and a planar receiver respectively and assume that the receivers consist of an infinite number of omni-directional point receivers. Afterwards, we will continue with the examination of a discrete line receiver.

## LINE RECEIVER

The directivity pattern in the x-z plane for a continuous line receiver along the x-axis with length L can be computed from equation 2.29 with  $\phi=0$  and

$$M(x,y,z,\omega) = \delta(y) \delta(z) \quad |x| \leq L/2$$

$$M(x,y,z,\omega) = 0 \quad |x| > L/2,$$

giving

$$\begin{aligned} Q(\theta, \phi, \omega) &= \int_{-\infty}^{\infty} M(x,y,z,\omega) e^{jk_x x} dx = \int_{-L/2}^{L/2} e^{jk_x x} dx \\ &= \frac{\sin(k_x \frac{L}{2})}{k_x/2} \quad \text{with } k_x = k \sin \theta. \end{aligned} \quad (2.30)$$

Figure 2.5 shows the directivity pattern of the line receiver as a function of  $\sin \theta$ . It is clear that a line receiver has a symmetry axis given by the x-axis and, therefore, it has a cylinder symmetric directivity. This means that the directivity pattern in e.g. the x,y plane will be the same as in the x,z plane.

Notches

The notches of the directivity pattern are determined by  $\sin(k_x L/2) = 0$  (except for  $k_x L/2 = 0$ ) :

$$k_x \frac{L}{2} = n\pi \quad n = \pm 1, 2, \dots$$

or

$$\sin \theta = \frac{n\lambda}{L} \quad n = \pm 1, 2, \dots \quad (2.31)$$

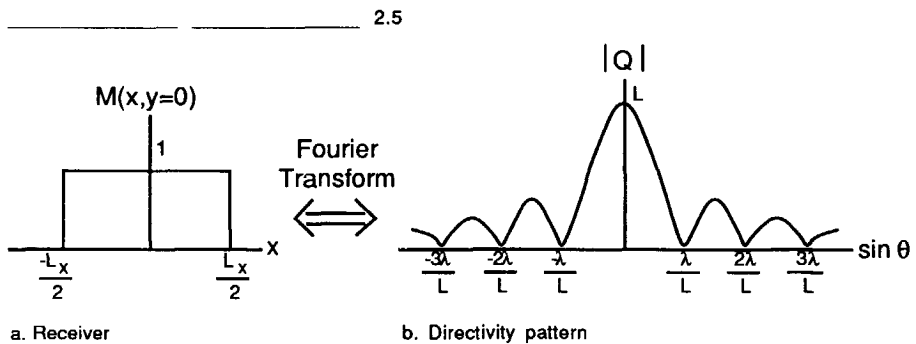


Figure 2.5 Directivity pattern (b) of a line receiver with length L (a). The directivity pattern is obtained by a Fourier transform of the line receiver to the spatial frequency domain.



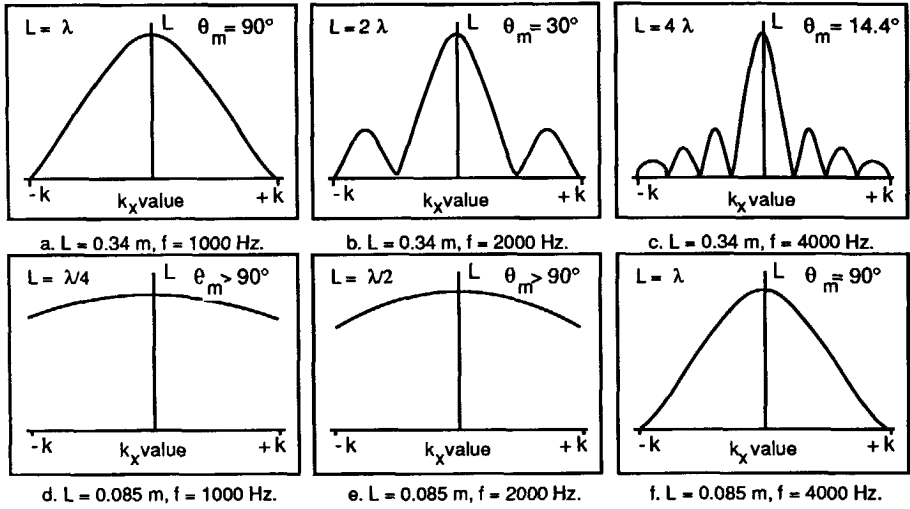


Figure 2.7 The directivity patterns for a receiver with length  $L = 0.34 \text{ m}$  and  $L = 0.085 \text{ m}$  at the frequencies  $f = 1000, 2000$  and  $4000 \text{ Hz}$ .

The first notch of the main beam is denoted by  $\theta_m$  and is only visible for  $L \geq \lambda$ . The examples show that a significant directivity is only obtained when  $L > \lambda$ .

#### PLANAR RECEIVER

The directivity pattern of a planar receiver  $\Delta M$  with dimensions  $L_x$  and  $L_y$  can be computed with equation 2.29 and

$$M(x, y, z, \omega) = \delta(z) \quad \text{inside } \Delta M$$

$$M(x, y, z, \omega) = 0 \quad \text{outside } \Delta M$$

giving (with  $k_x = k \cos \phi \sin \theta$  and  $k_y = k \sin \phi \sin \theta$ ):

$$\begin{aligned}
 Q(\theta, \phi, \omega) &= \int_{-\infty}^{\infty} \int_{-\infty}^{\infty} M(x, y, z, \omega) e^{j(k_x x + k_y y)} dx dy \\
 &= \int_{-L_x/2}^{L_x/2} \int_{-L_y/2}^{L_y/2} e^{j(k_x x + k_y y)} dx dy \\
 &= \left[ \frac{\sin k_x (\frac{L_x}{2})}{k_x/2} \right] \left[ \frac{\sin k_y (\frac{L_y}{2})}{k_y/2} \right] \quad (2.33)
 \end{aligned}$$

Equation (2.33) shows that the directivity pattern has three planes of symmetry. One plane of symmetry in the same plane as the receiver and two planes of symmetry perpendicular to  $\Delta M$ . In these planes ( $\phi = 0^\circ$  or  $90^\circ$ ) the directivity pattern equals the pattern of a line receiver. Furthermore, it is important to note that the beam width is mainly determined by the diameter of the receiver.

#### DISCRETE LINE RECEIVER

The directivity pattern in the x-z plane of a discrete line receiver with  $(2N+1)$  receivers and an intermediate distance  $\Delta x$  can be computed from the discretized version of equation 2.29

$$M(x, y, \omega) = \sum_{n=-N}^{+N} \delta(x - n\Delta x) \delta(y) ,$$

giving

$$Q(\theta, \phi, \omega) = \sum_{n=-N}^{+N} e^{+jk_x(n\Delta x)}$$

$$\frac{\sin \left[ k_x (2N+1) \frac{\Delta x}{2} \right]}{\sin \left[ k_x \frac{\Delta x}{2} \right]} \quad \text{with } k_x = k \sin \theta. \quad (2.34)$$

Figure 2.8 shows the directivity pattern of the discrete line receiver as a function of  $\sin \theta$ . The discrete line receiver has a symmetry axis given by the x-axis and a cylinder symmetric directivity pattern around the x-axis.

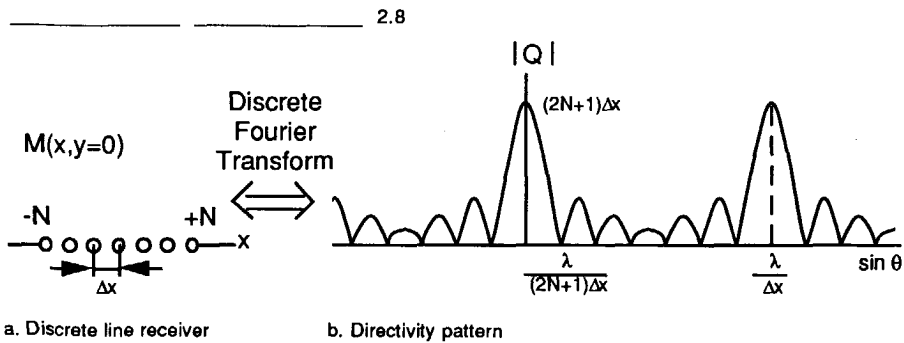


Figure 2.8 Directivity pattern (b) of a discrete line receiver with length  $(2N+1)\Delta x$  (a). The directivity pattern is obtained by a Discrete Fourier transform of the line receiver to the spatial frequency domain.

## Notches

The notches are determined by  $\sin(k_x(2N+1)\Delta x/2) = 0$  (except for  $\sin(k_x\Delta x/2) = 0$ ) :

$$k_x (2N+1) \frac{\Delta x}{2} = m\pi \quad m = \pm 1, 2, \dots$$

or

$$\sin \theta = \frac{m\lambda}{(2N+1) \Delta x} \quad m = \pm 1, 2, \dots \quad (2.35)$$

Equation 2.35 shows that the zeros depend on the wavelength  $\lambda$  and the length of the line receiver  $L=(2N+1) \Delta x$ . Next to the principal maximum at  $\sin \theta = 0$  maxima or so-called grating lobes occur at  $\sin(k_x\Delta x/2) = 0$  :

$$k_x \frac{\Delta x}{2} = i\pi \quad i = \pm 1, 2, \dots$$

or

$$\sin \theta = i \frac{\lambda}{\Delta x} \quad i = \pm 1, 2, \dots$$

This means that the directivity pattern has more than one main lobe when  $k \geq 2\pi/\Delta x$ . Figure 2.9 gives the  $k_x$ - $k$  diagram for the discretized line array.

## Spatial aliasing

The diagram shows that in the dark shaded area ( $|k_x| < \pi/\Delta x$ ) the directivity pattern is not influenced by the discretization. However, for values of  $k > \pi/\Delta x$  the directivity pattern is influenced in the light shaded areas. The effect is well-known as aliasing and, because we have applied a *spatial* Fourier Transform, is also called *spatial aliasing*. The aliasing effect gives at e.g.  $k = 2\pi/\Delta x$  the contribution of three main lobes.

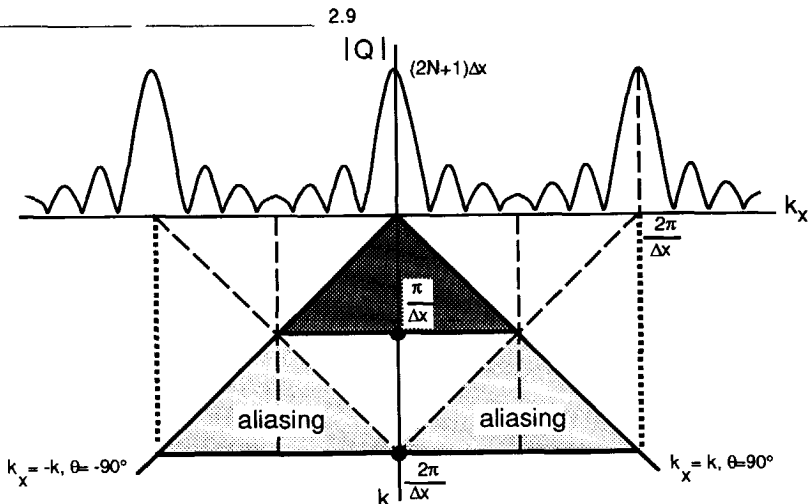


Figure 2.9 Representation of directivity pattern in a  $k_x$ - $k$  diagram showing the change of the directivity with frequency. For  $k > \pi/\Delta x$  spatial aliasing will occur.



For  $\pi/\Delta x < |k_x| < 2\pi/\Delta x$  aliasing does not occur if the angle is decreased (white triangle). We may conclude that aliasing does not occur if

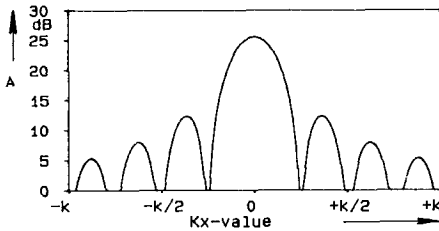
$$|k_x| \leq \frac{\pi}{\Delta x} \quad \text{or} \quad \Delta x \leq \frac{\lambda}{2 |\sin \theta|}. \quad (2.36)$$

For a diffuse sound field the angle of incidence  $\theta$  will be between  $0^\circ$  and  $90^\circ$  and therefore we must conclude that spatial aliasing can only be avoided when  $\Delta x < \lambda/2$ .

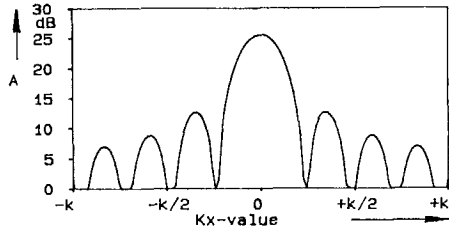
Example

Figure 2.10 gives the directivity patterns for a discrete microphone array with  $L=0.34$  m and  $f=4000$  Hz being equivalent with  $L=4\lambda$ . The directivity patterns are drawn for 17, 9, 5 and 3 equidistantly spaced microphones respectively, being equivalent with  $\Delta x = \lambda/4, \lambda/2, \lambda$  and  $2\lambda$  respectively. For  $\Delta x = \lambda$  and  $2\lambda$  extra main lobes occur due to spatial aliasing.

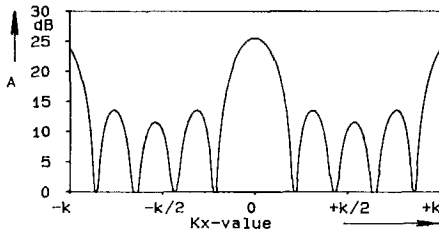
2.10



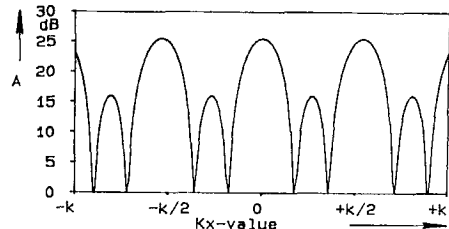
a.  $L=4\lambda$ ,  $n=17$ ,  $\Delta x = \lambda/4$ .



b.  $L=4\lambda$ ,  $n=9$ ,  $\Delta x = \lambda/2$ .



c.  $L=4\lambda$ ,  $n=5$ ,  $\Delta x = \lambda$ .



d.  $L=4\lambda$ ,  $n=3$ ,  $\Delta x = 2\lambda$ .

Figure 2.10 Directivity patterns of a discrete microphone array with  $L=0.34$  m and  $f=4000$  Hz being equivalent with  $L=4\lambda$ . The directivity patterns are drawn for 17 (a), 9 (b), 5 (c) and 3 (d) equidistantly spaced microphones respectively, being equivalent with  $\Delta x = \lambda/4, \lambda/2, \lambda$  and  $2\lambda$ .

## 2.4 Properties of Discrete Microphone Arrays: Broadside, Endfire and Jacobi Arrays

In this section we will examine the properties of different array configurations that are suitable for our purposes using the results of section 2.3. The directivity index will be introduced as a simple measure to differentiate between the different array configurations.

This examination will show the variation of the directivity patterns and the directivity index, dependent on the array configuration and the signal processing. In chapter 3 these parameters will be used to find an optimum solution for our problem.

### DIRECTIVITY INDEX

For the definition of the directivity index of a receiver array we start with the gain of a source in a given direction defined as the ratio of the transmitted intensity in that direction to the average transmitted intensity:

$$G_s(\theta, \phi, \omega) = \frac{|p(\theta, \phi, \omega)|^2}{W_s / 4\pi}, \quad (2.37)$$

where  $W_s$  is the total transmitted power represented by

$$W_s(\omega) = \int_0^{2\pi} \int_0^\pi |p(\theta, \phi, \omega)|^2 \sin \theta \, d\theta \, d\phi \quad (2.38)$$

Directivity factor      The *directivity* or *directivity factor*  $Q_s$  for an arbitrary frequency can now be defined as the *maximum* value of the source gain (Beranek, 1954):

$$Q(\omega)_{s,\max} = \frac{4\pi |p(\theta, \phi, \omega)_{\max}|^2}{\int_0^{2\pi} \int_0^\pi |p(\theta, \phi, \omega)|^2 \sin \theta \, d\theta \, d\phi} \quad (2.39)$$

Directivity index      The *directivity index* (DI) can now readily be obtained by taking the logarithm of (2.39):

$$DI(\omega) = 10 \log G(\omega)_{s,\max} \quad (2.40)$$

Consequently the directivity index is always larger than or equal to zero, the latter being the case for uniform radiation in all directions.

The directivity of an array in a plane wave field can now be obtained using reciprocity: the array gain in a given direction is defined as the ratio of the transmitted intensity in that direction to the average transmitted intensity:

$$G_r(\theta, \phi, \omega) = \frac{|I(\theta, \phi, \omega)|^2}{I_r / 4\pi}, \quad (2.41)$$

where  $I_r$  is the total transmitted intensity represented by

$$I_r(\omega) = \int_0^{2\pi} \int_0^\pi |I(\theta, \phi, \omega)|^2 \sin \theta \, d\theta \, d\phi. \quad (2.42)$$

Then, the directivity or directivity factor  $Q_r$  for a receiver array is given by the maximum of the array gain

$$Q(\omega)_{r, \max} = \frac{4\pi |I(\theta, \phi, \omega)|^2}{I_r(\omega)} \quad (2.43)$$

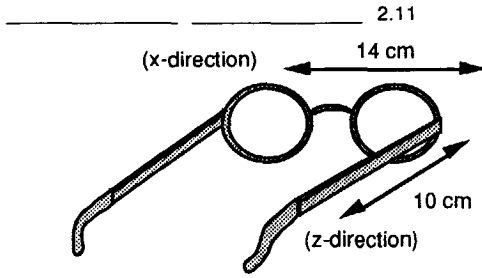
and the directivity index equals:

$$DI(\omega) = 10^{10} \log G(\omega)_{r, \max}. \quad (2.44)$$

The directivity index indicates the extent to which a sound field consisting of uncorrelated plane waves is attenuated in comparison with sound transmitted in the direction of the maximum array gain. According to this definition the directivity index of an omni-directional microphone is  $DI = 0$  dB for all frequencies. A directional microphone with a directivity pattern  $Q(\theta, \phi, \omega) = 1 + \cos \theta$ , being equivalent with a cardioid microphone, has a directivity index  $DI = 4.7$  dB (viz. equation 2.55 and figure 2.17).

#### DISCRETE MICROPHONE ARRAY

In the preceding section we have seen that a small beam width can be obtained for array length  $L > \lambda$ . For our purpose, however, we have to limit the maximum size for practical reasons. In section 1.5 we have proposed that the microphone array should be connected to, or built-in, a pair of spectacles. Therefore, we will limit ourselves to an examination of linear arrays that can be combined with the frame or legs of a pair of spectacles.



f (Hz)	$\lambda$ (cm)	Array length	
		10 cm	14 cm
500	68	$0.15 \lambda$	$0.21 \lambda$
1000	34	$0.29 \lambda$	$0.41 \lambda$
2000	17	$0.59 \lambda$	$0.82 \lambda$
4000	8.5	$1.18 \lambda$	$1.65 \lambda$

Figure 2.11 The array dimensions are limited by the length and the width of a pair of spectacles. The table gives the array length relative to the wavelength.

The maximum array length is determined by the length of the legs of a pair of spectacles or the width of the frame (figure 2.11) which is equivalent with approximately 10 cm and 14 cm respectively.

#### Array parameters

The directivity of a discrete microphone array depends on the array itself and the signal processing. Figure 2.12 shows a discrete microphone array with the following parameters:

- Length (L)
- Number of microphones (2N+1)
- Intermediate distance between the microphones ( $\Delta x$ )
- Time lag corrections ( $\tau_n$ )
- Amplitude weighting or pre-amplification ( $A_n$ )
- Directional properties of the individual microphones ( $D_n(\theta, \phi, \omega)$ ).

The influence of these parameters on the directivity of an equidistantly spaced linear array can be incorporated in equation (2.28). The directivity pattern is now equal to:

$$Q(\theta, \phi, \omega) = Q_0(\theta, \phi, \omega) D(\theta, \phi, \omega) \quad (2.45a)$$

with  $D(\theta, \phi, \omega)$  the directivity pattern of the individual microphones and

$$Q_0(\theta, \phi, \omega) = \sum_m \sum_n M(n\Delta x, m\Delta z, \omega) e^{+j [k_x(n\Delta x) + k_z(m\Delta z)]} \quad (2.45b)$$

with

$$M(n\Delta x, m\Delta z, \omega) = \sum_{n=-N}^{+N} \sum_{m=-M}^{+M} A_{n,m} e^{+j\alpha_{n,m}} \delta(x-n\Delta x) \delta(z-m\Delta z) \quad (2.45c)$$

and  $x, z$  the direction as given in figure 2.11,  $A_{n,m}$  the amplitude weighting,  $\alpha_{n,m}$  the phase correction of microphone  $n, m$ . The phase correction equals  $\alpha_{n,m} = -\omega\tau_{n,m}$  with  $\tau_{n,m}$  a frequency independent time-lag.

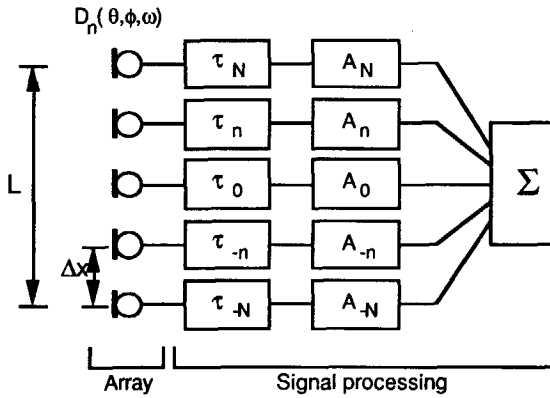


Figure 2.12 Diagram of a discrete microphone array with its parameters.

#### TIME LAG CORRECTION

Sum beam forming

The arrival time of a sound wave at each microphone is determined by the position of the microphone and the sound velocity in air. It results in phase differences between the microphone signals dependent on the angle of incidence. Using a discrete microphone array the phase can be corrected for the differences in arrival time for sounds coming from one specific direction:

$$\tau_n = \frac{n\Delta x}{c} \sin \theta_N \text{ or } \tau_m = \frac{m\Delta z}{c} \cos \theta_M \quad (2.46)$$

where the correction angle  $\theta_{N,M}$  determines the angle of the main beam of the array. The correction of the arrival times is also known as *sum beam forming*.

Now, we distinguish two important groups of linear arrays characterized by the position of the microphones and the angle  $\theta_{x,z}$ .

Broadside array

In **broadside arrays** the microphones are placed along the x-axis and the phase correction should be  $\alpha_n = 0$  by choosing  $\theta_N = 0$ , giving

$$\begin{aligned} Q_0(\theta, \phi, \omega) &= \sum_n M(n\Delta x, \omega) e^{+jk_x n\Delta x} \\ &= \sum_{n=-N}^{+N} A_n(\omega) e^{+jk_x n\Delta x} \end{aligned} \quad (2.47)$$

with  $k_x = k \cos \phi \sin \theta$ .

Endfire array

In **endfire arrays** the microphones are placed along the z-axis and the phase correction should be  $\tau_m = m\Delta z/c$  by choosing  $\theta_M = 0$  and with  $k_z = k\cos\theta$ , giving

$$\begin{aligned} Q_o(\theta, \phi, \omega) &= \sum_m M(m\Delta z, \omega) e^{+jk_z m\Delta z} \\ &= \sum_{m=-M}^M e^{-j\omega \frac{m\Delta z}{c}} A_m(\omega) e^{jk_z m\Delta z} \\ &= \sum_{m=-M}^M A_m(\omega) e^{jkm\Delta z (\cos\theta - 1)} \end{aligned} \quad (2.48a)$$

and for  $A_m(\omega) = 1$

$$Q_o(\theta, \phi, \omega) = \frac{\sin \left[ k(2M+1) \frac{\Delta z}{2} (\cos\theta - 1) \right]}{\sin \left[ k \frac{\Delta z}{2} (\cos\theta - 1) \right]} \quad (2.48b)$$

Notches

The notches of the directivity pattern are now determined by  $\sin[k(2M+1)\Delta z (\cos\theta - 1)/2]$  (except for  $\sin[k\Delta z (\cos\theta - 1)/2] = 0$ ):

$$k(2M+1) \frac{\Delta z}{2} (1 - \cos\theta) = i\pi, \quad i = 1, 2, \dots$$

or

$$1 - \cos\theta = \frac{i\lambda}{(2M+1)\Delta z}, \quad i = 1, 2, \dots \quad (2.49)$$

The first notches are determined by

$$\cos\theta = 1 - \frac{\lambda}{(2M+1)\Delta z}$$

For large M the notches of the main beam will be very close to  $0^\circ$ ; we can approximate  $\cos\theta$  with

$$\cos\theta \approx 1 - \frac{\theta^2}{2}$$

Beam width endfire

and the beam width of the endfire array equals

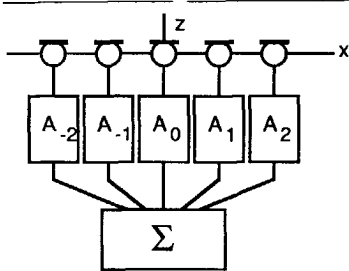
$$BW = 1.21 \sqrt{\frac{2\lambda}{L}} \quad (2.50)$$

with L the length of the array given by  $(2M+1)\Delta z$ .

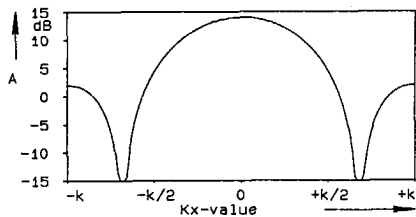
Example  
broadside array

An example of a broadside array is given in figure 2.13a. Figure 2.13b gives the computed directivity pattern  $Q(k_x, f = 4000 \text{ Hz})$  for a broadside array of 5 microphones ( $N=2$ ) with  $L = 10 \text{ cm}$ , assuming omni-directional microphones ( $D(\theta, \phi, \omega)=1$ ) and uniform amplitude weighting ( $A_n=1$ ). The beam maximum occurs in the direction perpendicular to the array for  $k_x=0$ . Further, figure 2.13c gives the full 3-dimensional directivity pattern as a function of  $\phi$  and  $\theta$  showing the cylinder symmetry around the x-axis. The polar diagram of figure 2.13d gives a cross section of the directivity pattern in the x-z plane as a function of the angle  $\theta$ . Due to the cylinder symmetry we have 'two main lobes' in the x-z plane. Computation of the directivity factor using equation (2.39) and assuming the maximum at  $\theta = 0^\circ$  gives a directivity index  $DI = 4.9 \text{ dB}$  at 4000 Hz.

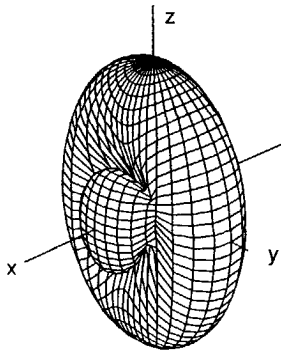
2.13



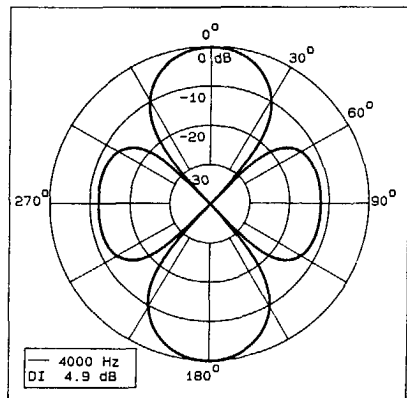
a. Scheme broadside array.



b. Directivity pattern  $Q(k_x, f=4000 \text{ Hz})$



c. Three-dimensional diagram

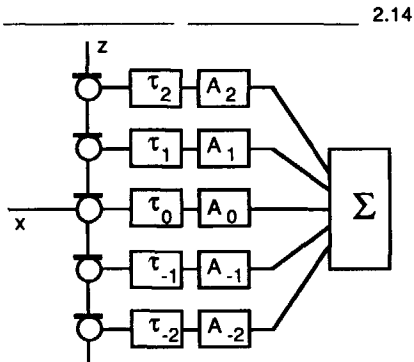


d. Polar diagram

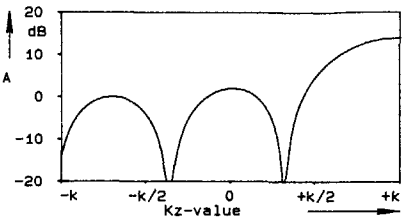
Figure 2.13 Scheme(a) and representation of directivity pattern in a  $k_x$ -diagram(b), three-dimensional diagram (c) and polar diagram (d) of a **broadside** array with length  $l = 10 \text{ cm}$ , 5 microphones, frequency  $f = 4000 \text{ Hz}$ .

Example  
endfire array

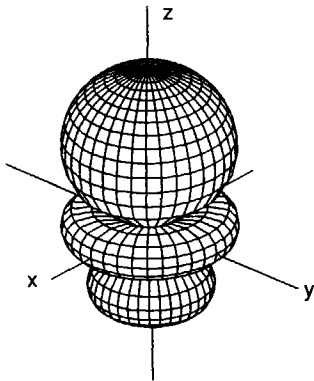
An example of an endfire array is given in figure 2.14a. The directivity pattern of an endfire array of 5 microphones ( $N=2$ ) with  $L = 10$  cm and  $\alpha_m = -\omega m \Delta z/c$  is computed and shown in figure 2.14b as a function of  $k_z$ . The beam maximum occurs in the direction of the array axis for  $k_z=k$ . The 3-dimensional directivity pattern (2.14c) is again cylinder symmetric around the array axis. The cross section given by the polar diagram shows that an endfire array has only one beam maximum. Computation of the directivity factor gives a directivity index  $DI = 7.6$  dB.



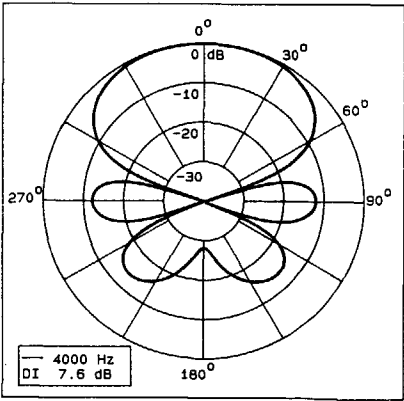
a. Scheme endfire array.



b. Directivity pattern  $Q(k_x, f=4000 \text{ Hz})$



c. Three-dimensional diagram



d. Polar diagram

Figure 2.14 Scheme(a) and representation of directivity pattern in a  $k_x$ -diagram(b), three-dimensional diagram (c) and polar diagram (d) of an **endfire** array with length  $l = 10$  cm, 5 microphones, frequency  $f = 4000$  Hz.



## Comparison

A comparison of equations (2.32) and (2.50) for the beam width and of the polar diagrams of the broadside and endfire array (figure 2.13d, 2.14d) shows that in the x-z plane the main beam of a broadside array is always narrower than that of an endfire array of the same size. Therefore, the use of a broadside array may be advantageous when a small beam width is wanted in one plane. However, the three-dimensional directivity patterns (figure 2.13c, 2.14c) and the computed directivity indices show that an endfire array of omni-directional microphones is advantageous for diffuse noise suppression.

## AMPLITUDE WEIGHTING

Amplitude weighting of each microphone signal is equivalent with the application of a window function. Window functions along the time axis and temporal frequency axis are generally applied in time series analysis and filtering applications (Harris, 1978), while window functions along the space axis and spatial frequency axis are applied in wave theoretical applications such as migration (Berkhout, 1984). In array techniques the amplitude weighting or window function is generally applied for adaptation of the directivity pattern and side lobe suppression (Ma, 1973).

## Window functions

We now apply some well-known window functions as an amplitude weighting function to a broadside microphone array. For a broadside array of omni-directional microphones the directivity pattern is equal to:

$$Q_0(\theta, \phi, \omega) = \sum_{n=-N}^{+N} A_n(\omega) e^{+jk_x n \Delta x}, \quad k_x = k \cos \phi \sin \theta. \quad (2.51)$$

Equation (2.51) shows that the directivity pattern  $Q_0(\theta, \phi, \omega)$  can be obtained by a discrete spatial Fourier Transform of the actual weighting function  $A_n(\omega)$  into the spatial frequency domain. Figure 2.15 gives five directivity patterns at  $f = 4000$  Hz for a broadside array with  $L = 14$  cm and 7 equidistantly spaced omni-directional microphones. Five different weighting functions have been used: the *concave upward* weighting function with larger weights towards the ends of the array; three cosine weighting functions  $\cos^\gamma(x)$ : *uniform* ( $\gamma = 0$ ), *cosine* ( $\gamma = 1$ ), *hanning* ( $\gamma = 2$ ) and a *dolph-chebyshev* weighting with binomial weights. The definition of the window functions, directivity index, first notch, beam width, and relative side lobe level are given in table 2.1.

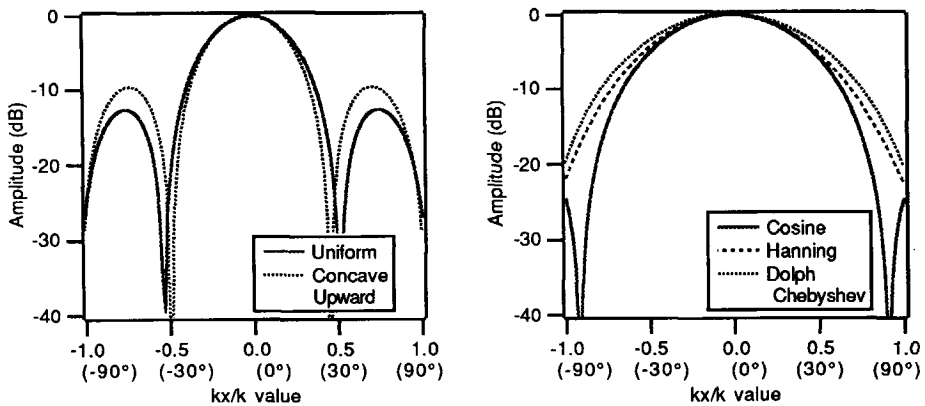


Figure 2.15 Directivity patterns of a broadside array with different amplitude weighting functions.

Table 2.1 Definition of window functions and influence on directivity at  $f = 4000$  Hz of a broadside array with  $l = 14$  cm.

Name	Weighting function		DI (dB)	$\theta_1$ BW	Sidelobe level (dB)
Concave Upward	$1 + (\gamma n)^2 \delta(x - n\Delta x), \gamma = 0.25$		6.0	29° 34°	-9
Uniform (Box-car, $\cos^0$ )	$\frac{1}{2N+1} \delta(x - n\Delta x)$		6.0	33° 38°	-13
Cosine ( $\cos^1$ )	$\cos \frac{\pi n}{2N} \delta(x - n\Delta x)$		4.1	68° 64°	-25
Hanning ( $\cos^2$ )	$\frac{1}{2} \left[ 1 + \cos \frac{2\pi n}{2N} \right] \delta(x - n\Delta x)$		3.9	>90° 68°	-32*
Dolph-Chebyshev	$\frac{(2N)!}{(N-n)!(N+n)!} \delta(x - n\Delta x)$		3.4	>90° 76°	-50*

\* Side lobe level for larger array.

#### Comparison

The uniform weighting gives a small main lobe with relative high side lobe levels. The concave upward weighting results in a narrower beam width at the expense of having higher side lobe levels. The opposite effect can be obtained with the Cosine, Hanning and Dolph-Chebyshev window functions. They reduce the side lobe levels at the cost of a broader main lobe and a lower directivity index. The broader main lobe is a result of the low amplitude weighting at both ends of the array giving an array with a relative shorter effective length.

We may conclude that the Cosine, Hanning and Dolph-Chebyshev weighting are attractive for side lobe suppression. However, the uniform weighting and the concave upward weighting give a narrow beam width and the highest directivity index.

Finally, it must be noted that the weighting functions can also be applied to an endfire array. The amplitude weighting is independent of the phase correction, but both can be used to shape the directivity pattern.

**Jacobi weighting** A special weighting function is the *Jacobi weighting* (Weston, 1986). It can be used in combination with a phase correction and defined by

$$A_n(\omega) = (-1)^{|N+n|} \frac{(2N)!}{(N-n)! (N+n)!} \quad (-N < n < N) \quad (2.52)$$

**Jacobi array** We call an array with such an amplitude weighting: **Jacobi array**. The main difference with a Dolph-Chebyshev weighting (table 2.1) is given by the factor  $(-1)^{|n|}$  resulting in an alternating sign of the amplitude and thus a sum of all coefficients equal to zero:

$$\sum_n A_n(\omega) = \sum_n (-1)^{|N+n|} \frac{(2N)!}{(N-n)! (N+n)!} = 0. \quad (2.53)$$

This means that the microphone signals which are in phase will be cancelled after summation (dependent on the phase correction). However, microphone signals being out of phase will not be cancelled.

To determine the directivity pattern of a Jacobi array we start with the most simple form: an array with two microphones. (According to our definition we have to take  $N=1/2$ ). The directivity pattern for two microphones on the z-axis equals:

$$\begin{aligned} Q_o(\theta, \phi, \omega) &= \sum_{m=-1/2}^{1/2} A_m(\omega) e^{j\alpha_m} e^{jk_z m \Delta z} \\ &= A_1(\omega) e^{+j(\alpha_1 + k_z \frac{\Delta z}{2})} + A_{-1}(\omega) e^{+j(\alpha_{-1} - k_z \frac{\Delta z}{2})} \end{aligned} \quad (2.54)$$

with  $A_1(\omega) = -A_{-1}(\omega) = 1$  and  $\alpha_1 = -\alpha_{-1} = \beta k \Delta z / 2$  where  $\beta$  can be used to change the phase correction. Equation (2.54) can now be written as:

$$\begin{aligned} Q_o(\theta, \phi, \omega) &= e^{+j(\alpha_1 + k_z \frac{\Delta z}{2})} - e^{+j(\alpha_{-1} - k_z \frac{\Delta z}{2})} \\ &= 2j \sin [ (\beta + \cos \theta) k \Delta z / 2 ] \quad k \Delta z \ll 1 \quad j (\beta + \cos \theta) k \Delta z \end{aligned} \quad (2.55)$$

Dipole

Figure 2.16 shows the directivity patterns for  $\beta=0$  with intermediate distance  $\Delta z = \lambda, \lambda/2, \lambda/4$  and  $\lambda/16$ . The directivity increases with diminishing  $\Delta z$  and the directivity pattern for a small intermediate distance equals the directivity pattern of a *dipole*. Further, equation 2.55 shows that the maximum value of the directivity pattern will depend on the intermediate distance  $\Delta z$  and the frequency. The frequency spectrum has a slope of 6 dB/octave.

Cardioid

Figure 2.17 gives the directivity patterns for  $\beta = 1$  and  $\beta = 0.3$  with  $\Delta z = \lambda/16$ . The responses are the well-known cardioid and hyper-cardioid directivity patterns. The directivity index for  $\beta = 1$  and  $\beta = 0.3$  are  $DI = 4.7$  dB and  $DI = 6.0$  dB respectively.

A Jacobi array with more elements may be very attractive because a high directivity can be obtained with a small intermediate distance  $\Delta z$ . This is

Low frequencies

especially advantageous for *low frequencies* where directivity can be obtained with an array with  $L < \lambda$ . Figure 2.18 gives the polar diagrams and the directivity patterns for a jacobi array with 2, 3 ( $N=1$ ) and 5 ( $N=2$ )

2.16

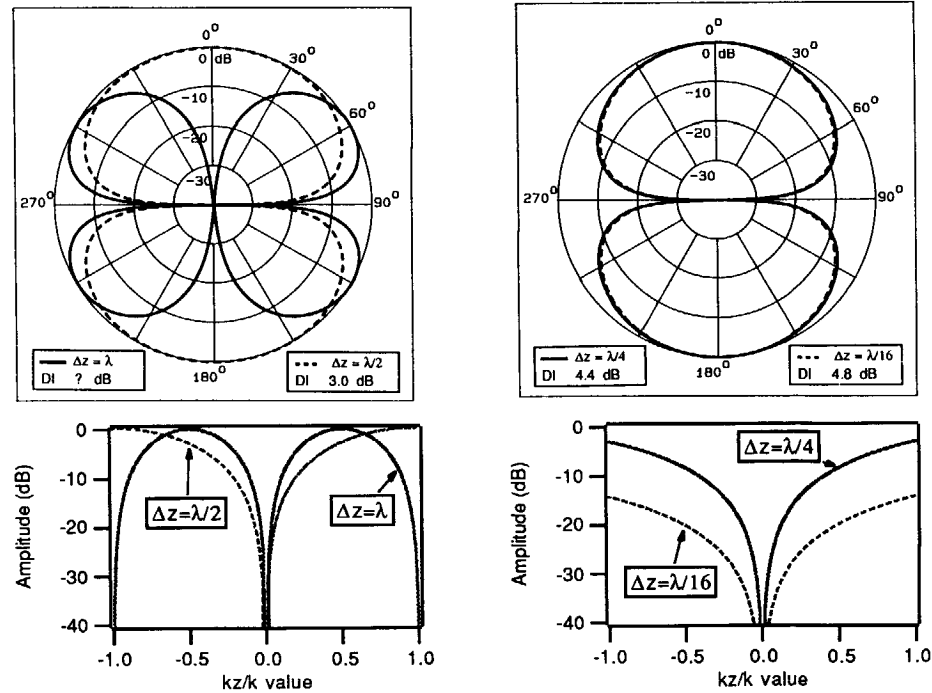


Figure 2.16 Directivity patterns of a Jacobi array with two elements for  $\beta=0$  and intermediate distance  $\Delta z$  is  $\lambda, \lambda/2, \lambda/4$  and  $\lambda/16$ .

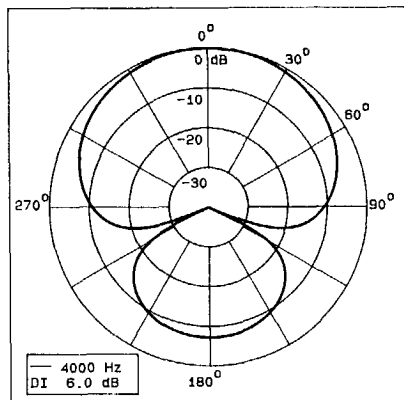
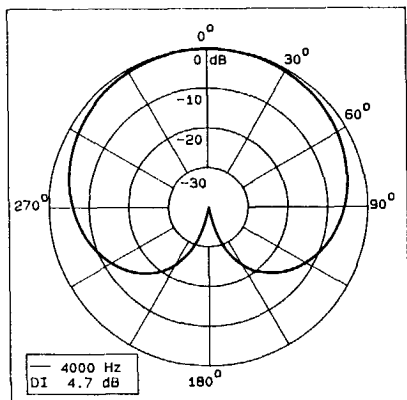
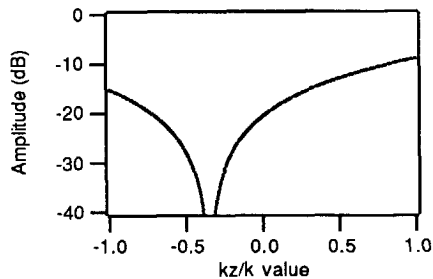
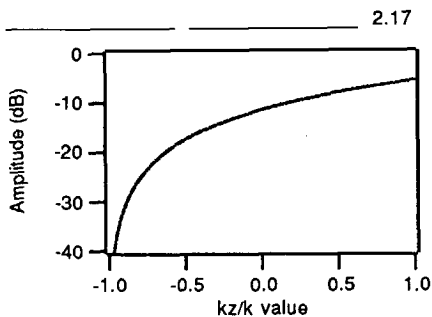


Figure 2.17 Directivity patterns of a Jacobi array with two elements for  $\beta=1$  and  $\beta=0.3$  with intermediate distance  $\Delta z$  is  $\lambda/16$  giving a cardioid and hyper-cardioid directivity pattern.

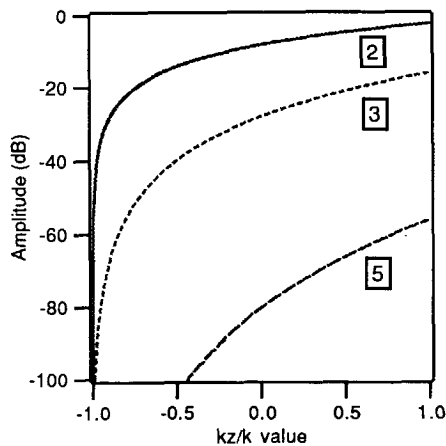
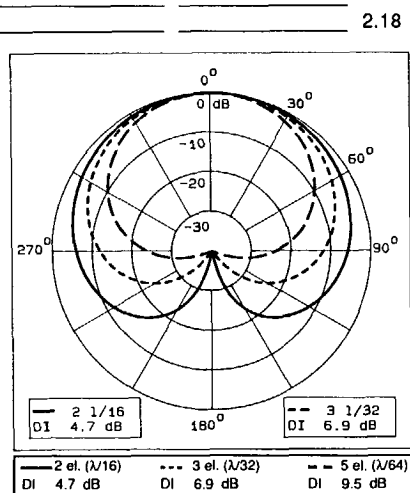


Figure 2.18 Polar diagram and  $k_z$ -diagram for a Jacobi array with 2, 3 ( $N=1$ ) and 5 ( $N=2$ ) elements. The time lag is applied with  $\beta=1$  and constant length  $L = \lambda/16$  giving a  $\Delta z = \lambda/16, \lambda/32$  and  $\lambda/64$  respectively.

elements. The time lag is computed for  $\beta = 1$  and the array length is constant  $L = \lambda/16$  giving  $\Delta z = \lambda/16, \lambda/32$  and  $\lambda/64$  respectively. The directivity index equals 4.7 dB, 6.9 dB and 9.5 dB.

Disadvantages

Although a high directivity index can be obtained with an array length  $L < \lambda$  the jacobi array will in practice have two important disadvantages. The maximum sensitivity decreases with more elements giving a low signal relative to the internal noise voltage (figure 2.18b). Furthermore, the high directivity will decrease dramatically due to a perturbation in the amplitude weighting or phase correction (instability) which will be shown in the next chapter.

### DIRECTIONAL MICROPHONES

In the preceding part of this chapter we have examined the directivity patterns of arrays with omnidirectional microphones. With a directional microphone the directivity pattern of an array can be improved for the lower frequencies, resulting in suppression of side lobes and sounds coming from behind.

Directional  
microphone

Figure 2.19 shows a cross-sectional view of a directional microphone with two sound inlets and two cavities in the microphone, separated by a very thin foil diaphragm. The diaphragm senses the difference between the instantaneous air pressures which impinge on its two surfaces. This pressure difference at the diaphragm causes it to move, and this mechanical movement is converted to an electrical output signal by the microphone. In the rear microphone inlet a time delay acoustic network is placed. This type of directional microphone functions as a Jacobi array of two elements and its directivity will depend on the time delay acoustical network:

$$D(\theta, \phi, \omega) \approx j (\beta + \cos \theta) k \Delta d$$

2.19

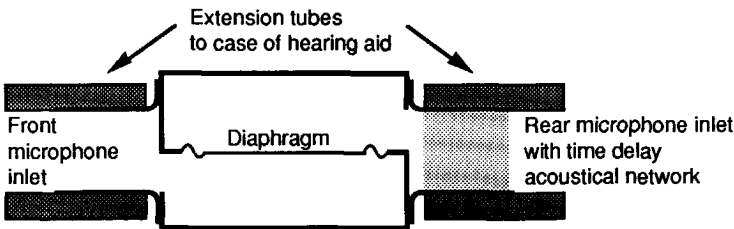


Figure 2.19 Cross-sectional view of a directional hearing aid microphone.

with  $\Delta d$  the distance between the sound inlets and  $\beta$  determined by the acoustical network. For an acoustical time delay resulting in  $\beta = 1$  we will obtain a cardioid directivity pattern (figure 2.17).

Application

Figure 2.20 shows the directivity pattern of a broadside array of 7 elements,  $l=14$  cm at  $f=4000$  Hz with omni-directional microphones(a) and directional microphones(b). The dashed line is the directivity pattern of one single cardioid microphone. The directional cardioid microphone suppresses the side lobes and the main lobe in the backward direction. We can conclude that a directional cardioid microphone can be very useful in array design to improve the directivity for the lower frequencies, suppress side lobes and/or unwanted main lobes.

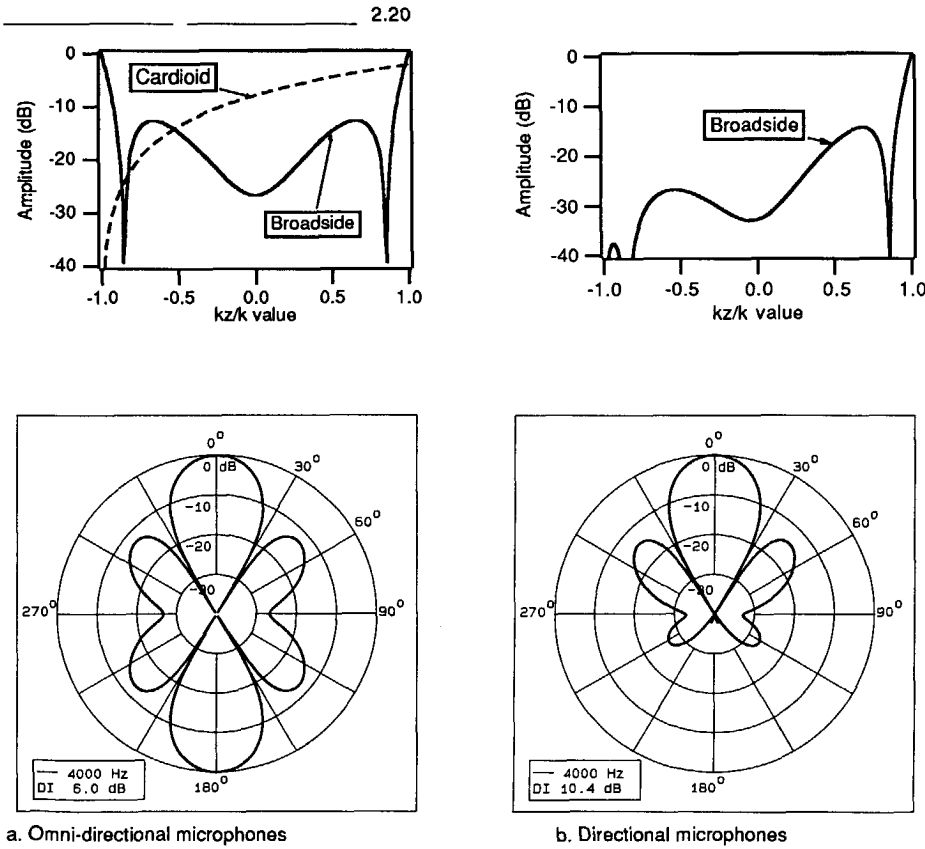
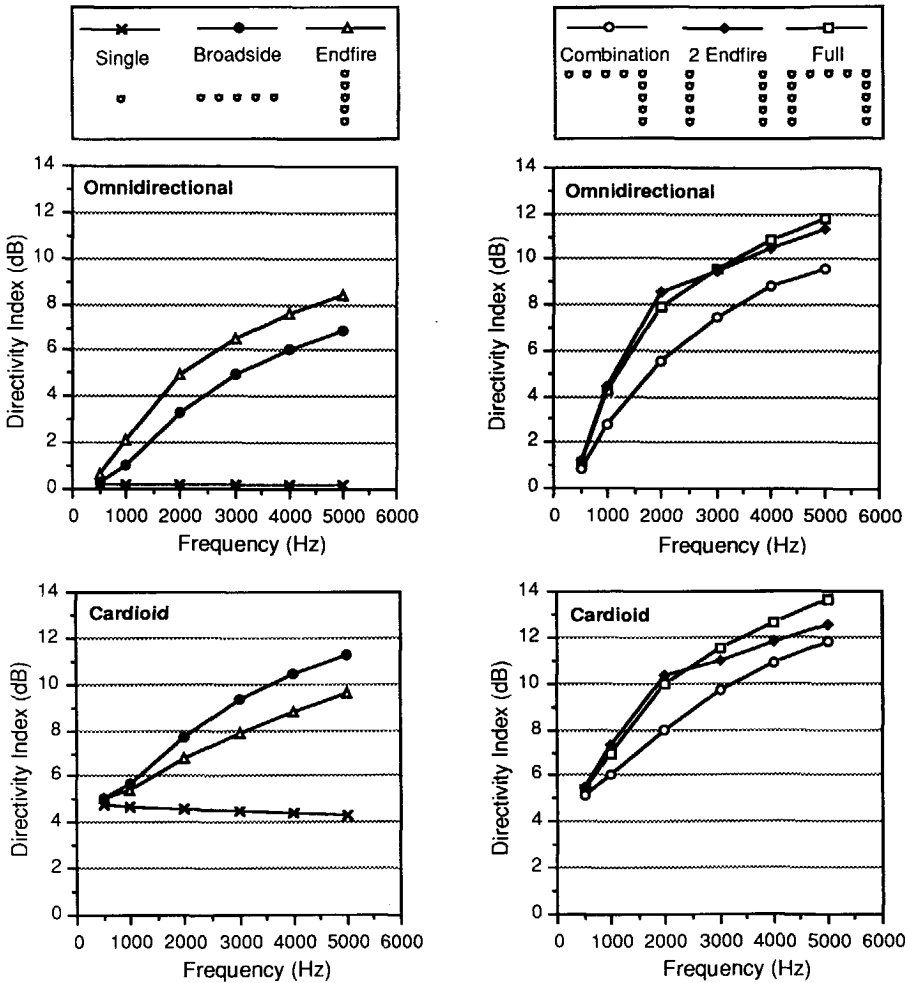


Figure 2.20 Directivity pattern of broadside array of 7 elements,  $l=14$  cm at  $f=4000$  Hz with omni-directional microphones(a) and directional microphones(b). The dashed line is the directivity pattern of one single cardioid microphone.

Finally, figure 2.21 gives the directivity index for different array configurations and microphone types used. The directivity index is computed for a free-field situation for a broadside array with  $L=14$  cm and an endfire array with  $L=10$  cm (figure 2.21a). Combinations are made of one endfire and one broadside array, two endfire arrays with intermediate distance  $L=14$  cm and a full configuration of two endfire arrays and one

2.21



a. Simple configurations

b. Combined configurations

Figure 2.21 Directivity index of one single microphone and different array-configurations as a function of frequency and microphone type: single microphone, endfire array and broadside array (a) and combined configurations (b).



broadside array giving the shape of one pair of spectacles (figure 2.21b). The directivity of the combined configurations is computed for a free-field situation and a simple summation of the (delayed) microphone signals giving one output signal (mono). Binaural profits of stereo fitting should be added by using two (combined) configurations.

#### Comparison

The array configurations of omni-directional microphones have a low directivity index at the lower frequencies because the array dimensions are small in comparison to the wavelength (figure 2.21a). A significant improvement of the directivity index at the lower frequencies can be obtained by using cardioid microphones (figure 2.21b). The use of the cardioid microphones is also important for the directivity index of one single broadside array. The cardioid microphones suppress the main lobe in the back giving a significant improvement of the directivity index for the higher frequencies. The full combined configuration of two endfire and one broadside array gives the highest directivity above 2500 Hz. The configuration with two endfire arrays only gives a higher directivity for the low frequencies. The 'under-sampling' in the horizontal direction results in a smaller main lobe and higher side lobes giving a small net profit of the directivity.

#### Conclusion

We may conclude that with one endfire array ( $L=10$  cm) or one broadside array ( $L=14$  cm) of cardioid microphones a directivity index can be reached of at least 5 dB at the lower frequencies rising to more than 9 dB at 4 kHz. The combined array configurations (mono, free-field) give an extra improvement of the directivity index between 2 and 3 dB.



---

# OPTIMIZATION AND STABILITY

## Chapter 3

### 3.1 Introduction

Optimization	<p>An effective array solution for speech intelligibility improvement in noise should not only have <i>highly directional characteristics</i>, but the solution should also be <i>robust</i>. In this chapter we will use array parameters e.g. number of microphones, time-lag correction and amplitude weighting to obtain the highest possible directivity index for a given fixed array length (see section 2.4). Also attention will be paid to the frequency spectrum of the different array configurations. Section 3.2 shows how the directivity of an endfire array can be improved by changing the time lag correction following a suggestion done by Hansen and Woodyard (1938). Section 3.3 gives a more general approach to optimization.</p>
Stability	<p>Robustness means that if the parameters change slightly or if the external acoustical conditions change, the array does not lose its favorable characteristics. Therefore, in section 3.4, the stability of the optimized array configurations will be examined. Finally, in section 3.5, choices are made</p>
Comparison	<p>based on directivity, stability and dynamic range.</p>

### 3.2 Endfire Solution with the Hansen-Woodyard Condition

For a normal endfire array with the microphones equidistant on the z-axis, a correction of the propagation time for each microphone  $m$  is carried out according to equation (2.46):

$$\tau_m = \frac{-\alpha_m}{\omega} = \frac{m\Delta z}{c}, \quad m = 0, 1, 2, \dots, \quad (3.1)$$

where the frequency independent delay time  $\tau_m$  is taken relative to the first microphone ( $m=0$ ) and  $\alpha_m$  represents the frequency dependent phase correction,  $\Delta z$  the intermediate distance and  $c$  the sound velocity in the medium. Hansen and Woodyard (1938) suggested that an increase in directivity can be achieved by changing the frequency dependent phase correction according to

$$\alpha_m = -m \left[ \frac{\omega}{c} \Delta z + \delta \right], \quad \delta > 0 \quad (3.2)$$

They also concluded that for an array with a large number of microphones  $2M+1$  and length  $L = 2M\Delta z$  the directivity factor will reach its maximum

$$Q_{\max} = 7.28 \frac{L}{\lambda} \quad (3.3a)$$

when

$$\delta_{\max} = \frac{2.94 \Delta z}{L} = \frac{2.94}{2M} \quad (3.3b)$$

Hansen-Woodyard  
condition

Equation 3.3b has since been known as the *Hansen-Woodyard condition* for maximizing the directivity of endfire arrays. This condition was derived originally for arrays with length  $L > \lambda$  and a relatively small  $\Delta z$  giving a large number of elements. If we substitute equation (3.2) into (3.1) we obtain:

$$\tau_m = \frac{m \left( \frac{\omega}{c} \Delta z + \delta \right)}{\omega} = m \frac{\Delta z}{c} (1 + \varepsilon) \quad (3.4a)$$

with

$$\varepsilon = \frac{c}{\omega \Delta z} \delta \stackrel{\delta=\delta_{\max}}{=} \frac{2.94}{2\pi} \frac{\lambda}{L} \quad (3.4b)$$

The multiplication factor  $(1 + \varepsilon)$  now represents the correction of the time lag and depends on the relation between the wavelength  $\lambda$  and array length  $L$  only. When  $\varepsilon = 0$  we have the normal time lag correction.

Application

For our application we can also use the Hansen Woodyard suggestion. Table 3.1 gives the values of  $\varepsilon$  according to equation (3.3b) for an array with

length  $L = 10$  cm. Figure 3.1 gives the directivity patterns as a function of  $k_z$  for an endfire array of omnidirectional and cardioid microphones with a length of  $L = 10$  cm. The computation is done for  $f = 4000$  Hz and an array with 5 microphones ( $\Delta z = 2.5$  cm). The value of  $\epsilon = 0$  gives a normal time lag correction and  $\epsilon = 0.4$  follows the Hansen-Woodyard condition.

Ordinary and  
improved array

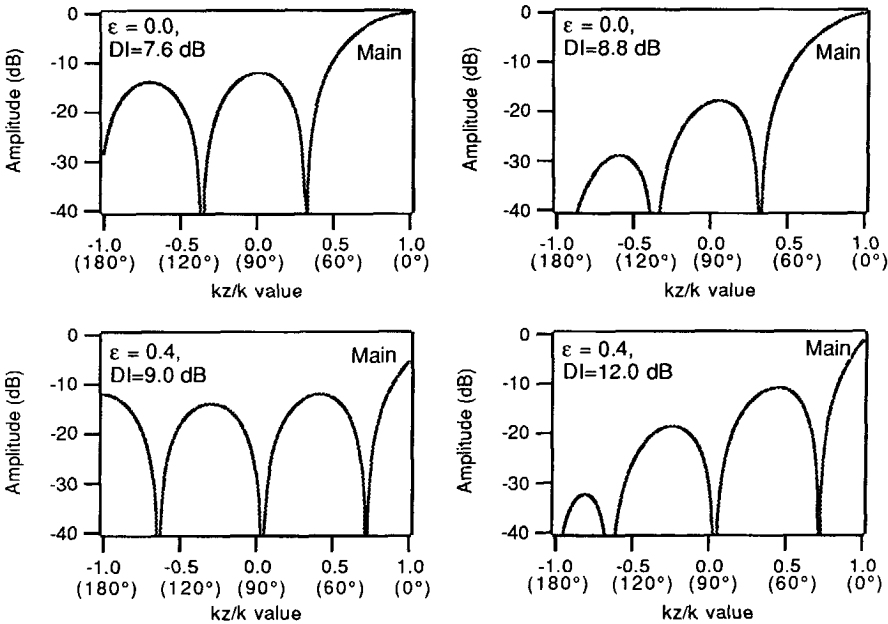
Using the Hansen-Woodyard condition the directivity can be improved significantly with 1.4 dB and 3.2 dB for the arrays with omnidirectional and cardioid microphones respectively.

Table 3.1 Maximum values according to the Hansen-Woodyard condition for an array with length  $L = 10$  cm.

	500 Hz	1000 Hz	2000 Hz	4000 Hz
$\epsilon$	3.2	1.6	0.8	0.4
$1+\epsilon$	4.2	2.6	1.8	1.4
$L$	$0.15\lambda$	$0.29\lambda$	$0.59\lambda$	$1.18\lambda$

3.1

3.1



a. Omnidirectional microphones

b. Cardioid microphones

Figure 3.1 The directivity patterns as function of  $k_z$  of an endfire array with length  $L = 10$  cm and values of  $\epsilon$ : a. Omnidirectional microphones b. Cardioid microphones.

Therefore, the arrays are usually referred to as *ordinary* endfire array ( $\epsilon = 0$ ) and *improved* endfire array ( $\epsilon = \epsilon_{\max}$ ). The improved directivity pattern has a narrower main lobe which is obtained at the expense of having an extra lobe in the back direction. The relative output level in the front direction is also lower.

Optimum

The time lag correction in the preceding example has been done according to the Hansen-Woodyard condition. Although an improvement has been reached it is important to verify the validity of this condition by computation of the directivity index for more values of  $\epsilon$ . Figure 3.2 gives the results of the computation of the Directivity Index for an endfire array of omnidirectional and cardioid microphones with a length of  $L = 10$  cm. The computation is done for  $f = 4000$  Hz and an array with 3, 4 and 5 microphones ( $\Delta z = 5$  cm,  $\Delta z = 3.33$  cm and  $\Delta z = 2.5$  cm respectively). The value of  $\epsilon$  ranges from  $-1$  until  $2$ , so the time lag  $\tau_m$  has been multiplied with a factor ranging from 0 to 3.

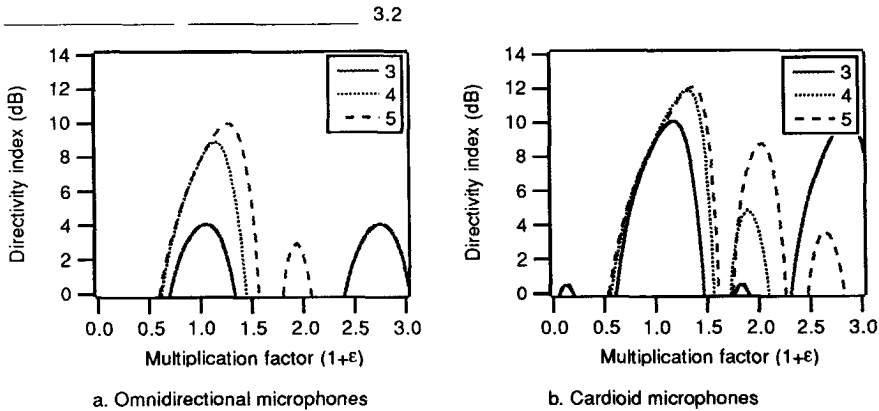


Figure 3.2 The directivity index of an endfire array with length  $L = 10$  cm and 3 , 4 and 5 microphones: a. Omnidirectional microphones b. Cardioid microphones.

Table 3.2 Values of the directivity index at  $f = 4000$  Hz, for  $\epsilon = 0$  and  $\epsilon = \epsilon_{\max}$  for an endfire array with length  $L = 10$  cm and 3, 4 and 5 microphones.

Number of microphones	Omnidirectional		Cardioid	
	Improved $1+\epsilon$	DI (dB)	Improved $1+\epsilon$	DI (dB)
3	1.05	4.1	1.15	10.1
4	1.15	8.9	1.35	11.8
5	1.30	9.9	1.40	12.0

3.2

The values of the directivity index for  $\epsilon = 0$  and  $\epsilon = \epsilon_{\max}$  are given in table 3.2. Figure 3.2 shows that the maximum value of the directivity index for an array with 3 or 4 microphones is reached for a lower value of  $\epsilon$  than the value according to Hansen-Woodyard. The maximum value for an improved array with 5 microphones is  $1+\epsilon=1.3$  and  $1+\epsilon=1.4$  for omnidirectional and cardioid microphones respectively.

Although we have an array with  $L \sim \lambda$  the values of  $\epsilon$  for 5 microphones correspond well with the value of the Hansen-Woodyard condition given in table 3.1. Because the computed values of  $\epsilon$  correspond with the value of  $\epsilon$  given in table 3.1, we can expect that the use of 6 or more microphones will not give any significant improvement.

Next, figure 3.3 gives the computed directivity index for the frequencies 500, 1000, 2000 and 4000 Hz with the same array length but now for 5 microphones only. The maximum value of the directivity index depends on frequency and multiplication factor  $1+\epsilon$ . Table 3.3 gives the values of the directivity index for omnidirectional and cardioid microphones. The values are given for the optimum value of  $1+\epsilon$  for each frequency and for one fixed value of  $\epsilon$  being the optimum value at  $f = 4000$  Hz.

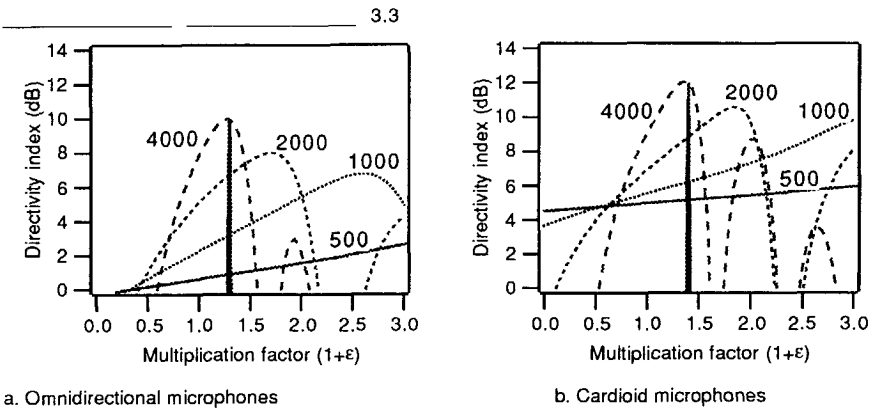


Figure 3.3 The directivity index for  $f = 500, 1000, 2000$  and  $4000$  Hz as a function of the multiplication factor  $1+\epsilon$  of an endfire array ( $L = 10$  cm) and 5 microphones.

Table 3.3 The directivity index for  $f=500, 1000, 2000$  and  $4000$  Hz of an improved endfire array with length  $L = 10$  cm and 5 microphones.

Frequency (Hz)	Omnidirectional				Cardioid			
	Improved $1+\epsilon$	DI (dB)	Improved (fixed) $1+\epsilon$	DI (dB)	Improved $1+\epsilon$	DI (dB)	Improved (fixed) $1+\epsilon$	DI (dB)
500	5.20	6.5	1.30	0.9	5.70	9.4	1.40	5.1
1000	2.60	6.7	1.30	3.1	3.05	9.8	1.40	6.1
2000	1.70	7.9	1.30	6.6	1.85	10.5	1.40	8.7
4000	1.30	9.9	1.30	9.9	1.40	12.0	1.40	12.0

The Hansen-Woodyard suggestion gives the opportunity to reach a high directivity for one specific frequency and one choice of  $\epsilon$ . However, in practice, we can only apply one fixed delay time for all frequencies. Therefore, we must choose one value of  $\epsilon$ . For our application this means that we will choose  $\epsilon$  less than the maximum value at  $f = 4000$  Hz. If we would take  $\epsilon > 0.4$  the directivity will decrease significantly for the higher frequencies. The values of the directivity index given in the last column of table 3.3 show that an improved endfire array of cardioid microphones with one optimum value of  $\epsilon (=0.4)$  will have a directivity ranging from 5.1 dB to 12.0 dB.

### 3.3 Numerical Approach to Optimization

In the preceding sections 2.4 and 3.2 the amplitude weighting and the time lag correction of the microphone signals were done according to well-known principles in areas of signal theory and specific solutions by several authors. Several authors have also tried to give a theoretical, mathematical proof of the maximum directivity which can be obtained for one specific monochromatic situation. Examples of this mathematical approach are Hansen and Woodyard (1938) (see section 3.2), Ma (1973) with several proofs for (in-)equidistant arrays, Weston (1986) with a Jacobi sensor arrangement and Parsons (1987) with a maximum directivity proof for three-dimensional arrays.

Numerical approach Although it would be possible to adapt some of these mathematical approaches for our situation we decided to optimize our arrays numerically. As a criterium for the optimization we have chosen the directivity index. The directivity index of an array will depend on the array parameters : number of microphones( $N,M$ ), intermediate distance( $\Delta x, \Delta z$ ), time lag correction( $\tau_{n,m}$ ), amplitude weighting ( $A_{n,m}$ ) and the directivity pattern of the individual microphones ( $D$ ) (see section 2.4, eq. 2.45).

#### OPTIMIZATION ALGORITHM

For our optimization problem a comprehensive quasi-Newton algorithm was used (Gill, 1981). The algorithm searches for an unconstrained maximum of a function vector  $F$  of parameters (represented by parameter vector  $\mathbf{x}$ ), where no mathematical derivatives of the function are required. The variables can be subjected to fixed lower and/or upper bounds. Figure 3.4 gives a schematic structure of the algorithm.



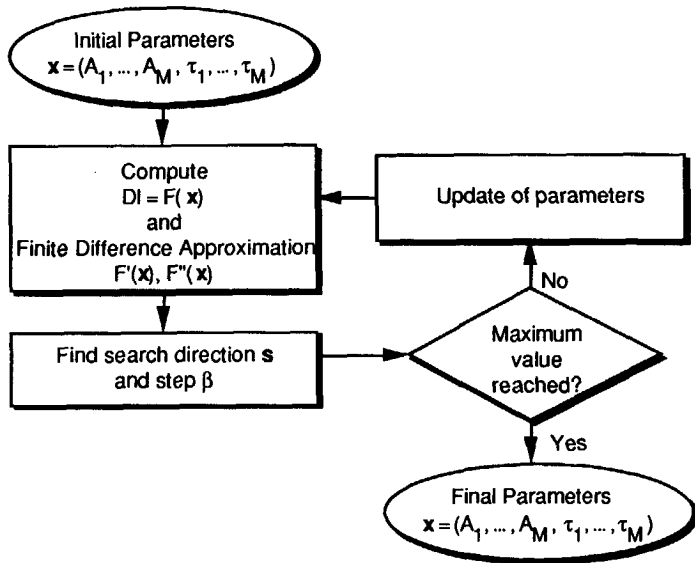


Figure 3.4 Schematic structure of the quasi-Newton algorithm for optimization. The derivatives are computed by finite difference approximation.

A typical iteration starts with the computation of finite difference approximations of the vectors  $F'(\mathbf{x})$  and  $F''(\mathbf{x})$  with the use of the initial values of parameter vector  $\mathbf{x}$  and the definition of function  $F(\mathbf{x})$ . Then the derivatives are used to find a search direction vector  $\mathbf{s}$  and search step  $\beta$  is found such that  $F(\mathbf{x} + \beta\mathbf{s})$  is maximum, etc. If the convergence criteria are not achieved parameter vector  $\mathbf{x}$  is replaced by the vector  $\mathbf{x} + \beta\mathbf{s}$ . The optimization stops when the maximum value is reached.

#### Implementation

The implementation of the optimization program is done using the above mentioned algorithm. The program needs the function for the directivity index and an initial configuration of the microphone array consisting of the coordinates  $(x_m, z_m)$ , the amplitude weighting  $(A_m)$  and the time lag correction  $(\tau_m)$  of the individual microphones. The optimization process is done with respect to the amplitude weighting and the time lag correction of each microphone.

#### OPTIMIZATION OF ENDFIRE ARRAYS

At the start of the optimization we decided to focus on an endfire array with a high directivity for frequencies ranging from 500 Hz to 4000 Hz. Therefore, in this section the results will be presented of the optimization of an endfire array consisting of cardioid microphones only.

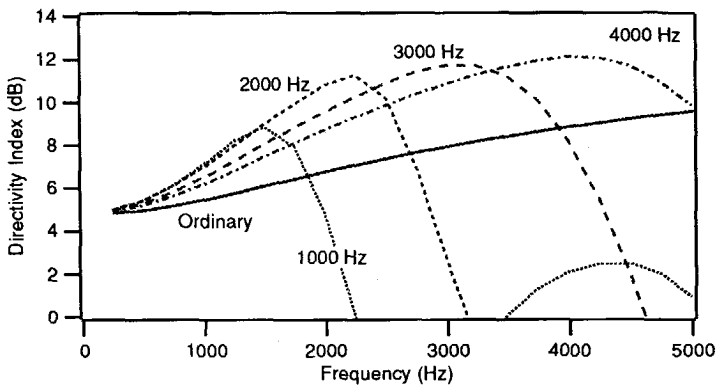


Figure 3.5 The directivity index as a function of the frequency for an ordinary (continuous line) and optimized endfire array of 4 cardioid microphones. Parameters are optimized for one frequency:  $f = 1000, 2000, 3000$  and  $4000$  Hz.

The use of cardioid microphones is necessary for a sufficient directivity at the lower frequencies.

#### Two-step approach

The optimization of the time lag variables was considered to be of major importance for a high directivity in comparison with the amplitude weighting variables. Therefore, the optimization of endfire arrays has been done in two steps giving a reduction of parameters to be optimized and reduction of the computation time. The first step is the optimization of the time lag variables only. The amplitude variables are fixed. The second step has been done by optimization of all parameters, i.e. the time lag and amplitude variables, using as initial time lag values the output of the first step.

#### Monochromatic optimization

Figure 3.5 gives the Directivity Index as a result of four optimization processes. The optimization processes were done at four different frequencies: 1000, 2000, 3000 and 4000 Hz for an endfire array with a length of 10 cm consisting of 4 cardioid microphones. So, the optimization program searched for the best amplitude weighting and time lags for that frequency. As initial parameter values an endfire configuration was taken with a uniform amplitude weighting and time lags following the optimum of the Hansen Woodyard condition as given in table 3.2. The boundary conditions of the parameters were set to:  $0 < A_m < 2$  and  $0 < \tau_m < (2m\Delta z/c)$   $\mu s$  (time lag correction microphone  $m$  relative to outer microphone at  $-M\Delta z$ ). The choice of these boundaries is based on the demand that a stable solution with a high output level is wanted. The optimum of a Jacobi array with negative amplitude weighting will be part of the stability investigation in the next section. Regarding figure 3.5, we can see that the optimization-program did its job well in adjusting the array parameters.

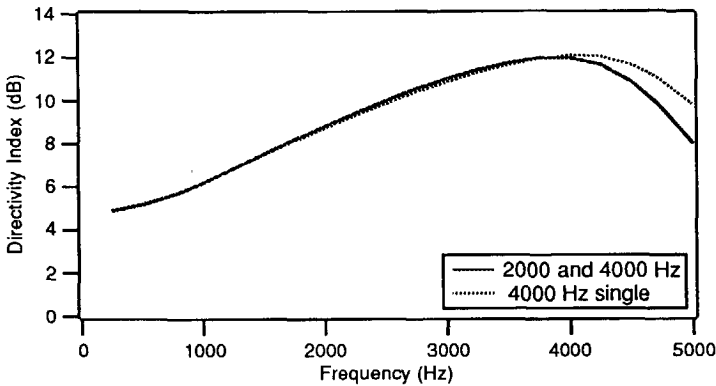


Figure 3.6 The directivity index as a function of the frequency for an optimized endfire array of 4 cardioid microphones. Optimization at  $f=2000$  and  $4000$  Hz and single optimization at  $f=4000$  Hz.

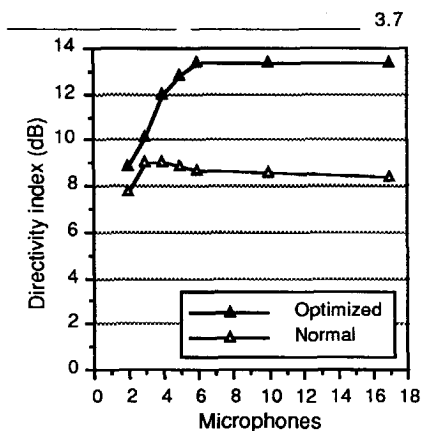
#### Two frequencies

However, in developing an array with fixed parameters for all frequencies we have to choose one optimum parameter set for all frequencies. Therefore, the optimization process was repeated for optimization of the mean directivity at two frequencies  $f=2000$  Hz and  $f=4000$  Hz. Figure 3.6 gives the directivity index as a result of the optimization process for both frequencies and optimization at one single frequency  $f=4000$  Hz.

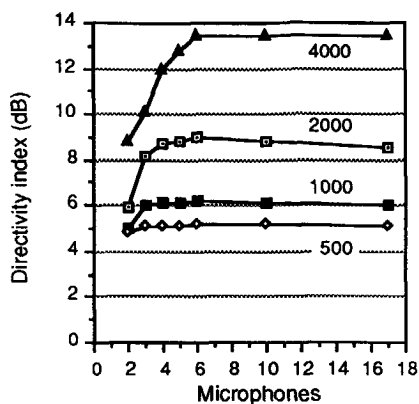
We may conclude that optimization of the parameter set at  $f=4000$  Hz will be sufficient for a high directivity index for all frequencies. Based on the results of figures 3.5 and 3.6 the optimum parameter set of the next examples is computed for a frequency of  $f=4000$  Hz expecting a high directivity index for all other frequencies too.

#### Number of microphones

The next optimization step was done for an endfire array with a *fixed* overall length of 10 cm. The optimization process was repeated for a changing number of microphones ranging from 2 to 17. The input-parameter set was taken in the same way as the previous one with the same boundary conditions. Figure 3.7 gives the directivity index as a result of the optimization for 2,3,4,5,6,10 and 17 microphones respectively. The directivity index at 4 kHz has improved by 4 dB when 5 or more microphones are used (figure 3.7a). Using 6 or more microphones gives no further improvement. The optimization process gives a mean improvement of 1 dB in comparison with the maximum values of the Hansen-Woodyard suggestion. Figure 3.7b gives the resulting directivity index of the endfire array at four different frequencies. A minimum directivity of 5 dB is obtained for the lower frequencies.



a. Optimized and ordinary endfire  $f=4000\text{Hz}$ .



b. Optimized endfire all frequencies

Figure 3.7 The directivity index of an ordinary uniform and optimized endfire array as a function of the number of microphones within a fixed length of 10 cm.

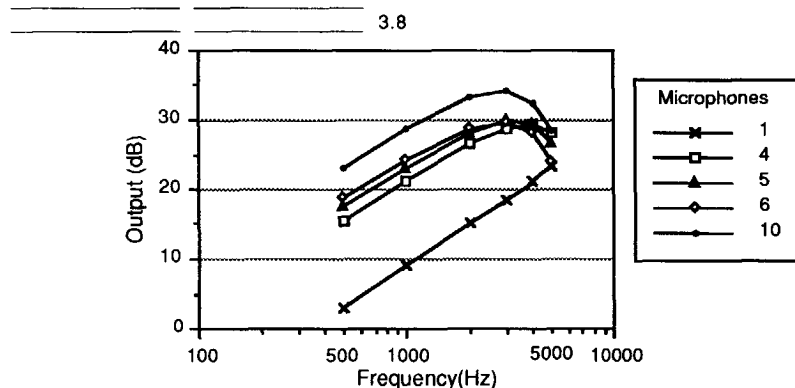


Figure 3.8 Output of one single cardioid microphone and optimized endfire arrays for the main direction  $0^\circ$ .

Spectrum

Finally, figure 3.8 gives the computed output of one single cardioid microphone and the output of the optimized endfire arrays for the main direction at  $0^\circ$ . We can see that the shape of the spectrum of the optimized arrays is nearly the same as the spectrum of one cardioid microphone. The output level is higher than the output of one single microphone thus providing a high dynamic range with less influence of internal electronic noise.

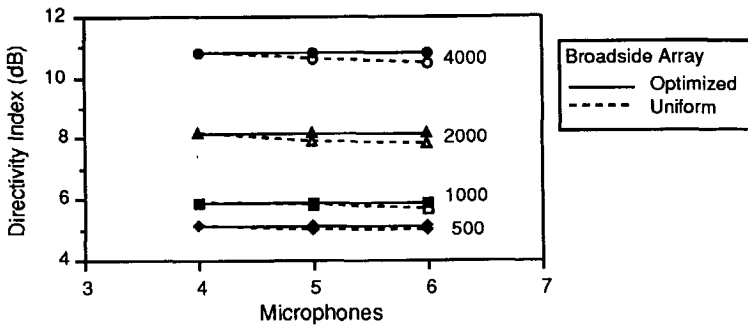


Figure 3.9 Directivity Index of Broadside arrays before and after optimization.

#### OPTIMIZATION OF BROADSIDE ARRAYS

The optimization of a broadside array can be done with respect to the position of the microphones and the amplitude-weighting. However, Ma (1973) showed that the directivity of an array with variable microphone spacing will, at its optimum, only be a little bit higher than an array with equidistant microphone spacing. Therefore, we will only optimize the amplitude-weighting of an equidistant broadside array.

The optimization has been done for a broadside array with a fixed length of 14 cm consisting of 4, 5 and 6 microphones. The optimization process started with a uniform amplitude-weighting and was done for a frequency of 4000 Hz. Figure 3.9 presents the directivity of the optimum amplitude-weighting for the frequencies 500, 1000, 2000 and 4000 Hz. We can conclude that the profit of the optimization is very small and also that the directivity is mainly determined by the length of the array in relation to the wave length.

#### Spectrum

The spectrum of the optimized broadside array is hardly influenced by the optimization and is equal to the spectrum of one single cardioid microphone. The output signal is equal to the sum of the microphone signals and will therefore be higher than the output of one single microphone.

### 3.4 Stability

An array configuration with a high directivity may not always be a stable solution. The high value of the directivity index may be reached for a special theoretical parameter choice that can be created in a laboratory situation but cannot be maintained in a practical situation. Therefore, in a practical situation it is important to choose a stable array solution with a sufficient directivity which is hardly influenced by variations between the microphones (amplitude and phase characteristics), amplitude weighting (amplifiers and resistor values) and/or time lag correction.

#### Parameters

In this section we will study the stability of the optimized endfire and broadside arrays (section 3.3) and the Jacobi arrays (section 2.4). We will mainly investigate the dependence of the directivity on the variation of two parameters: *time lag correction* and *amplitude weighting*. Other array parameters like intermediate distance, phase and amplitude characteristics of the individual microphones are directly related to time lag correction and amplitude weighting.

#### OPTIMIZED ENDFIRE ARRAYS

#### Error-space

In the preceding section we have optimized endfire arrays with a fixed length (10 cm) and changing number of microphones. A sufficiently high directivity was reached with at least 4 microphones. The directivity depends on the variations in the time lag correction (electronic delay time) and amplitude weighting of each microphone. This results in a complex multi-dimensional 'error-space'. To gain insight in this multi-dimensional space we will limit ourselves to cross-sections to be obtained by variation of two parameters.

#### Contour diagram

Figure 3.10 gives the contour diagrams and sections at the optimum parameter choice for the optimized array of 4 cardioid microphones with  $L = 10$  cm. The contour diagrams show the change in the value of the directivity index as function of the amplitude weighting and delay time of one microphone. The delay time is given relative to the first microphone and the other parameters are kept constant. The asterisks denote the optimum parameter choice computed by the optimization program. The maximum value of the directivity index at 4000 Hz lies in a stable area.

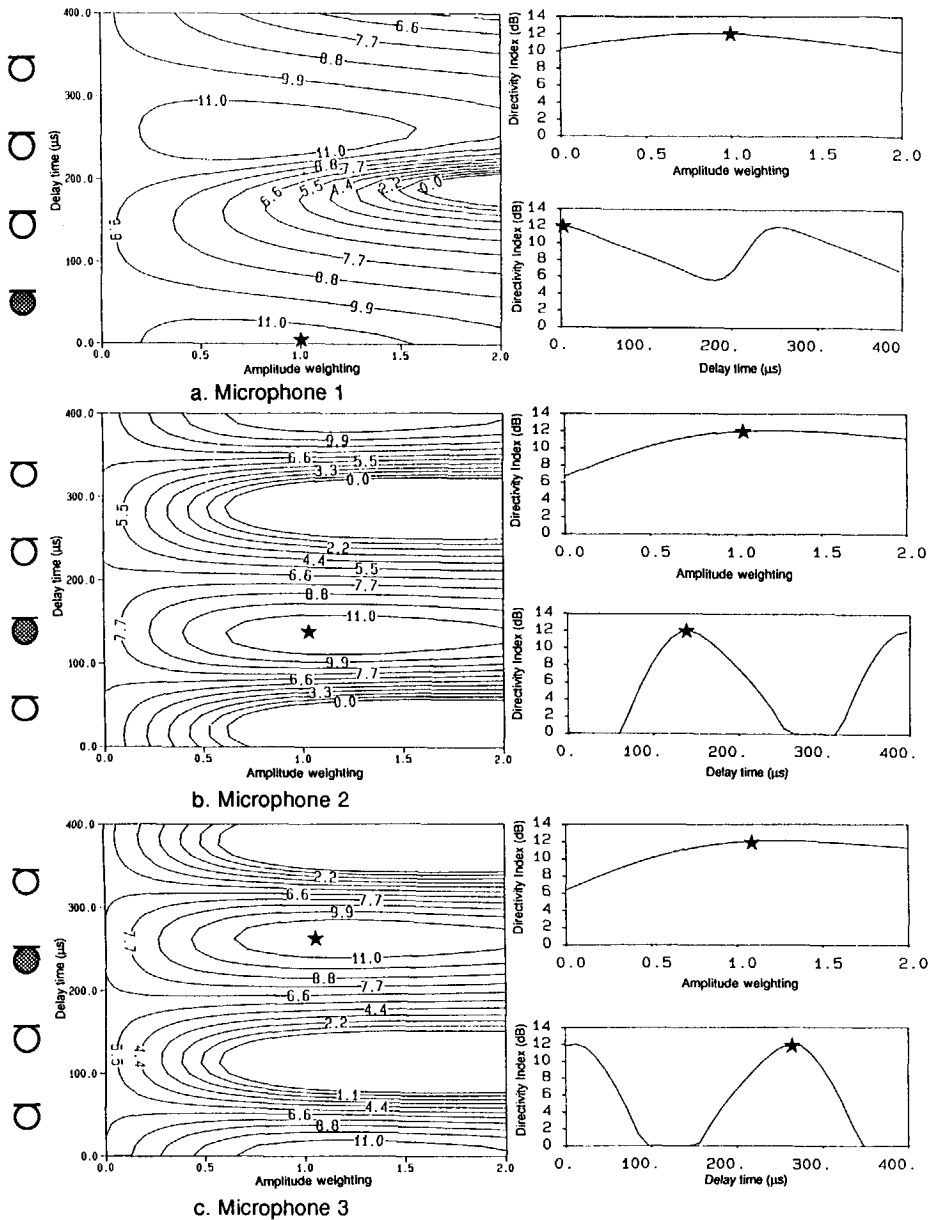


Figure 3.10 Contour diagrams and cross sections of the value of the Directivity Index of an endfire array of 4 cardioid microphones at a frequency of 4000 Hz as a function of the setting of one microphone. The asterisks denote the desired microphone setting for an optimum Directivity Index at 4000 Hz. Variation of delay-time and weighting of microphone 1 (a), microphone 2 (b) and microphone 3(c). Contour diagram of microphone 4 is given in figure 3.11a.

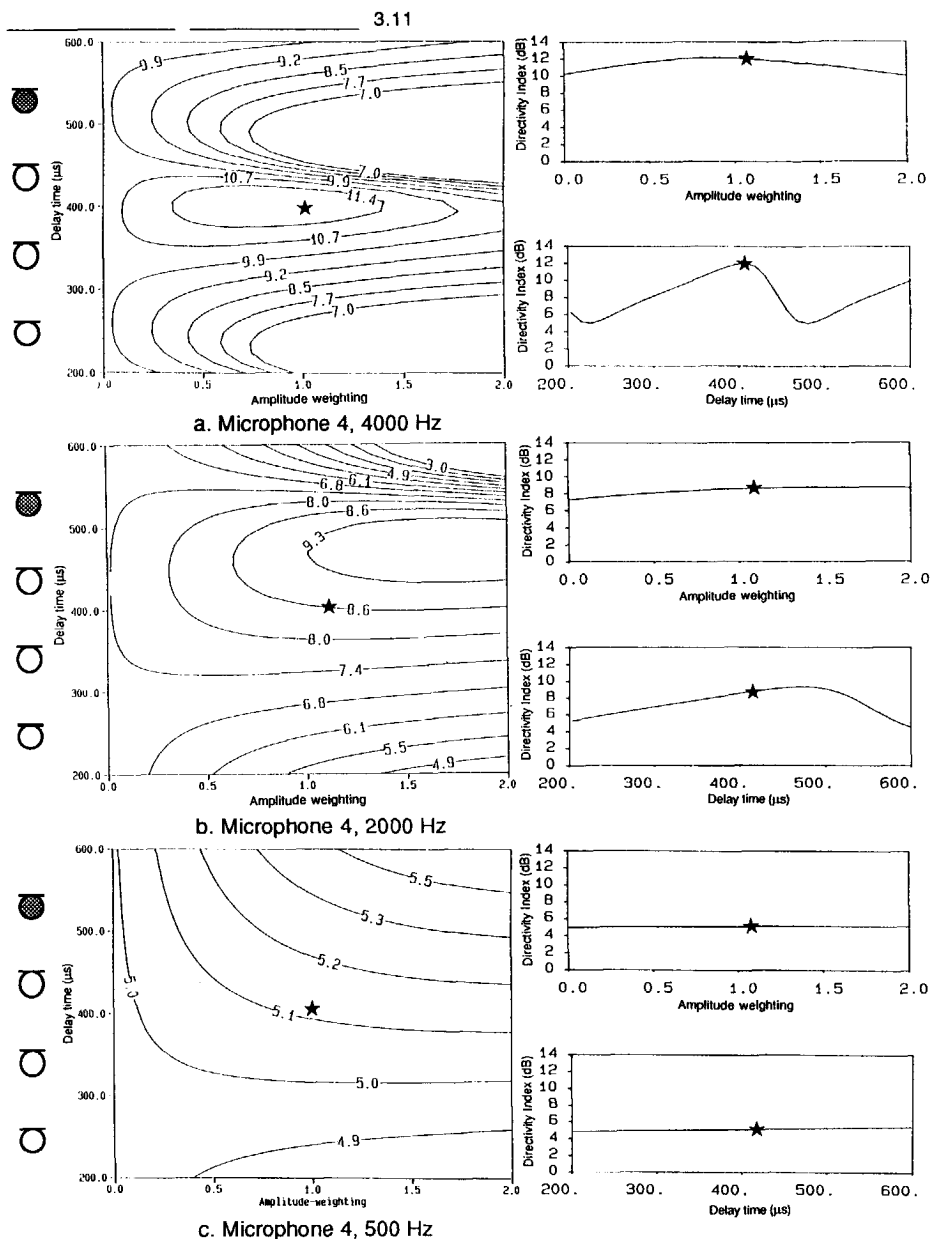


Figure 3.11 Contour diagrams and cross sections of the value of the Directivity Index of an endfire array of 4 cardioid microphones as a function of the variation in the setting of the fourth microphone. The asterisks denote the desired microphone setting for an optimum Directivity Index at 4000 Hz. Variation of delay-time and weighting at 4000 Hz (a), 2000 Hz (b) and 500 Hz (c).



Next, figure 3.11 gives the contour diagrams of the endfire array at four different frequencies when the delay time and amplitude weighting on the fourth microphone are changed. The fixed parameter choice of the optimization program results in a stable directivity for the lower frequencies with widely spread contour lines.

Stable solution

We may conclude that the influence of variation in amplitude weighting and delay times on the value of the directivity index of an optimized endfire array with 4 microphones is small. In addition, we may expect that this is even better for the optimized endfire arrays with more microphones. Therefore, we may conclude that optimized endfire arrays with 4 or more microphones offer a stable solution in practical situations.

### OPTIMIZED BROADSIDE ARRAYS

Weighting

The directivity of a broadside array can only be influenced by variations in microphone positions, amplitude weighting and variations between the used microphones. In the preceding section we have already mentioned that the influence of a variation in the position of the microphones on an optimum directivity is very small. Further, the influence of variations in the amplitude weighting appears to be very small as well. The difference of 0.2 dB between the directivity index of the uniform broadside array and the optimized array was reached by a variation in the amplitude weighting of

Microphones

more than 50%. Variations between the used microphones can occur with respect to sensitivity and phase characteristics. It is clear that sensitivity variations will not give problems (see influence of amplitude weighting). Figure 3.12 gives the directivity index as a function of the phase error of the central microphone of the broadside microphone for different frequencies.

3.12

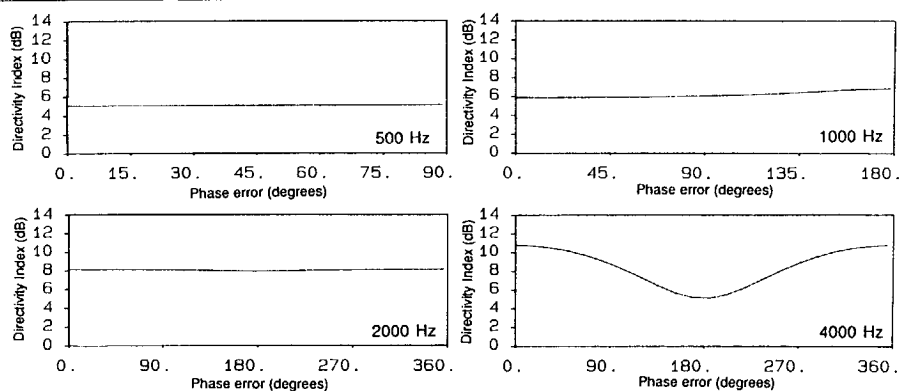


Figure 3.12 Influence of a phase error of the central microphone of a broadside array ( $L = 14$  cm) at 500 Hz, 1000 Hz, 2000 Hz and 4000 Hz.

Stable solution      The diagrams show that a large phase error can reduce the directivity for frequencies above 2000 Hz, but not below 6 dB. We may conclude that a broadside array is very stable with respect to variations in the individual microphones.

#### JACOBI ARRAYS

$L < \lambda$       In section 2.4 it was concluded that with a Jacobi array a high directivity can be obtained for all frequencies and array length  $L < \lambda$ ! The high directivity is obtained with the characteristic solution of a Dolph-Chebyshev weighting with *alternating* sign. The sum of the weights equals zero.

2 Microphones      Figure 3.13 shows the contour diagrams and sections of a Jacobi array of 2 microphones at a frequency of 4000 Hz. Cardioid microphones are used to obtain the highest possible directivity. The diagrams are computed for three intermediate distances  $\Delta z = 2.5, 1.0$  and  $0.5$  cm. The amplitude weighting and delay time are taken relative to the other microphone. The parameter set giving maximum directivity can easily be obtained from the contour diagram. For  $\Delta z = 2.5$  cm, the directivity index reaches a maximum of 8.7 dB in a stable area. However, the reduction of the intermediate distance decreases the area where this maximum is reached. For an intermediate distance  $\Delta z = 0.5$  cm a small variation in amplitude weighting or delay time will give a low directivity index. At this moment we may conclude that the intermediate distance between the microphones should not be too small to get a stable directivity at 4000 Hz.

Low frequencies      Figure 3.14 gives the contour diagram of the same Jacobi array with  $\Delta z = 2.5$  cm at  $f = 500$  Hz. Although a high directivity can be obtained, the Jacobi array appears to be very sensitive to parameter variations. The value of the directivity index will decrease dramatically due to an incorrect delay time or a small variation in the amplitude weighting.

More microphones      Furthermore, we may expect that a Jacobi array with more elements will be even more unstable. Figure 3.16 shows the computed polar diagrams of a Jacobi array with 3 microphones for a correct amplitude weighting and a variation of only 1.5% in the amplitude weighting of the central microphone! The directivity, particularly for the low frequencies, appears to be very unstable when more microphones are used. In practice, a usable Jacobi array of 3 or more elements can hardly be built.

Careful design      Summarizing, we may expect that in practice a Jacobi array of 2 cardioid microphones will only have a sufficient and stable directivity for high frequencies. The small stability area for the low frequencies asks for a matched pair of microphones and well adjusted signal processing. This is not a practical proposition.

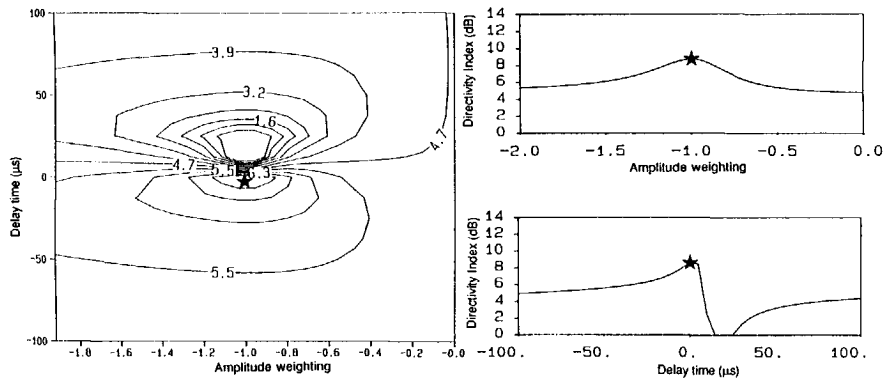
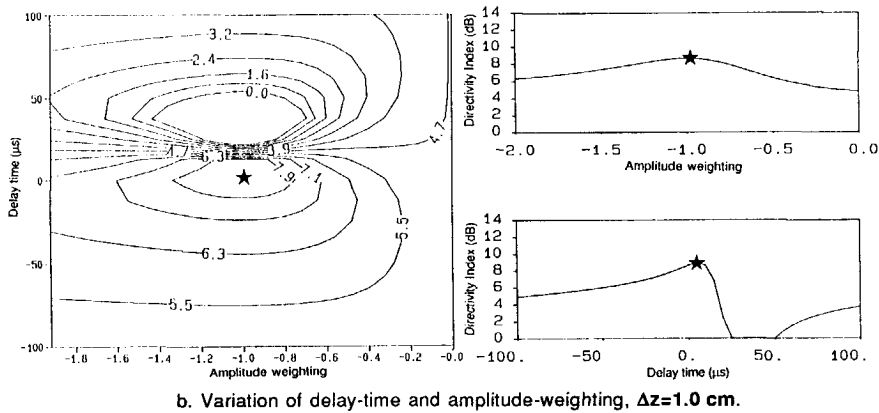
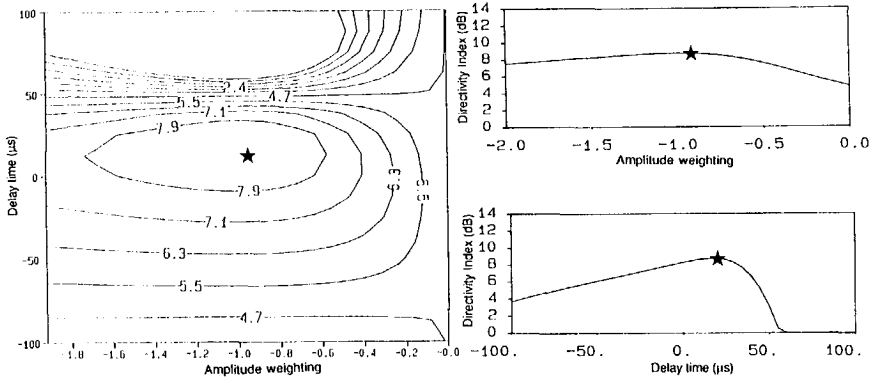
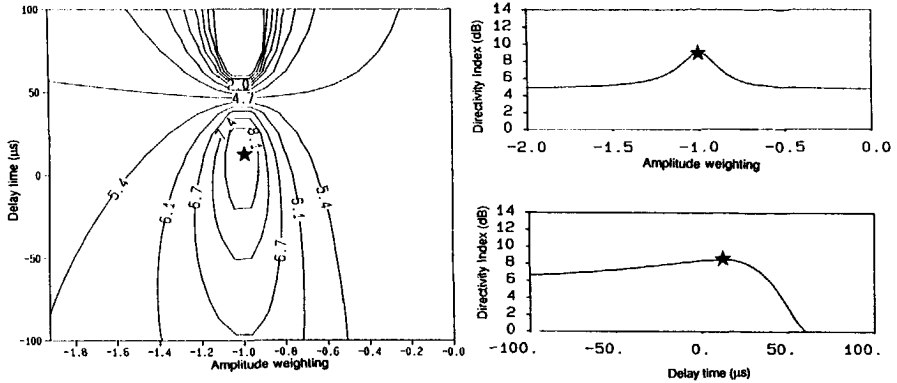


Figure 3.13 Contour diagrams of the value of the directivity index of a Jacobi array of 2 cardioid microphones at a frequency of 4000 Hz as a function of the variation in the setting of one microphone.



## DIRECTIVITY

### Directivity Index

A comparison of the directivity, which can be achieved by the different optimized array configurations, is given in the bar diagram of figure 3.16. This diagram shows the directivity index at different frequencies for one simple cardioid microphone, a Jacobi array of 2 cardioid microphones ( $L=2.5$  cm, delay time  $\tau_m = 0$ ), an optimized endfire array ( $L=10$  cm, 5 cardioids) and an optimized broadside array ( $L=14$  cm, 5 cardioids). The computed directivity indices show an important difference between the Jacobi array and the endfire and broadside array: the value of the directivity index of the Jacobi array reaches a maximum of 8 dB for all frequencies. In contrast, the value of the directivity index of the endfire and broadside array rises with the frequency from 5.1 dB at 500 Hz to 12.8 dB (endfire) and 10.8 dB (broadside) at 4000 Hz. On the one hand the directivity of the Jacobi array will give a better suppression of low frequency background noise while on the other hand the directivity of the endfire and broadside array has the advantage of better suppression of high frequency noise.

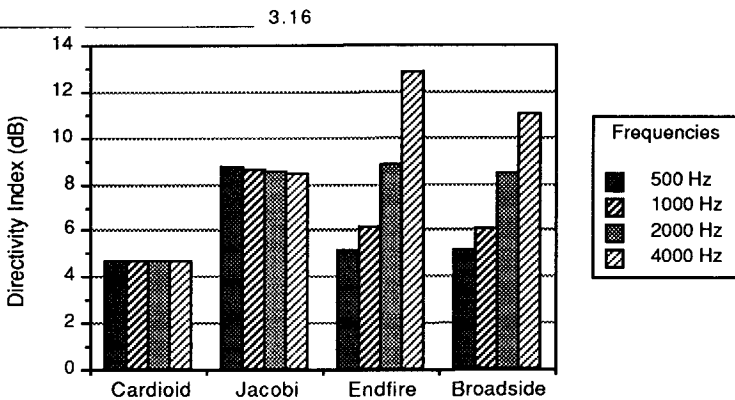


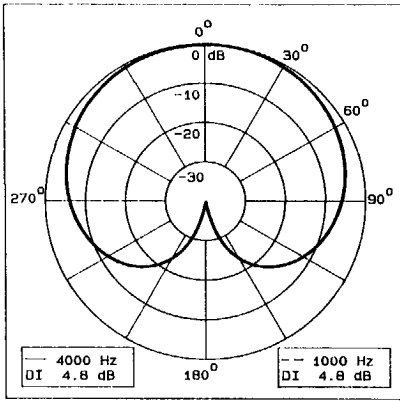
Figure 3.16 The Directivity Index of one cardioid microphone and three different array types: Jacobi array ( $L=2.5$  cm), optimized endfire array ( $L=10$  cm) and an optimized broadside array ( $L=14$  cm).

### Directivity Pattern

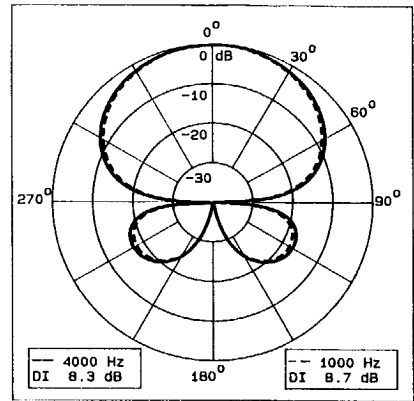
In the preceding part of this chapter the optimization of the directivity index has been done without any restrictions on the resulting beam width or side lobe levels of the directivity pattern. Therefore, it is now important to compare the directivity patterns of the optimized configurations. Figure 3.17 gives the polar diagrams of the directivity pattern of one cardioid microphone and the Jacobi array at 4000 and 1000 Hz. The main beam of the Jacobi array is broad with a very low relative side lobe level of  $-25$  dB. Figures 3.18 and 3.19 give the three dimensional representation of the directivity pattern at 4000 Hz.

### Cardioid

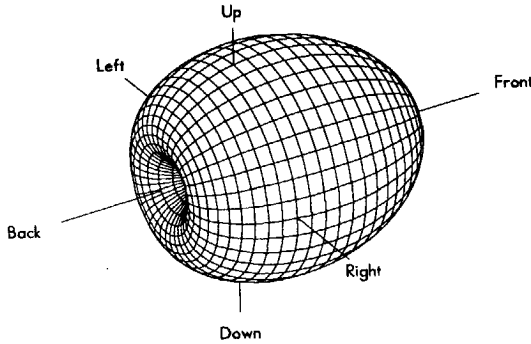
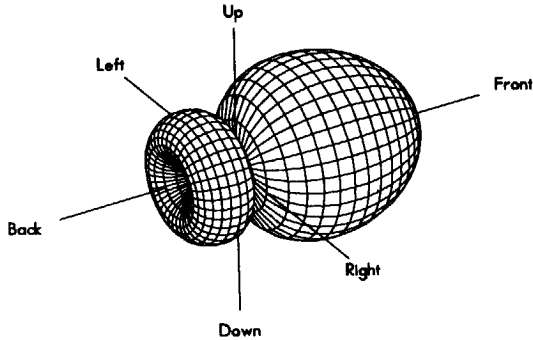
### Jacobi

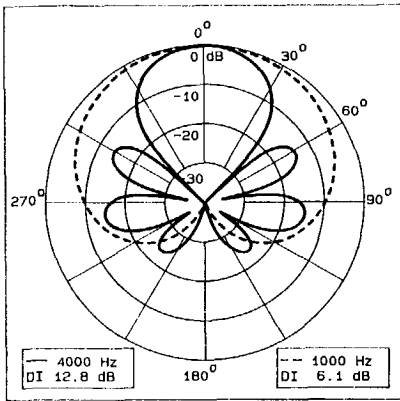
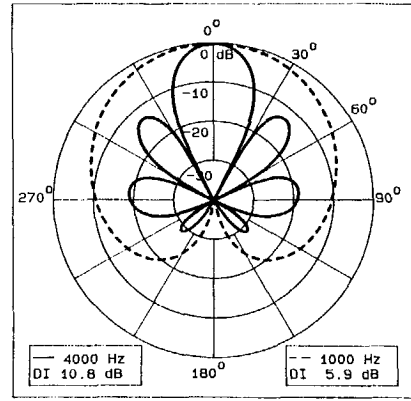


a. Cardioid microphone



b. Jacobi array

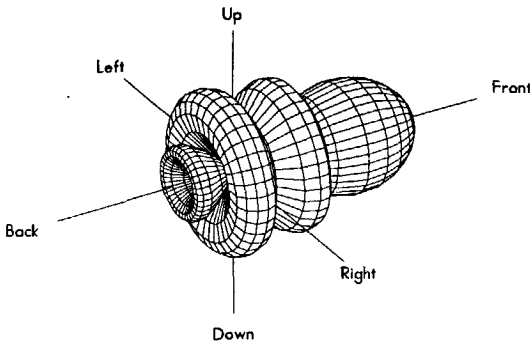
Figure 3.17 Polar diagram of *cardioid microphone* and a perfect *Jacobi array* ( $L=2.5$  cm).Figure 3.18 Directivity pattern of *cardioid microphone*,  $f=4000$  Hz,  $DI=4.8$  dB.Figure 3.19 Directivity pattern of perfect *Jacobi array*,  $L=2.5$  cm,  $f=4000$  Hz,  $DI=8.3$  dB.

a. Endfire array ( $L = 10$  cm)b. Broadside array ( $L = 14$  cm)Figure 3.20 Polar diagram of *optimized endfire and broadside array*.

---



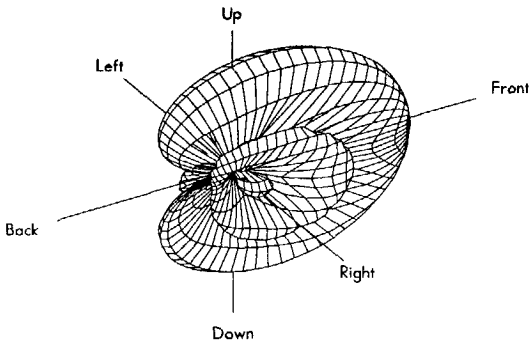
---

3.21
Figure 3.21 Directivity pattern of *optimized endfire array*,  $L = 10$  cm,  $f = 4000$  Hz,  $DI = 12.8$  dB.

---



---

3.22
Figure 3.22 Directivity pattern of *broadside array*,  $L = 14$  cm,  $f = 4000$  Hz,  $DI = 10.8$  dB.

On behalf of a clearer presentation we have rotated the diagrams and renamed the axis: left-right equals x-axis, front-back equals z-axis and up-down equals y-axis. The Jacobi array has a cylinder symmetric directivity pattern around the front-back axis.

Endfire

Broadside

Next, figures 3.20-3.22 give the same diagrams for the optimized endfire and broadside array. The polar diagrams at 4000 Hz of figure 3.20 are equal to cross-sections in the horizontal plane of the three dimensional directivity patterns. The polar diagrams at 4000 Hz show that in the horizontal plane both arrays have a narrow main lobe and side lobe levels less than -13 dB. The main lobe of the broadside array is narrower than the main lobe of the endfire array. Further, the three-dimensional diagrams show an important difference between the array types. The endfire array is cylinder symmetric around the front back axis (z-axis). Using cardioid microphones, the broadside array has only one plane of symmetry given by the vertical plane. This results in a narrow main beam in a cross-section along the left-right axis. In the vertical symmetry plane the directivity pattern equals the pattern of one single (cardioid) microphone (see also section 2.4, figure 2.13). The narrower beam width of the broadside array in the horizontal plane may be advantageous in many practical situations with noise in the horizontal plane.

#### SPECTRUM AND OUTPUT LEVEL

A hearing impaired listener needs amplification with a spectrum which is carefully adapted to the hearing loss. A small variation in the overall transfer function can result in a significant change of speech intelligibility with or without noise. Therefore, it is important that the adaptation of the overall amplification and spectrum of the hearing system is not limited by the properties of the microphone. Figure 3.23 gives a block diagram of an (array) microphone with spectral shaping and amplification. The block diagram shows that we have to deal with two types of noise: *acoustic* and *electronic*.

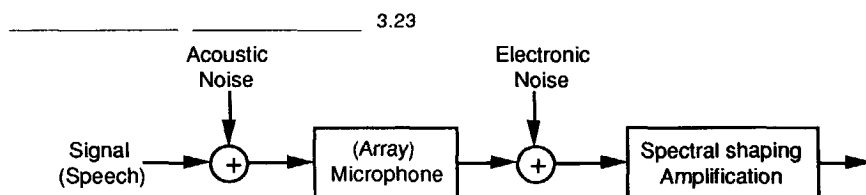


Figure 3.23 A system with an (array) microphone, spectral shaping and amplification has to deal with two types of noise: acoustic and electronic.



A directional (array) microphone is used for suppression of acoustic noise. However, the influence of electronic noise of the next subsystem is only limited when an (array) microphone has a high output level relative to the electronic noise level and a spectrum suitable for spectral shaping. A simple miniature electret cardioid microphone for a hearing instrument will have a high pass transfer function with a slope of 6 dB/octave. This might be advantageous for suppression of low frequency noise. However, if a flat spectrum (or any other shape) is wanted an extra correction filter is necessary.

Figure 3.24 gives the computed spectra in the main direction of one single cardioid microphone and the optimized array configurations with cardioid microphones.

The endfire and broadside array have a high output level resulting in a high dynamic range. The spectrum equals the spectrum of a cardioid microphone. Above 3000 Hz the spectrum of the endfire array is flattened due to optimization. The broadside array has the highest output level at the high frequencies. The spectrum of the Jacobi array is steeper than the spectrum of one cardioid microphone. The combination of the spectrum of the cardioid microphone (6 dB/octave) and the spectrum of a Jacobi array (equation 2.55) results in a slope of 12 dB/octave. This seems advantageous for suppression of acoustic low frequency noise but is especially disadvantageous when the spectrum needs to be less steep.

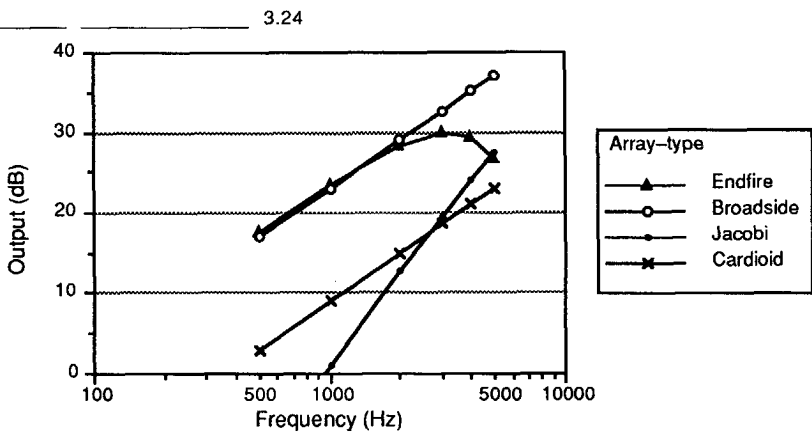


Figure 3.24 The spectrum in the main direction  $0^\circ$  of three array-types in comparison with a single cardioid microphone: optimized broadside array of 5 microphones, optimized endfire array of 5 microphones and a perfect Jacobi array of 2 microphones.

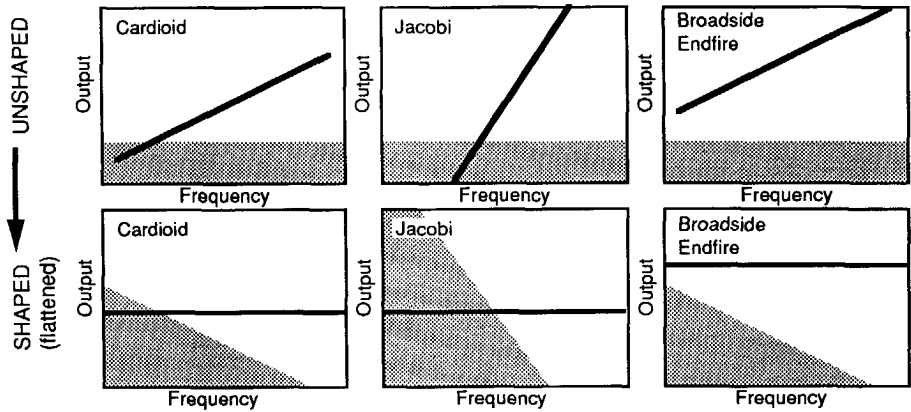


Figure 3.25 The output level of an (array) microphone in relation to internal electronic noise before and after spectrum shaping (flattening).

Figure 3.25 gives the output level of the microphones in relation to the internal electronic noise. The spectral shaping and amplification of the output of the Jacobi array will result in a limited dynamic range due to amplification of internal electronic noise, particularly at the low frequencies.

#### CHOICES

We will now compare and evaluate the three array types Jacobi, endfire and broadside with respect to: number of microphones, size, cosmetic aspects, directivity, spectrum, electrical S/N-ratio, stability and electrical circuit. For each array type table 3.4 gives the value of each parameter or aspect and a valuation of that specific aspect. This is done with a simple +/- system as a primary indication and is based on the following arguments.

Number of  
microphones

The number of microphones, necessary for a sufficient directivity without aliasing, is not only important for power consumption and the final design and size of the electronic signal processing but is also relevant from an economic point of view. The valuation is based on power consumption and the electronic circuit for signal processing. In section 1.4 it was proposed that the microphone array should be connected to, or built in, a pair of spectacles. The maximum size of the endfire and broadside array corresponds with this proposal. The size of the Jacobi array is even smaller. The size, position and design of the array microphone is important for acceptance by the user. The Jacobi array is preferable because it is small and can be placed near the ear. The endfire array can be placed at the side of the head and may be combined with the legs of a pair of spectacles.

Size

Table 3.4 Comparison of three array types: Jacobi, endfire and broadside. The +/- signs denote a valuation of the aspect.

Aspects	Jacobi		Endfire		Broadside	
N microphones	2	++	4 or 5	+	4 or 5	+
Size	2.5 cm	++	10 cm	+	14 cm	+
Cosmetics/ Position	above ear	++	along head	+	front head	-
Directivity Index						
500 Hz	8.8	+	5.1	-	5.1	-
1000 Hz	8.7	+	6.1	+	5.9	+
2000 Hz	8.6	+	8.8	+	8.2	+
4000 Hz	8.3	+	12.8	++	10.8	++
Output level	low	--	high	++	very high	++
Spectrum	12 dB/oct	-	6 dB/oct	++	6 dB/oct	++
Stability	low	--	high	+	very high	++
Electrical Circuit	subtraction	+	delays summation	-	summation	++

### 3.4

A broadside array needs to be placed in front of the head and should be built in the frame of a pair of spectacles.

#### Directivity

The directivity is considered to be the principal aspect. A directivity index of at least 5 dB is necessary for a significant improvement of the speech intelligibility in noise. As already mentioned in the first part of this section the directivity of the Jacobi array is advantageous for low frequency noise suppression. The high directivity index of the endfire and broadside array for the frequencies above 2000 Hz is very valuable for the speech intelligibility of consonants.

#### Spectrum

#### Output level

A hearing impaired listener needs an amplification with a spectrum which is carefully adapted to the hearing loss. This demand complicates the applicability of the Jacobi array because it has a steep spectrum of 12 dB/octave and low output level.

#### Stability

In section 3.4 we have concluded that the Jacobi array will have a very small stability area. It requires a matched pair of microphones and well adjusted signal processing. This is disadvantageous for an industrial series production of the microphone array and reliable operation in the user situation. On the other hand, the endfire and broadside array will have a very stable directivity for all frequencies. The signal processing of the broadside array is very simple while the endfire needs an extra electronic delay circuit.

Based on the comparison and the valuation given in table 3.4 we must conclude that a Jacobi array will be an unpractical choice. The Jacobi array has a low stability particularly for the low frequencies, an unfavorable spectrum shape and a low output level. Therefore, we choose a stable array solution with an endfire or broadside array. While cosmetic drawbacks can be overcome, the endfire and broadside array offer a stable and high directivity, a spectrum of 6 dB/octave with a high output level. The narrower beam width of the broadside array in the horizontal plane may be advantageous in practical situations with noise in the horizontal plane.

---

# ARRAY MEASUREMENTS

## Chapter 4

### 4.1 Introduction

In the preceding chapter we made the choice for an endfire or broadside microphone array because of high directivity and robustness. For a practical assessment of the microphone array we decided to develop a laboratory model of an endfire array and a broadside array. In this chapter the most important results will be presented of measurements carried out with these prototype models in an anechoic room. Because it was expected that the directivity of an array might be influenced by reflections and diffractions at the head, the measurements have been carried out with the models placed in free field conditions as well as in combination with an artificial head.

Section 4.2 gives a description of the measurement system in the anechoic room and discusses the newly developed measurement system for directivity patterns.

#### Free field

The results of the free field measurements are presented in section 4.3. First, attention is paid to the directivity pattern of one single directional (cardioid) microphone. Next, directivity measurements have been done with an endfire array model and a broadside array model. Results are

Artificial head

presented of the optimum parameter choice for a high directivity and of the influence of using incorrect parameters. Section 4.4 gives the results of the measurements with an artificial head.

Development

On the basis of the measurements with the laboratory models we decided to build portable models of an endfire array and a broadside array for a clinical assessment with hearing impaired listeners. Section 4.5 gives a description of these models and measurements carried out with these models in the anechoic room. In chapter 5 and 6 these portable models are used for measurements in a diffuse noise field and for listening tests.

## 4.2 Set-up of Directivity Measurements

The directivity measurements, presented in the next sections, have been carried out in the anechoic chamber of the Delft University. The chamber has glass wool wedges of 1 m length and a volume of  $1000 \text{ m}^3$ . The directivity patterns were measured monochromatically with the microphone (array) mounted on a Brüel and Kjaer 3921 turntable and a loudspeaker at a distance of 6.4 m (figure 4.1).

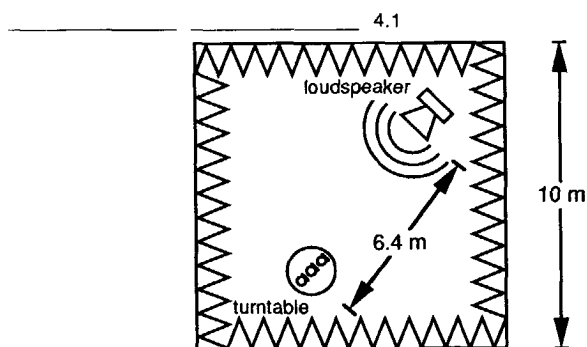


Figure 4.1 Sketch of the measurement set-up in the anechoic room.

Polaris

The output level of the microphone (array) signal as a function of the angle of incidence of a local plane wave is measured with a newly developed measurement system. The measurement system is called '*Polaris*' (*Polar Investigation System*) and offers the following possibilities:

- Control of the turntable and data acquisition
- Real time graph of the measured directivity pattern
- Fast computation of the directivity index of the measured data (assuming a symmetric directivity pattern)
- Data file system with accountancy of important parameters.

With the Polaris measurement system the directivity pattern as well as the directivity index can easily be compared with other measurements or simulations. Figure 4.2 gives a schematic drawing of the measurement system. The main part of the system is an AT personal computer with a MS-DOS operating system. The PC controls, through the RS232-port, the turntable with an intelligent I/O-controller. The data acquisition is carried out with an in-house developed RMS-DC converter and a Data Translation DT2814 A/D converter.

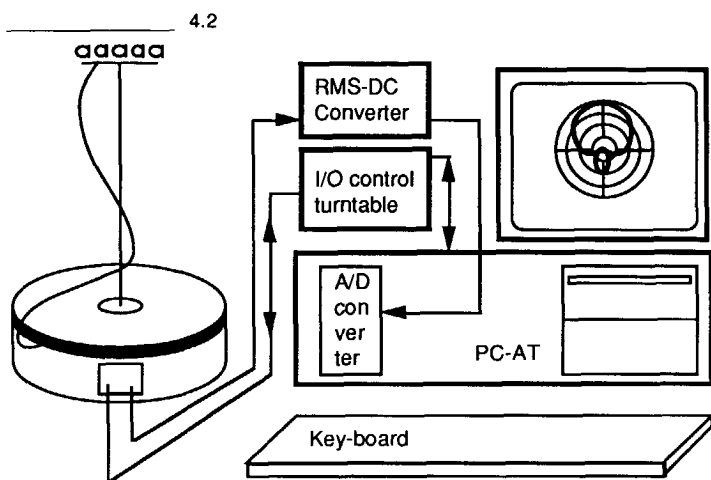


Figure 4.2 Schematic drawing of 'Polaris' (Polar Investigation System) consisting of an AT-personal computer with a built-in A/D converter. Control of the turntable is done with an intelligent I/O controller. The RMS-value of the output signal of the microphone is determined with a RMS-DC converter.

### 4.3 Free Field Directivity Measurements

In this section the results of free field directivity measurements are presented in three parts. In the first part measurements are presented with one single directional miniature electret condenser microphone. The directivity is measured as a function of the distance between the two sound inlets of the directional microphone. Based on these measurements a choice is made for one suitable distance to be used in the subsequent measurements with arrays. The second and third parts show the results of measurements with a laboratory model of an endfire microphone array and a broadside microphone array respectively.

## SINGLE DIRECTIONAL MICROPHONE

miniature  
microphone

The microphone used in the following experiments is a miniature electret condenser microphone with directional characteristics (Microtel M61). This miniature microphone is developed for application in hearing aids and is usually mounted in a behind the ear hearing aid. The properties and operation of this microphone are essentially comparable with the directional microphone as discussed in section (2.4). The directivity pattern equals:

$$D(\theta, \phi, \omega) = (\beta + \cos\theta) k \Delta d \quad (4.1)$$

where

$$\beta = \frac{c \tau}{\Delta d}$$

with  $\tau$  the time delay of the acoustical network of the microphone and  $\Delta d$  the intermediate distance between the sound inlets. Figure 4.3a shows the microphone with two sound inlets and intermediate distance of 5.0 mm. The nominal delay time of the acoustical network of  $\tau = 28 \mu s$  and the effective distance of  $\sim 1$  cm between the two sound inlets at the hearing aid case result in a value  $\beta \sim 1$  (figure 4.3b).

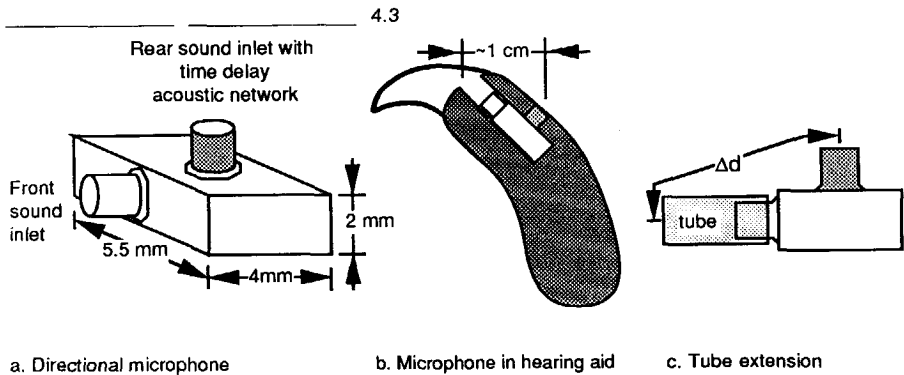


Figure 4.3 Drawing of a miniature electret condenser microphone (Microtel M61) with two sound inlets and time delay acoustical network (a). Microphone built in hearing aid case (b). The effective distance  $\Delta d$  between the sound inlets can be changed with a tube (c).

measurement

For our measurements we have changed the intermediate distance  $\Delta d$  between the sound inlets with a tube placed on the front sound inlet (figure 4.3c). A selection of the measured directivity patterns is given in figure 4.4. The polar diagrams are given for intermediate distances  $\Delta d = 5.5, 8.5$  and  $16.5$  mm. The measured directivity patterns of the microphone with a tube are similar with measurements done by Madaffari (1983) for microphones built in a hearing aid case.



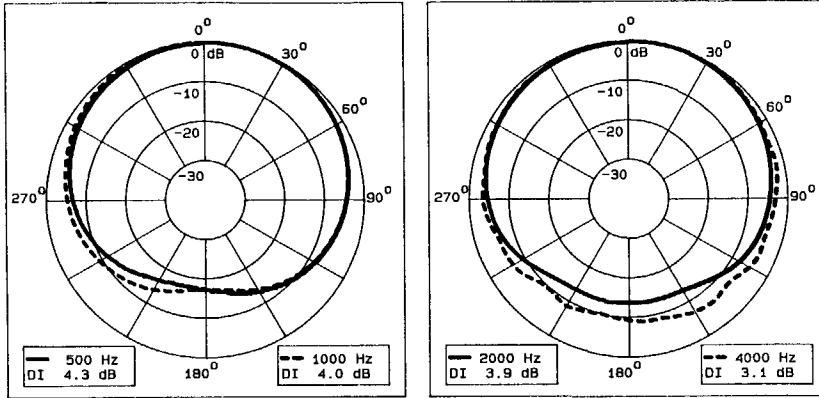
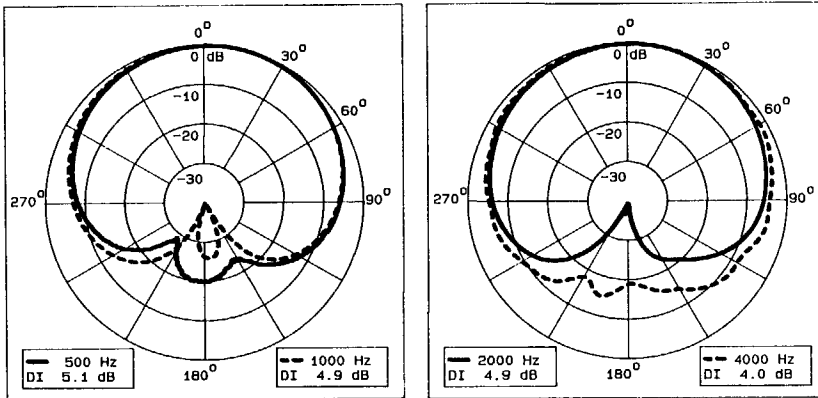
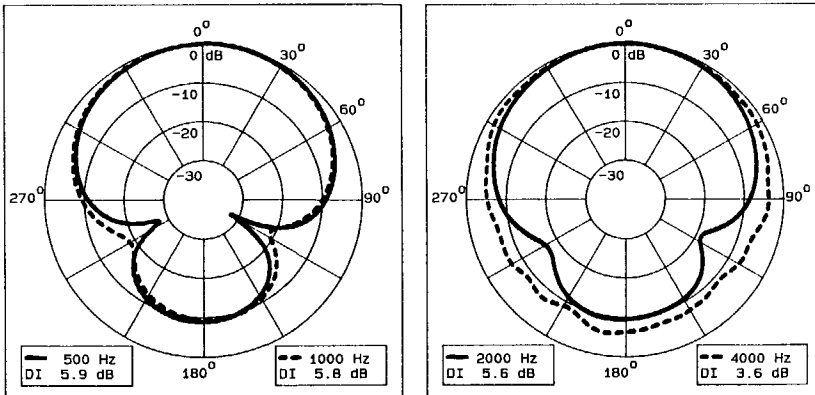
a.  $\Delta d = 5.0$  mm.b.  $\Delta d = 8.5$  mm.c.  $\Delta d = 16.5$  mm.

Figure 4.4 Measured directivity patterns of one single miniature electret microphone for intermediate distances  $\Delta d = 5.5, 8.5$  and  $16.5$  mm.

Cardioid

For  $\Delta d = 8.5$  mm we have a *cardioid* directivity pattern. The value of  $\beta$  equals 1.12 ( $\tau = 28 \mu s$ ) which agrees with the theoretical value of  $\beta = 1$  for a true cardioid microphone. For  $\Delta d = 16.5$  mm we have a so-called *super cardioid* directivity pattern for the lower frequencies. The value of  $\beta$  equals 0.57 which agrees very well with the theoretical value of  $\beta = 1/\sqrt{3}$  for a true super cardioid microphone.

Super cardioid

The results of directivity measurements with more tube lengths are given in figure 4.5. Table 4.1 gives a review of the used tube lengths, the approximated distances  $\Delta d$  as noted in figure 4.3c and the corresponding values of the factor  $\beta$  for an internal delay of  $\tau = 28 \mu s$ . The values for  $k\Delta d$  are computed at  $f = 500$  and  $1000$  Hz. The values of factor  $\beta$  are used for the simulation of the directivity index of a directional microphone at  $f = 500$  Hz and  $k\Delta d \ll 1$ . Figure 4.5 shows that the directivity index for  $f = 500$ ,  $1000$  and  $2000$  Hz increases with the distance  $\Delta d$ . The measured values are even better than the simulated values and reach a mean value of 5 dB. The internal delay of the microphone has most probably been shorter than  $28 \mu s$  resulting in a smaller  $\beta$  and a higher directivity.

$\Delta d \ll \lambda$

The directivity index at 4000 Hz is about 4 dB, being 1 dB lower in comparison with the other frequencies. In section 2.4 it was shown that with a Jacobi array, being equivalent with a directional microphone, directivity can be obtained when  $k\Delta z \ll 1$  or  $\Delta z \ll \lambda$  (equation 2.55, figure 2.16). However, table 4.1 shows that the intermediate distance was made too large in comparison with the wavelength at 4000 Hz resulting in  $k\Delta d \sim 1$ . Therefore, the directivity at the higher frequencies of one directional microphone can only be improved when the effective delay time of the internal acoustical delay network is reduced.

Table 4.1 The value of  $\Delta d$ ,  $\beta$  and the resulting  $k\Delta d$  for the used tube lengths.

Tubelength (mm)	$\Delta d$ (mm)	$\beta$	$k\Delta d$	
			500 Hz	4000 Hz
0.0	5.5	1.72	0.10	0.41
3.0	7.0	1.35	0.13	0.52
4.5	8.5	1.12	0.16	0.63
6.5	10.3	0.92	0.19	0.76
8.0	11.7	0.81	0.22	0.86
10.0	13.6	0.69	0.25	1.01
13.0	16.5	0.57	0.31	1.22

4.1

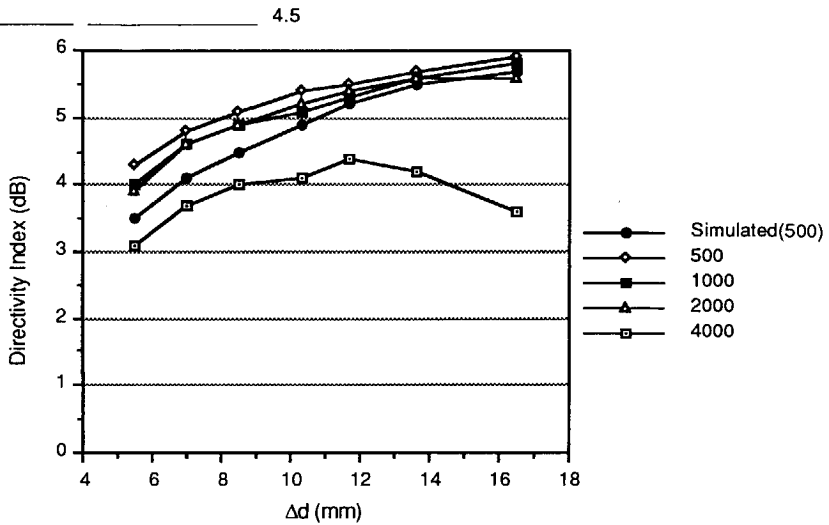


Figure 4.5 The change of the Directivity Index dependent on the length of a tube-extension placed on the 'A-port' of one single cardioid microphone.

#### Conclusion

Summarizing, we may conclude that the value of the directivity index and the directivity pattern of one microphone can be changed by a variation in the distance between the two sound inlets. The best choice for a high directivity for all frequencies is an intermediate distance  $\Delta d = 11.7$  mm. The directivity index at 4000 Hz is about 1 dB lower than the theoretical value because of the internal delay time of the microphone resulting in a  $k\Delta d \sim 1$ .

Although the highest directivity can be obtained when  $\Delta d = 11.7$  mm, in the following array measurements an intermediate distance of  $\Delta d \sim 8.5$  mm will be used. The value of the factor  $\beta \approx 1$  results in a true cardioid directivity pattern which corresponds with the theoretical directivity pattern ( $DI = 4.7$  dB) used during the simulations of the preceding chapters.

#### ENDFIRE ARRAY OF CARDIOID MICROPHONES

For the measurements of the directivity of an endfire array we made a flexible laboratory model consisting of adjustable delay and weighting units. This model enabled us to do measurements with respect to an ordinary endfire array, improved endfire array following Hansen and Woodyard, numerically optimized endfire array and measurements on the influence of errors in weighting and delay time.

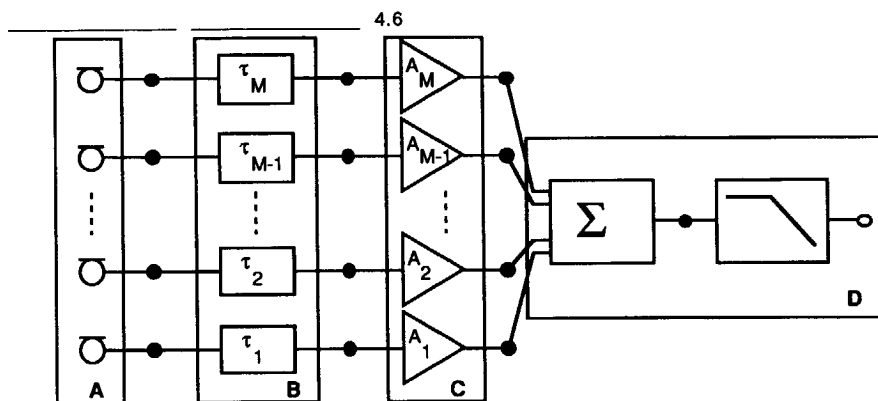


Figure 4.6 Block-diagram of the laboratory model, consisting of microphones (A), delay-elements for each microphone signal (B), adjustable amplifiers for amplitude weighting (C) and an active low-pass filter after summation of the signals (D).

Model

Figure 4.6 gives a block diagram of the developed laboratory model. The array consisted of cardioid microphones with tube extensions of  $\sim 4.5$  mm connected to movable little sockets. Each microphone was placed in the endfire configuration with its maximum sensitivity to  $\theta = 0^\circ$  (along the bar). The signal of each microphone is delayed relative to the first microphone signal. The delay elements are Panasonic MN3012 bucket-delays. The delay time of each microphone can be changed independently of the other delays by variation of the clock frequency of the bucket-delay. The amplitude weighting is done with an adjustable amplifier. Finally, the summed signal is low-pass filtered with an active filter having a cut-off frequency of 5.5 kHz. This filter is necessary for suppression of audible cross-products ( $> 6$  kHz) of the clock signals of the bucket-delays. The cross-products originate from the differences in clock frequencies as used for the setting of the delay times.

Ordinary

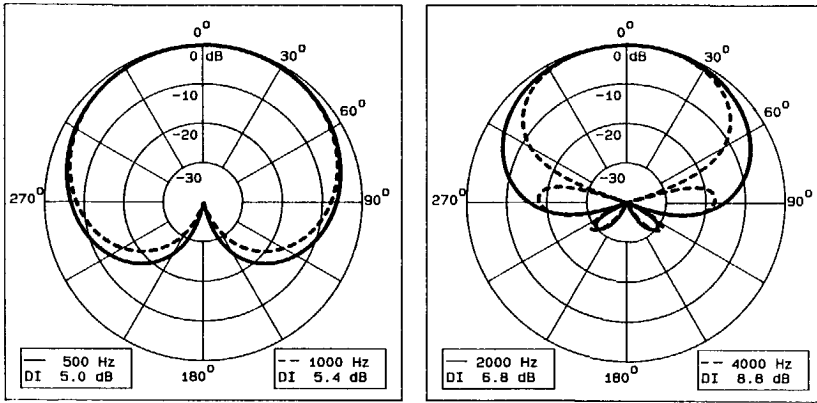
Endfire array

The simulated and measured directivity patterns of an ordinary endfire array ( $\tau_m = m \Delta z/c$ ) with uniform weighting ( $A_m = 1$ ) are given in figure 4.7. The length of the array is  $L = 10$  cm and thus  $\Delta z = 2.5$  cm. A comparison between simulation and measurement shows that the simulation gives a good prediction of the directivity patterns as well as of the value of the directivity index.

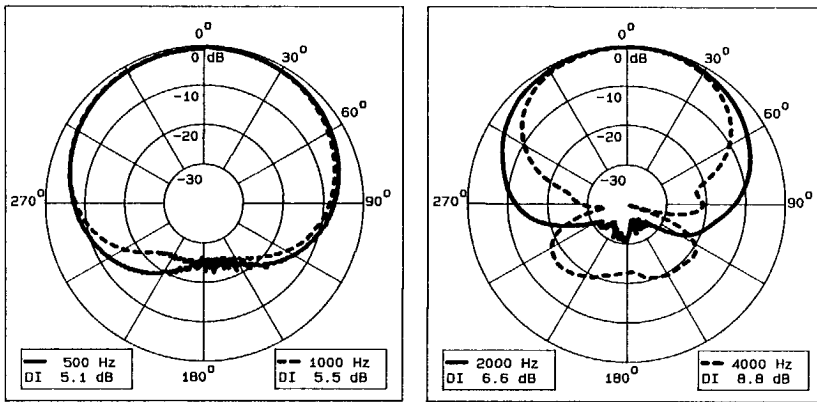
Hansen Woodyard

In section 3.2 it was shown that the directivity of an endfire array could be improved, following a suggestion by Hansen and Woodyard, by multiplying the delay time of microphone  $m$  with a factor  $1 + \epsilon$ :

$$\tau_m = m \frac{\Delta z}{c} (1 + \epsilon) . \quad (4.2)$$



a. Simulation of directivity pattern.



b. Measured directivity pattern.

Figure 4.7 Simulated (a) and measured (b) directivity patterns of an ordinary endfire array of 5 cardioid microphones with uniform weighting ( $A_m = 1$ ) and  $L = 10$  cm.

The improvement of the directivity as a function of the factor  $1+\epsilon$  was measured with an endfire array of 5 cardioid microphones. The length of the array was  $L = 10$  cm with uniform amplitude weighting. The delay time of each delay unit was multiplied with  $1+\epsilon$ .

Figure 4.8 gives the values of the directivity index computed from the measured directivity patterns. We can see that the values of the directivity index rise to a maximum value at 4000 Hz of 11.5 dB for a value of the multiplication factor  $1+\epsilon=1.37$ . The maximum value of the directivity index and the value of  $\epsilon$  agree very well with the theoretical values of  $DI = 12.0$  dB and  $1+\epsilon=1.4$  predicted by the simulations and the Hansen Woodyard condition (Table 3.3 and figure 3.3).

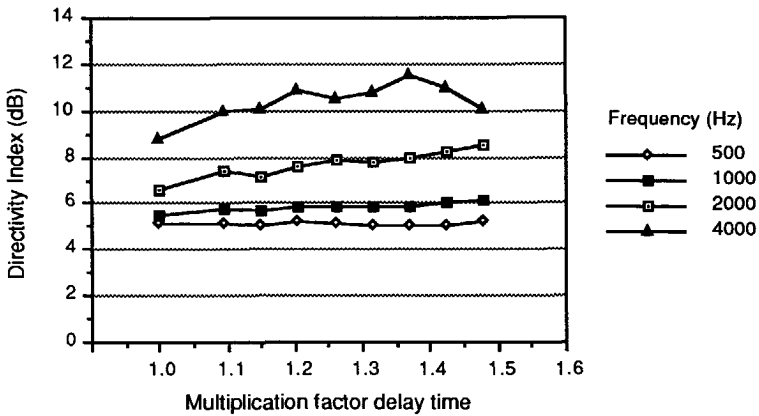


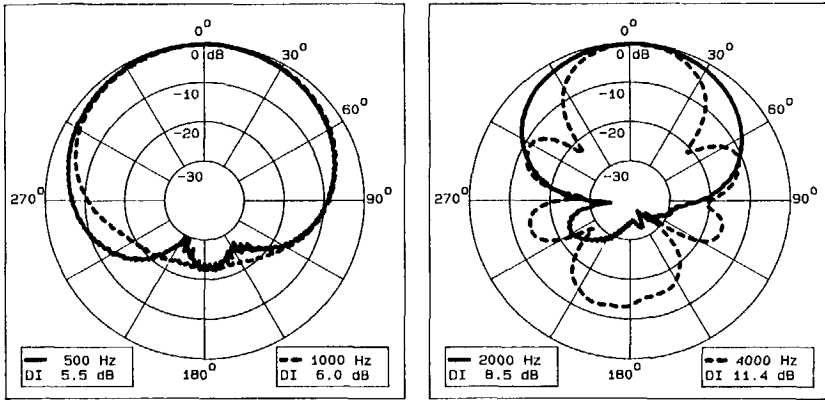
Figure 4.8 The measured values of the Directivity Index of a uniform endfire array of 5 cardioid microphones dependent on the delay-time multiplied by the factor  $1+\epsilon$ . The length of the array is 10 cm.

For larger values of  $1+\epsilon$  the value of the directivity index at  $f = 4000$  Hz decreases and increases for the lower frequencies, which corresponds with the simulated directivity index of figure 3.3b. Therefore, we can conclude that an improvement of the directivity at all frequencies of a uniform endfire array can be achieved when  $0.35 < \epsilon < 0.40$ .

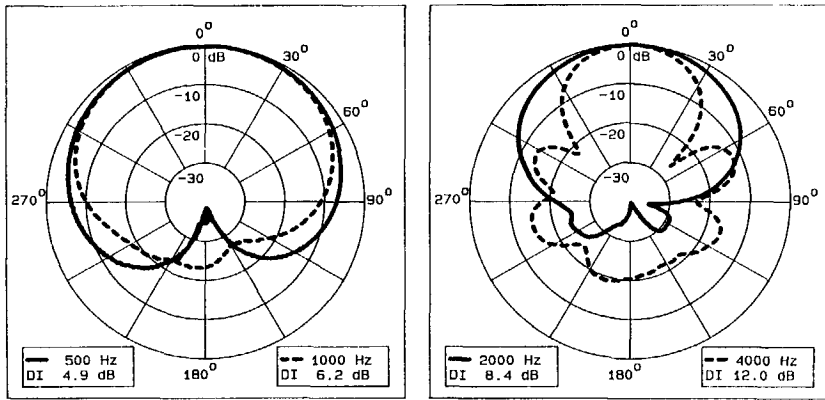
Optimized  
parameters

In section 3.3 the results were presented of the optimization of the array parameters of an endfire array with fixed length  $L = 10$  cm and true cardioid microphones ( $DI = 4.7$  dB). A high directivity was obtained when 4 or 5 microphones were used. Using the optimized weights and delay times, figure 4.9 gives the results of measurements for an endfire array of 4 and 5 microphones respectively. The measured directivity patterns are given for  $f = 500, 1000, 2000$  and  $4000$  Hz. The computed directivity indices of the simulations and measurements are given in figure 4.10.

The figures show that the simulations predict the directivity of the real arrays very well up to  $4000$  Hz. A directivity index ranging from  $4.9$  dB ( $500$  Hz) to  $12.0$  dB ( $4000$  Hz) can be achieved. Above  $4000$  Hz the difference between simulation and measurement originates from the low directivity of the used cardioid microphones. This is especially disadvantageous for the endfire array of 4 microphones where a significant backward lobe as a result of spatial aliasing is not suppressed as a result of the low directivity of the cardioid microphones. Therefore we may conclude that the highest directivity can be obtained with the optimized endfire array of 5 microphones.

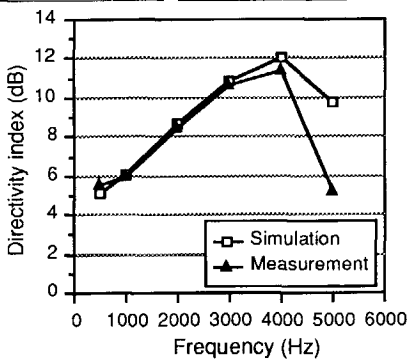


a. Measured directivity patterns endfire microphone array of 4 microphones.

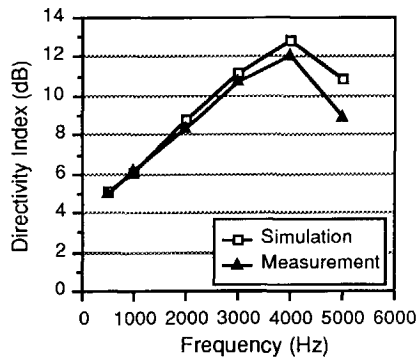


b. Measured directivity patterns endfire microphone array of 5 microphones.

Figure 4.9 Directivity patterns of optimized endfire arrays of 4 microphones (a) and 5 microphones (b).



a. Optimized endfire of 4 microphones.



b. Optimized endfire of 5 microphones.

Figure 4.10 Comparison of the values of the Directivity Index for simulated array and measured result.

Influence of errors In section 3.4 we have seen that an endfire array offers a high and stable directivity. Therefore, we will now introduce some errors in amplitude weighting or delay times for the endfire array of 5 microphones. Figure 4.11 shows the change of the directivity index due to two extreme errors in the amplitude weighting measured with the laboratory model. First, the amplitude weighting of microphone 5, at  $z = 10$  cm, is set to zero.

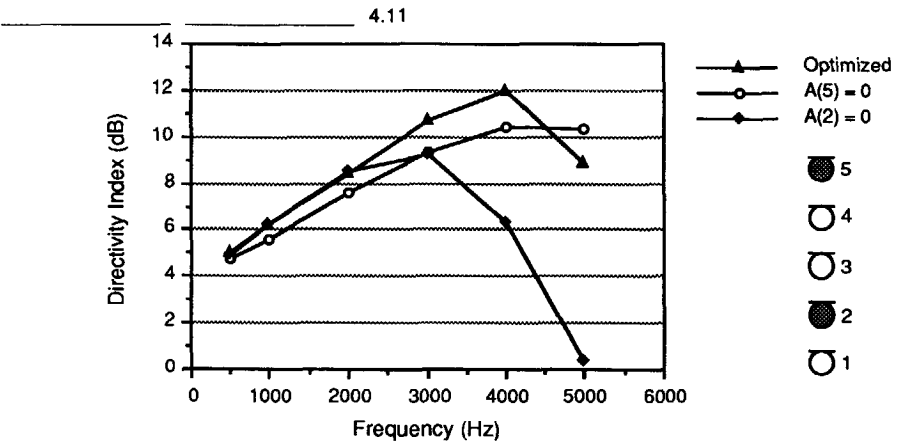


Figure 4.11 Influence of errors in amplitude weighting on the measured values of the directivity index of an optimized endfire array ( $L=10\text{cm}$ ). The values of the directivity index are computed from measurements with the optimized endfire array of 5 microphones, the same array with  $A_5=0$  (at  $10.0$  cm) or  $A_2=0$  (at  $2.5$  cm).

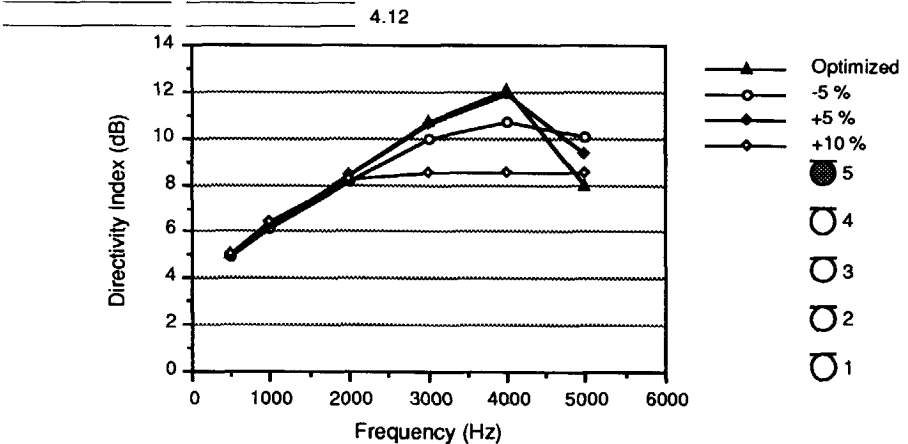


Figure 4.12 Influence of errors in delay time on the values of the measured values of the directivity index of an optimized endfire array ( $L=10\text{cm}$ ). The values of the directivity Index are computed from measurements with the optimized endfire array of 5 microphones, and the delay time of microphone 5 (at  $10$  cm) is varied with  $-5\%$ ,  $0\%$ ,  $+5\%$ ,  $+10\%$ .



The effective length of the array is reduced to 7.5 cm giving a reduction of the directivity for all frequencies up to 4000 Hz. Secondly, the amplitude weighting of microphone 2, at  $z = 2.5$  cm, is set to zero. The error in the amplitude weighting leads to a gap in the array and thus an incorrect spatial sampling for frequencies above 3000 Hz results.

Next, we will change the delay time of one microphone (The Hansen Woodyard measurements were done with variation of the delay times with 50 %!). Figure 4.12 shows the values of the directivity index when the delay times of microphone number 5, at  $z = 10$  cm, is changed with  $-5\%$ ,  $+5\%$  and  $+10\%$  respectively. Variation of the delay time by  $\pm 5\%$  leads to a small change in the values of the directivity index. The significant error in delay time of  $+10\%$  reduces the maximum directivity index from 12 to 8.5 dB.

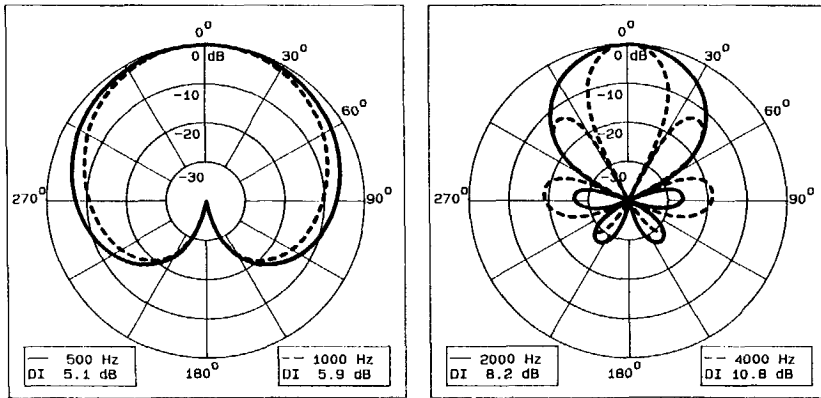
**Conclusion** We may conclude that large errors in amplitude weighting or delay time influence the directivity, but the directivity index up to 4000 Hz stays above 5 dB. In practice, variations in amplitude weighting and delay time will even be smaller and therefore, we may expect that in practice the optimized endfire array of 5 cardioid microphones has a high and stable maximum.

### BROADSIDE ARRAY OF CARDIOID MICROPHONES

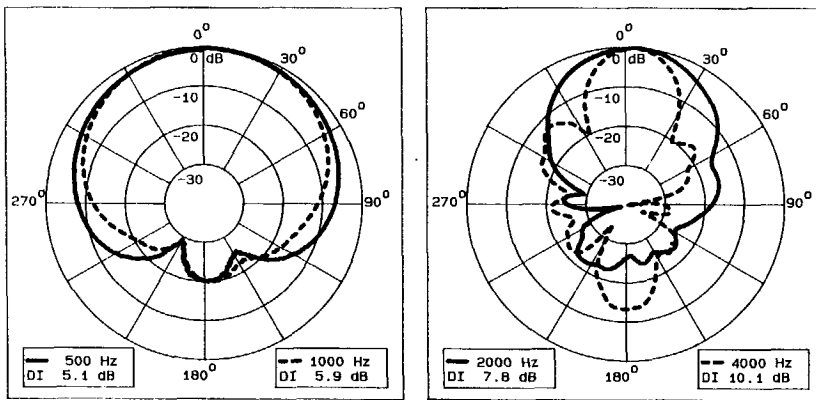
For the measurements of the directivity of a broadside array we used a simple laboratory model. The array consisted of cardioid microphones with tube extensions of  $\sim 4.5$  mm connected to movable little sockets. Each microphone was placed in the broadside configuration with its maximum sensitivity to  $\theta = 0^\circ$  (perpendicular to the bar). The electronic model consisted of adjustable amplifiers and a summation unit.

**Asymmetrical directivity pattern** In section 3.5 (figure 3.22) we have seen that a broadside array of cardioid microphones has only one plane of symmetry given by the vertical plane. In that vertical plane the directivity pattern equals the pattern of one cardioid microphone. The following measurements with the broadside array model have been done in the horizontal ear plane. Therefore, the directivity index is computed for the horizontal directivity pattern and corrected for the cardioid-like directivity pattern in the vertical plane. The measured directivity pattern in the vertical plane was equal to the directivity pattern of one microphone as given in figure 4.3b.

**Measurement** The simulated and measured directivity patterns of an optimized broadside array of 5 microphones are given in figure 4.13. The 5 microphones are equidistantly placed with an array length of 14 cm.



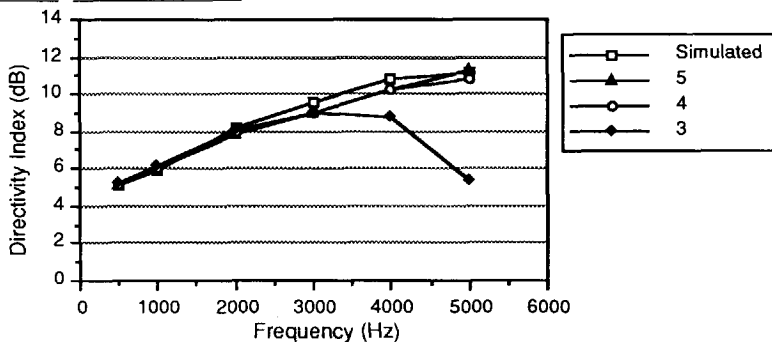
a. Simulated directivity pattern



b. Measured directivity pattern.

Figure 4.13 Directivity patterns of a broadside array of 5 cardioid microphones with a length of 14.0 cm.

4.14

Figure 4.14 Directivity index of a simulated broadside array of 5 microphones ( $L = 14$  cm) and directivity index computed from measurements with a broadside array consisting of 5, 4 and 3 microphones and fixed length  $L = 14$  cm.

The simulations of the directivity patterns predict the measured patterns very well. Figure 4.14 gives the values of the directivity index of the simulated optimized broadside array and the values of the directivity index computed from the measurements with the broadside array model with fixed length  $L = 14$  cm. The results are given of measurements with 5, 4 and 3 cardioid microphones. The directivity of the broadside array model of 4 and 5 microphones is comparable with the directivity of the simulated broadside array. The results of the measurement with 3 microphones show that the directivity decreases for frequencies above 3000 Hz. The intermediate distance between the microphones of  $\Delta x = 7$  cm results in spatial aliasing for the high frequencies ( $\Delta x \sim \lambda$ ) giving extra side lobes and a low directivity (see also figures 2.9 and 2.10).

**Influence of errors** In section 3.4 we assumed that a broadside array is very robust. This is implicitly confirmed by the preceding measurements. A broadside array with 4 or 5 microphones gives nearly the same directivity: the microphones have different x-positions but a sound wave coming from the front is summed in phase. Nevertheless, figure 4.15 gives the results of some additional measurements with extreme errors in the amplitude weighting of a broadside array with 5 and 4 microphones and  $L = 14$  cm. First, the amplitude weighting of microphone 5 is set to zero ( $A(5)=0$ , figure 4.15a). The effective length of the array reduces to  $L = 10.5$  cm giving a small reduction of the directivity.

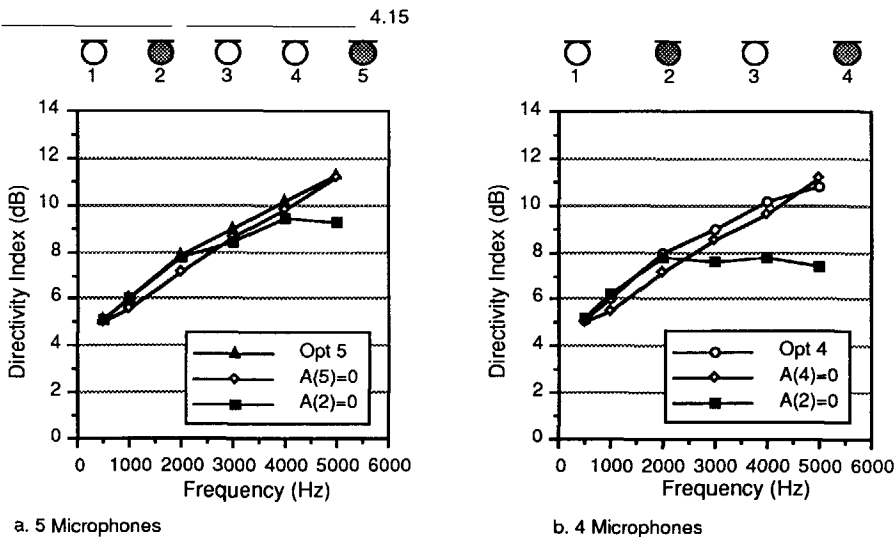


Figure 4.15 Directivity index computed from measurements with a broadside array with  $L=14$  cm showing the influence of errors in amplitude on the directivity.

The error in the amplitude weighting of the second microphone ( $A(2)=0$ ) results in a gap in the array and thus a lower directivity above 3000 Hz due to spatial aliasing. Figure 4.15b shows the results of measurements carried out with 4 microphones and  $L = 14$  cm. The reduction of the effective length of the array to  $L = 9.3$  cm by setting  $A(4)=0$  gives only a small reduction of the directivity. When the amplitude weighting of the second microphone is set to zero the large gap in the array results in spatial aliasing and thus a lower directivity above 2000 Hz. However, a directivity index of more than 7.5 dB is still reached. Therefore, we may conclude that a broadside array has a very stable directivity.

#### CONCLUSION OF FREE FIELD MEASUREMENTS

The free field measurements show that the free field simulations in the preceding chapter give a good prediction of the directivity and stability that can be obtained with a practical endfire or broadside array. A stable directivity can be reached with an optimized endfire array consisting of 5 miniature electret microphones ( $L = 10$  cm). Further, a broadside array of 4 or 5 microphones ( $L = 14$  cm) will give a high and very stable directivity.

### 4.4 Directivity Measurements with an Artificial Head

Until now, we have simulated and measured the directivity patterns of arrays placed in a free field situation. However, in practice we will place the directional microphone array along the side (endfire) or in front of (broadside) a human head. This means that the directivity of a microphone array may be disturbed due to sound waves being reflected and diffracted by the head. Therefore, we decided to do measurements with the microphone(s) connected to the head of a KEMAR manikin (Knowles Electronics Manikin for Acoustic Research). This manikin which conforms to the IEC-959 standard has been developed for measurements with hearing aids (IEC-959).

#### Measurements

In this section the directivity patterns will be presented of one omnidirectional and one cardioid microphone and the optimized endfire and broadside microphone arrays. The directivity patterns are measured in the anechoic room with the KEMAR manikin placed on a turntable and the microphone connected to the head (figure 4.16).

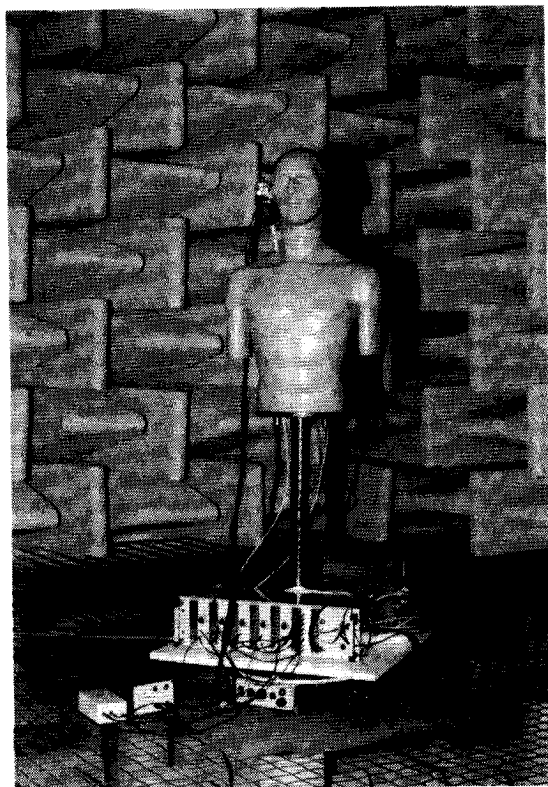


Figure 4.16 KEMAR manikin with endfire microphone array placed on a turntable.

Determination of  
Directivity Index

For practical reasons, the directivity patterns are measured in the horizontal plane. In consequence, the computed directivity index can only be an *estimation* of the real three dimensional value and will be dependent on the azimuth of the source. The real value of the directivity index can only be determined when the complete three dimensional directivity pattern is

Diffuse noise field

measured. However, placing the KEMAR set-up in a *diffuse noise field* for the determination of the directivity index is more convenient. Results of measurements in a diffuse noise field will be presented in the next chapter. For the measurements in this section the directivity index is computed from the directivity pattern assuming the main beam at  $0^\circ$  and a cylinder symmetry of the directivity pattern (Actually, this gives an estimation of the so-called front-random index, see also section 5.3). The value of the broadside array with KEMAR is corrected for the vertical asymmetry of the broadside array.

#### KEMARS OWN EAR

First, figure 4.17 gives the measured directivity patterns of the ear-simulator of the right ear of KEMAR. The directivity patterns for the lower frequencies at 500 Hz and 1000 Hz are mainly determined by shadowing of the head. The main direction is  $80^\circ$ ; sound coming from the left of the head is 6 dB lower. The directivity pattern at the higher frequencies 2000 Hz and 4000 Hz is determined by the head as well as by the auricle. The main direction of the directivity pattern is now  $30^\circ$ .

4.17

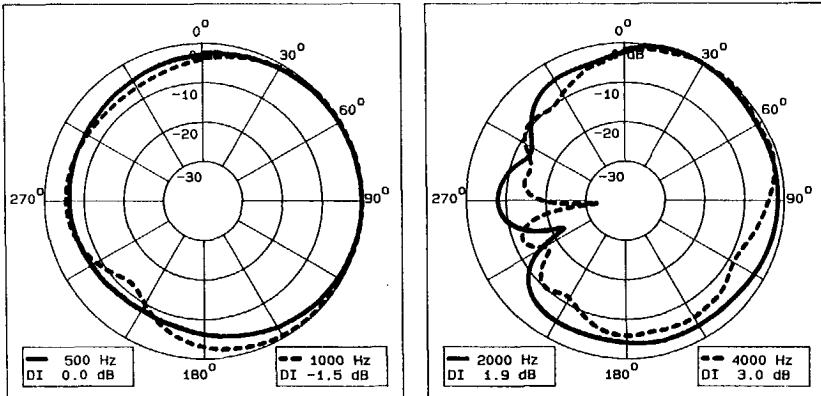


Figure 4.17 Measured directivity patterns of the right internal ear simulator of KEMAR.

#### KEMAR WITH OMNIDIRECTIONAL AND CARDIOID MICROPHONE

Next, figure 4.18 gives the measured directivity pattern of one single omnidirectional microphone mounted above the right auricle of KEMAR. The directivity patterns are now mainly influenced by the shadowing of the head; the main direction is  $90^\circ$ . The estimated directivity indices are very low. Figure 4.19 gives the directivity pattern of one single cardioid microphone. The microphone was mounted above the right auricle of KEMAR. The main direction of the cardioid microphone was  $0^\circ$ . A comparison of the directivity patterns of the cardioid microphone with the patterns of the omnidirectional microphone shows that the main direction is turned from  $\sim 90^\circ$  to  $\sim 30^\circ$ . The estimated values of the directivity index are 4 dB higher than for one omnidirectional microphone. However, listening tests have shown that the improvement, especially in reverberant situations, is lower (Mueller 1981). A possible explanation is the insufficient directivity for the higher frequencies and the main beam pointing to  $30^\circ$ .

Cardioid

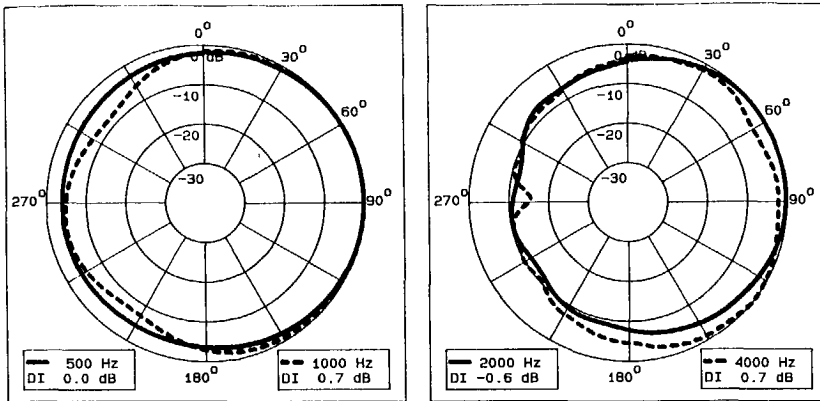


Figure 4.18 Measured directivity patterns of KEMAR with an omnidirectional microphone above the right auricle.

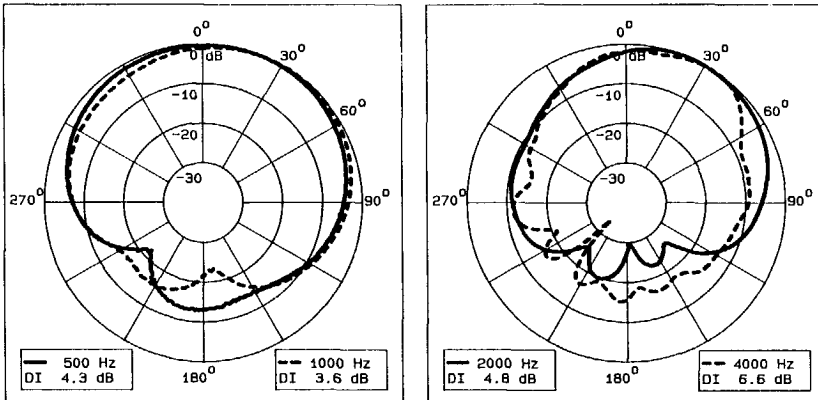


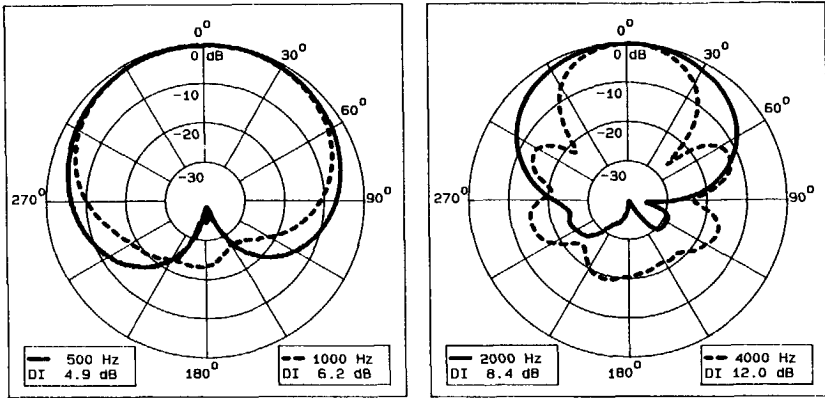
Figure 4.19 Measured directivity patterns of KEMAR with a cardioid microphone above the right auricle.

#### KEMAR WITH OPTIMIZED ENDFIRE ARRAY AND BROADSIDE ARRAY

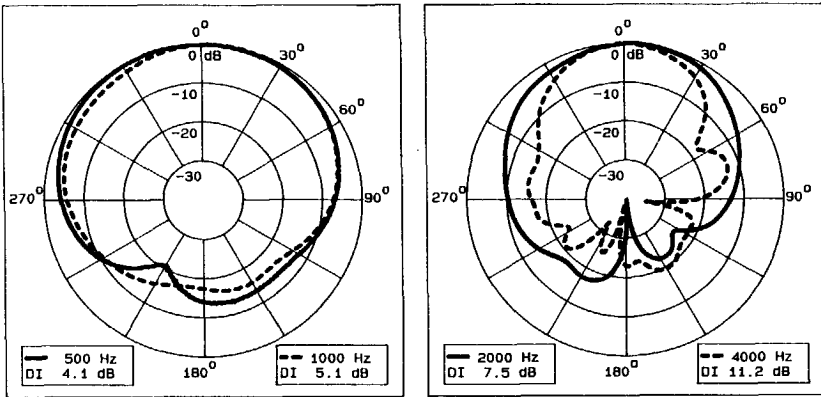
The KEMAR measurements with the optimized endfire array ( $L = 10$  cm, 5 cardioids) and the broadside array ( $L = 14$  cm, 5 cardioids) are presented in figure 4.20 and 4.21 respectively. The free field directivity patterns are added for comparison.

#### Endfire array

The directivity of the endfire array is hardly decreased by the addition of reflections or diffraction of the sound by the head. A comparison of the free field directivity patterns and those measured with KEMAR show that, especially when the sound is coming from the right side of KEMAR,



a. Free field measurement



b. Measurement with KEMAR

Figure 4.20 Measured polar diagrams of an optimized endfire array consisting of 5 cardioid microphones and an overall length of 10 cm. Measurement of array free field (a) and mounted near the right ear of KEMAR (b).

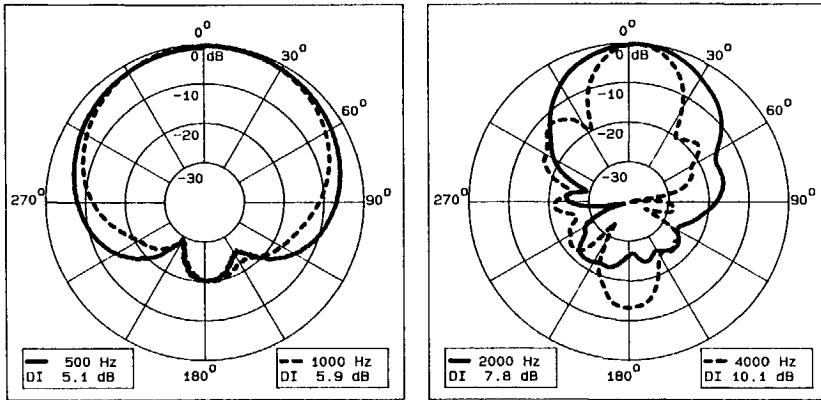
the influence of the head on the performance of the array is relatively small. The decay of the estimated directivity index is less than 1 dB for all frequencies. The main beam is for all frequencies in the direction of 0°.

#### Broadside array

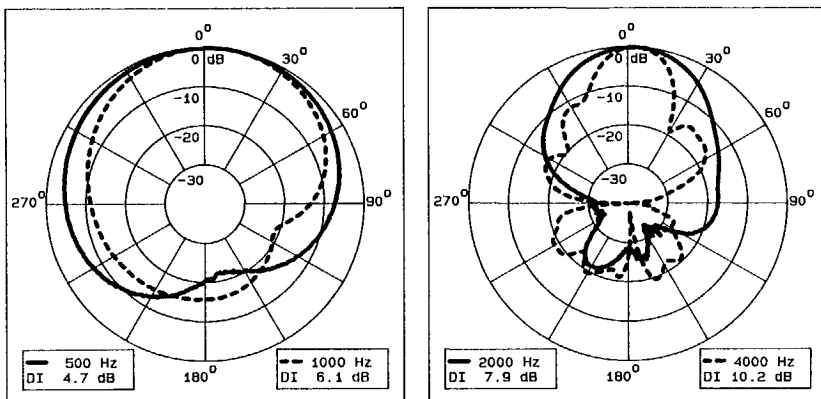
The directivity patterns measured with the broadside array show that the influence of the head on the directivity patterns is again very small and is even advantageous for suppression of the backward lobes. The loss of the directivity index at 500 Hz is less than 0.5 dB.

The KEMAR measurements with the endfire and broadside microphone arrays show that a directivity of more than 7.5 dB can be obtained for frequencies above 2000 Hz.





a. Free-field measurement



b. Measurement with array in front of the head of KEMAR

Figure 4.21 Measured polar diagrams of a broadside array consisting of 5 cardioid microphones and an overall width of 14.0 cm. Free-field (a) and KEMAR (b).

## CONCLUSIONS

The measurements with the KEMAR manikin show that the array effect is only slightly influenced by diffraction or reflections by the head. The estimated values of the directivity index computed from the directivity patterns show that one cardioid microphone may give a mean improvement of 4 dB in comparison with one omnidirectional microphone. The estimated directivity of the endfire microphone array as well as the broadside microphone array ranges from 4 dB at 500 Hz to more than 10 dB at 4000 Hz, where the directivity at the higher frequencies may be considered as very important for speech intelligibility in noise (chapter 1).

## 4.5 Portable Microphone Arrays: Development and Measurements

The free field and KEMAR measurements carried out with a laboratory model of the endfire and broadside arrays showed that in practice a high and stable directivity can be obtained (section 4.3 and 4.4). Therefore, we decided to build portable array models suitable for psychophysical assessment with (hearing impaired) listeners. In this section a short description will be given of the portable models and the results will be presented of directivity and frequency spectrum measurements.

### DEVELOPMENT OF PORTABLE ARRAY MODELS

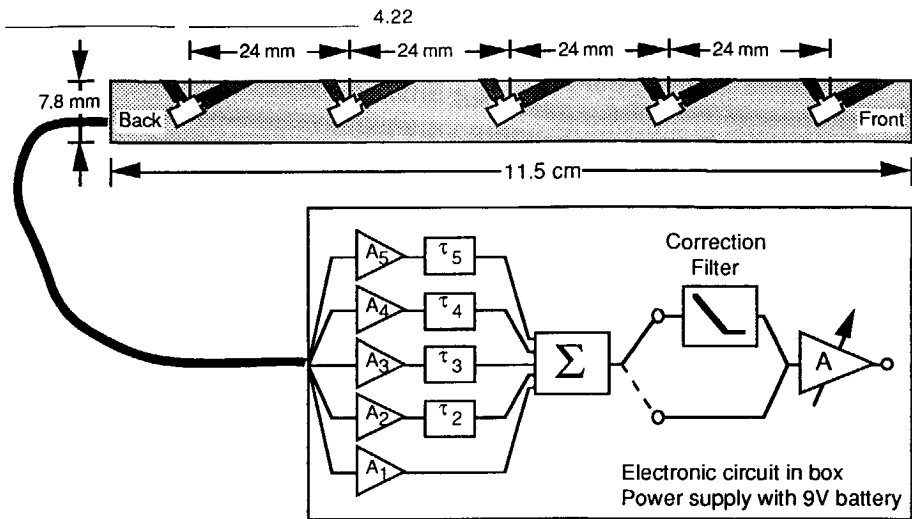
The measurements in the preceding sections were sufficiently encouraging for us to develop a portable endfire microphone array with  $L \sim 10$  cm and a portable broadside microphone array with  $L \sim 14$  cm. Because of directivity and stability we decided to use 5 cardioid microphones in each array. Later on, if economically interesting, the use of 4 cardioid microphones may be taken into consideration for the final implementation after these portable models have proved themselves to be robust and showing a sufficient directivity.

Portable endfire  
array

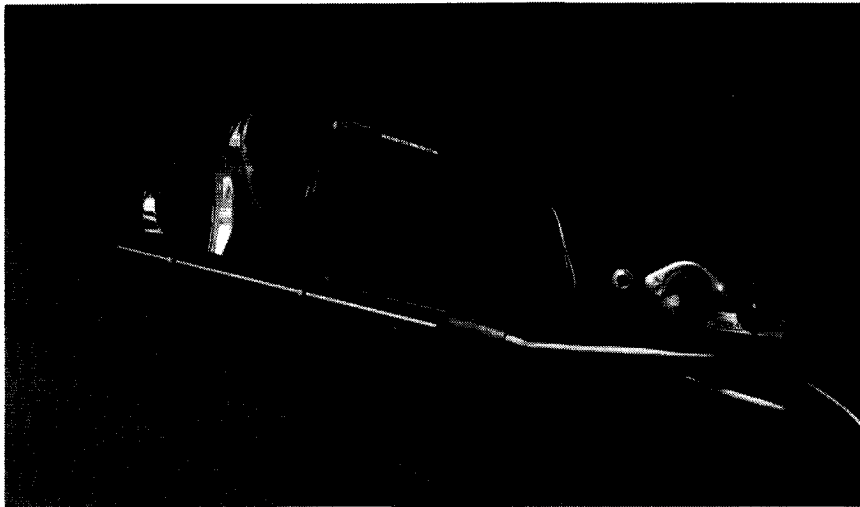
Figure 4.22 gives a diagram and picture of the endfire microphone array developed. The 5 cardioid microphones are placed in a bar with dimensions  $115 \times 8.6 \times 7.8$  mm and an intermediate distance between the microphones of 24 mm. The positioning of each microphone and the length of the bore holes are chosen in such a way that a cardioid directivity pattern is obtained with the main direction along the axis of the array bar. The electronic signal processing is built in a box ( $118 \times 66 \times 33$  mm) and can be fed by a 9V battery or by external power supply. The signal of each microphone is pre-amplified, delayed and summed (figure 4.22a). Because the summed signal will have a spectrum rising with 6 dB/octave, a correction filter can be optionally switched on for flattening of the spectrum. Finally, the (corrected) signal is amplified with an adjustable amplifier.

Portable Broadside  
Array

Figure 4.23 gives a diagram and picture of the developed portable broadside microphone array. The 5 cardioid microphones are placed in a bar with dimensions  $140 \times 12 \times 6.5$  mm and an intermediate distance between the microphones of 33 mm. The position and the length of the tube extensions of the sound inlets are chosen in such a way that a cardioid directivity pattern is obtained. The electronic circuit is the same as the endfire circuit without the delay units.



a. Diagram of endfire array bar with electronic circuit.

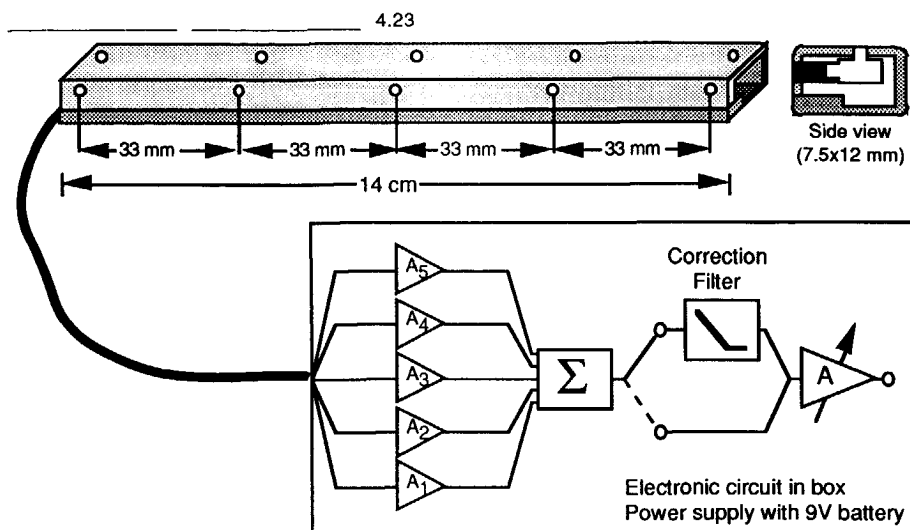


b. Picture of portable endfire microphone array connected to a pair of spectacles.

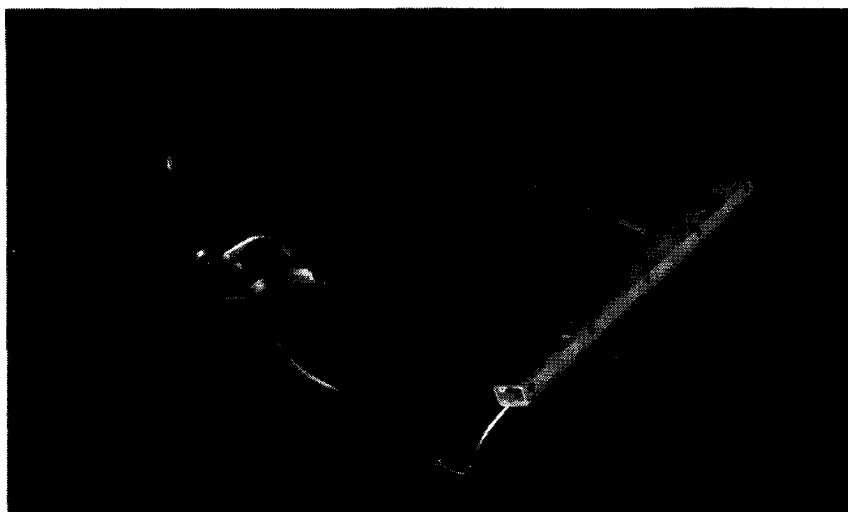
Figure 4.22 Diagram and picture of the developed portable endfire microphone array.

## DIRECTIVITY

Figure 4.24 gives the measured directivity patterns for these portable arrays. The measurements have been carried out with the arrays in a free field situation in the anechoic room. The developed portable arrays have a horizontal directivity pattern comparable to the directivity patterns measured of the laboratory models in section 4.3 (see figures 4.10 and 4.13).



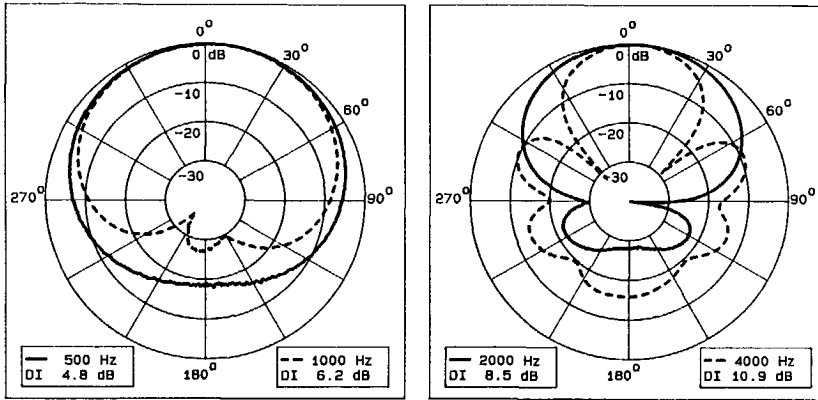
a. Diagram of broadside array bar with electronic circuit.



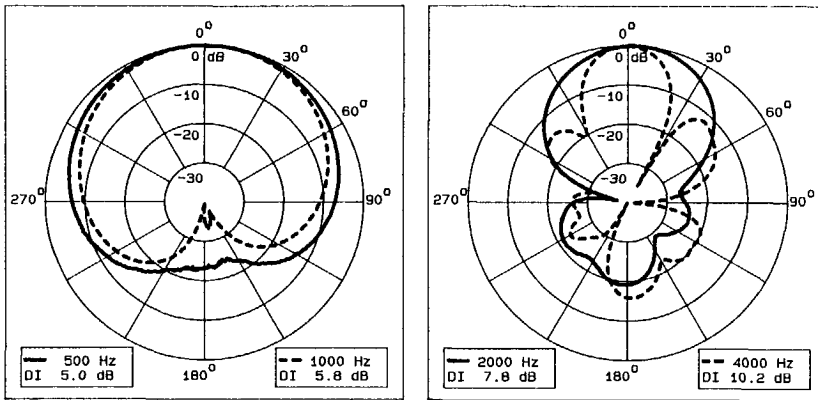
b. Picture of portable broadside microphone array on a pair of spectacles.

Figure 4.23 Diagram and picture of the developed portable broadside microphone array.

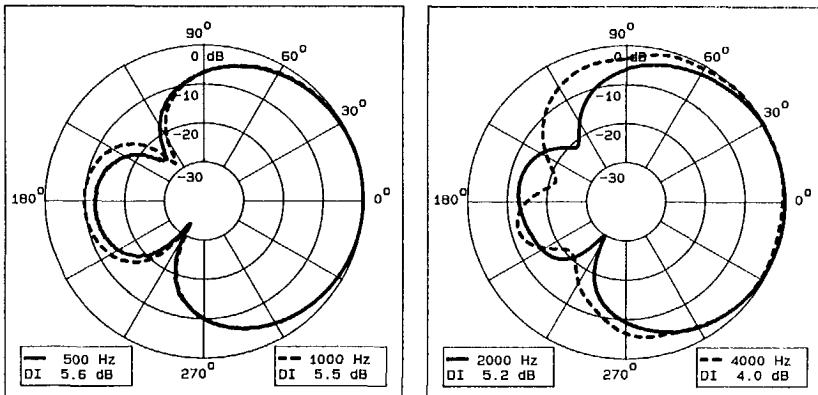
After the directivity measurements in the horizontal plane, figure 4.24c gives the measured directivity pattern of the broadside array in the vertical plane. As expected, the directivity pattern equals the directivity pattern of one directional microphone. Note, that the directivity index is computed under the assumption of a cylinder symmetry.



a. Free field directivity pattern of portable *endfire* array in **horizontal** plane.



b. Free field directivity pattern of portable *broadside* array in **horizontal** plane.



c. Free field directivity pattern of portable *broadside* array in **vertical** plane.

Figure 4.24 Measured directivity patterns of the developed portable microphone arrays.

Repeatability

The directivity patterns of 6 endfire and 7 broadside microphone arrays (made for other purposes) could also be measured. Figure 4.25 gives the measured mean and standard deviation of the directivity index at  $f = 500, 1000, 2000$  and  $4000$  Hz. The mean and standard deviation ( $<0.34$  dB) of the directivity indices show that both array types have a high and repeatable directivity!

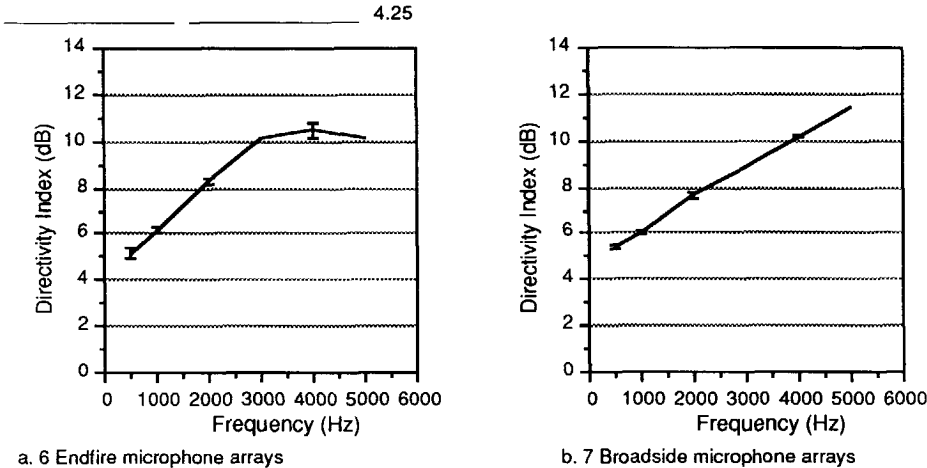
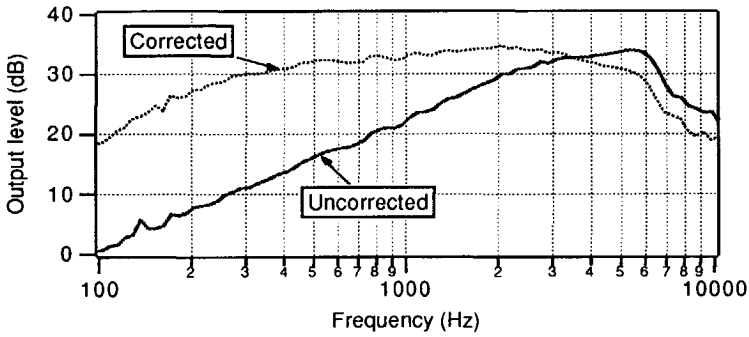


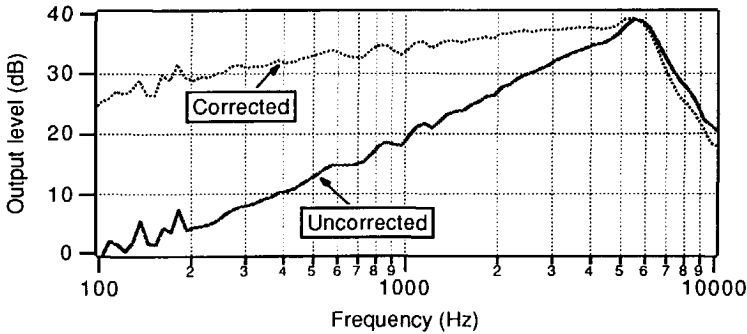
Figure 4.25 Mean and standard deviation of the directivity index computed from measurements carried out with 6 endfire array models (a) and 7 broadside array models (b)

TRANSFER FUNCTION

In the preceding part of this chapter we paid attention to directivity only. However, as discussed in section 3.4 (figure 3.23 and 3.24), the transfer function and output level of the microphone array are important for shaping and eventual amplification of electronic internal noise. Figure 4.26 gives the measured transfer functions of the portable endfire and broadside arrays. The measurements have been carried out with and without the correction filter. The uncorrected transfer functions have a slope of  $+6$  dB/octave up to  $4000$  Hz. Above  $5500$  Hz the output level diminishes. When high frequency amplification is sufficient the uncorrected transfer functions are very useful for suppression of low frequency noise. The correction filter has been designed in such a way that the spectrum of both arrays is flattened resulting in a flat spectrum ( $\pm 2$  dB) between  $500$  and  $4000$  Hz. Above  $3500$  Hz the frequency spectrum of the broadside array is superior in comparison with the frequency response of the endfire array.



a. Portable endfire array



b. Portable broadside array

Figure 4.26 Transfer functions of the endfire and broadside array without and with application of a correction filter.

## CONCLUSION

The developed portable endfire and broadside microphone arrays have a high and repeatable directivity. Both arrays have a spectrum with a slope of +6 dB/octave which can, optionally, be flattened between 500 and 3500 Hz with a correction filter. Above 3500 Hz the frequency spectrum of the broadside array is superior to the frequency response of the endfire array. We may conclude that with the developed portable array microphones a high directivity with an appropriate spectrum can be achieved.





---

# TECHNICAL ASSESSMENT IN NOISE FIELDS

## Chapter 5

### 5.1 Introduction

Cocktailparty	In a typical cocktailparty situation the background noise has two constituents: direct noise of the voice babble of all competing talkers and reverberation noise, being the voice babble reflected by the room. In relatively large halls the listeners will mainly hear the voice babble of the people surrounding them, but in small reverberant halls, often with relatively low ceilings, the listeners mainly hear a general noise <i>filling the entire space</i> . It may be expected that in a lot of practical situations the microphone array has to attenuate noise coming from all directions with a diffuse character. Therefore, we decided that the developed microphone arrays should be tested in a situation with a noise field having a diffuse character.
Technical Assessment	In this chapter the results will be presented of the technical assessment of our arrays in two noise fields. In section 5.2 the equationmanikin for the reverberation distance is generalized for the directivity at the source as well as at the receiver side. A description of the experimental set-up is given.

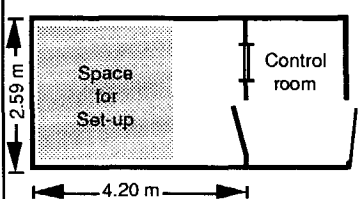
Artificial diffuse noise field	<p>The experimental equipment simulates a true cocktailparty: one loudspeaker in front of the listener simulates the partner in a discussion and eight loudspeakers produce an <i>artificial diffuse noise field</i>.</p> <p>The experimental set-up is used in section 5.3 for measurements with the KEMAR manikin. The manikin was placed in the centre of the set-up and the attenuation of the noise field was measured for the (portable) microphone arrays developed and also for a hearing aid with an omni-directional and directional microphone respectively. The same experimental set-up is also used in chapter 6 for the listening tests (main objective).</p>
Reverberation distance	<p>Finally, section 5.4 gives the results of measurements carried out in a large church-hall. The sound pressure level as function of the distance to a loudspeaker is measured with an omni-directional microphone and the developed microphone arrays. The influence of the microphone arrays on the reverberation distance in the hall is determined.</p>

## 5.2 Experimental Set-up with an Artificial Diffuse Noise field

Soundtreated room The experimental set-up, described in this section, was primarily developed for the assessment of the microphone arrays with (hearing impaired) subjects. For this reason, the experimental set-up has been built in a small sound insulated room of the ENT-department in the University Hospital Rotterdam. The small rectangular room is 2.59 x 4.20 meters and has a height of 2.20 meters. The room is soundtreated and the resulting high sound absorption and very low reverberation time make the room suitable for several clinical tests. Table 5.1 gives a survey of important parameters and a sketch of the room with a control room next to it.

For the assessment of the microphone arrays we wanted to simulate a cocktailparty situation and we decided to create an artificial diffuse noise field with a sufficient number of independent sound sources.

Table 5.1 Parameters of sound treated room in the University Hospital Rotterdam.

	Size	Acoustic parameters
	length 4.20 m width 2.59 m height 2.20 m volume 23.9 m <sup>3</sup> surface 46.6 m <sup>2</sup>	mean absorption $\bar{\alpha}_s$ 0.4 reverberation time $T$ 0.2 s reverberation distance $r$ 1.0 m

5.1

Artificial sound field In principle, such an artificial sound field can be theoretically produced in an anechoic room using an infinite number of independent, but equally intense, single sound sources being uniformly distributed over a sphere. Veit (1987) showed that in a practical realization with only 8 independent sound sources at the corners of an imaginary cube a spatially limited diffuse sound field could be obtained in an anechoic room. Based on this article we decided to simulate a cocktailparty in the sound insulated room with 8 loudspeakers. We used 8 independent noise sources with a spectrum equal to the long time average spectrum of speech and adapted the arrangement of the loudspeakers giving a better diffusivity: the four loudspeakers at the top were positioned at the edges of the cube (see figure 5.2).

First, we give a short description of a diffuse sound field and use this description to generalize the critical distance between a source and receiver in a room. Afterwards, a description and characterization of the experimental set-up will be given.

#### THEORETICAL NOTES ON A DIFFUSE SOUND FIELD

A sound field can be called diffuse when it is homogenous and isotrope; it may be considered as an infinite number of uncorrelated plane waves with equal intensity and an equal distribution over all directions. For a sound field the intensity  $I_{\Omega}$  coming from a certain angle in space  $d\Omega$  can be defined as:

$$I_{\Omega} = \frac{dI}{d\Omega} \quad (5.1)$$

with the intensity being defined as

Intensity  $I = \lim_{T \rightarrow \infty} \frac{1}{T} \int_0^T p \cdot v \, dt$  . (5.2)

For a diffuse sound field the modulus  $I$  of  $I_{\Omega}$  will be constant for all angles. Now, consider the far field of a point source. The intensity of a travelling plane wave in air equals:

$$I_{\text{plane}} = \frac{p_{\text{eff}}^2}{\rho c} \quad (5.3)$$

where  $p_{\text{eff}}^2$  represents the mean square effective sound pressure,  $\rho c$  the acoustic impedance of air with  $\rho$  and  $c$  the density and sound velocity in air.

Diffuse sound field In a diffuse sound field we will define the intensity  $I_{dS}$  as the acoustic power flow in *one* direction through an incremental area  $dS$ . (If we considered the power flow of a diffuse sound field in two directions we would obtain  $I_{\text{diffuse}}=0$ ).

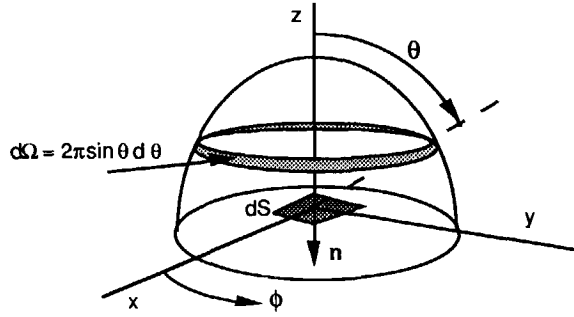


Figure 5.1 Contribution by  $d\Omega$  to the acoustic power flow through  $dS$ .

The acoustic power flow through  $dS$  will be built up by the normal components of the intensities of all plane waves in a halfspace above  $dS$ . Take a hemisphere with unit radius ( $r=1$ ) around  $dS$  (figure 5.1). The contribution of the surface  $d\Omega = 2\pi \sin\theta d\theta$  to the acoustic power flow equals:

$$dI_{dS} = I_{\Omega} \cdot n \cdot d\Omega = 2\pi I_{\Omega} \sin\theta \cos\theta d\theta \quad (5.4)$$

resulting in a total  $I_{dS}$  through the surface:

$$I_{dS} = \int_0^{\pi/2} 2\pi I_{\Omega} \sin\theta \cos\theta d\theta = \pi I_{\Omega} \quad (5.5)$$

Further, in the surface  $dS$  the effective pressure is given by :

$$p_{\text{eff}}^2 = \sum \delta p_{\text{eff}}^2 \quad (5.6)$$

where the effective pressures  $\delta p_{\text{eff}}^2$  of all uncorrelated plane waves in  $dS$  according to equation (5.3) are equal to:

$$\delta p_{\text{eff}}^2 = \rho c I_{\Omega} d\Omega \quad (5.7)$$

For an infinite number of plane waves  $p_{\text{eff}}^2$  equals (with  $I_{\Omega}$  is constant):

$$p_{\text{eff}}^2 = \rho c I_{\Omega} \int_S d\Omega = 4\pi \rho c I_{\Omega} \quad (5.8)$$

Equation 5.8 shows that in a diffuse sound field the intensity  $I_{\Omega}$  as well as the effective acoustic pressure will be constant.

The acoustic power flow through a surface  $dS$  can now be obtained combining equations (5.5) and (5.8):

$$I_{dS} = \frac{p_{\text{eff}}^2}{4 \rho c} \quad (5.9)$$

Sound source  
in a room

Consider a receiver with a directivity factor  $Q_r$  (equation 2.43) at a distance  $r$  from a sound source in a closed room. The stationary sound source emits a total acoustic power  $W$  and it has a directivity factor  $Q_s$  in the direction of the receiver. The direct sound field  $p_{d,eff}$  at the receiver equals:

$$p_{d,eff}^2 = \frac{\rho c}{4\pi r^2} Q_s W \quad (5.10)$$

The direct sound will be absorbed and partially reflected at the boundaries of the room. The reflected power  $W'$  is available for the build-up of a reverberated acoustic sound field:

$$W' = W (1 - \bar{\alpha}_s) \quad (5.11)$$

where  $\bar{\alpha}_s$  represents the average energy absorption coefficient of the surface of the room. For a stationary situation the reflected power  $W'$  will be absorbed by the total absorption of the room:

$$W_{abs} = W' \quad (5.12a)$$

and assuming a diffuse reverberated sound field:

$$W_{abs} = I_S A \stackrel{(5.9)}{=} \frac{p_{rev,eff}^2}{4\rho c} A \quad (5.12b)$$

where  $A$  represents the total acoustic absorption in the room being equal to  $A = \bar{\alpha}_s S$ ,  $S$  the total surface of the room and  $p_{rev,eff}$  the effective sound pressure level of the reverberated sound field. We can rewrite equation (5.12b) and substitute (5.11) giving the effective reverberated sound pressure level:

$$p_{rev,eff}^2 = 4\rho c \frac{(1 - \bar{\alpha}_s)}{A} W \quad (5.13)$$

Reverberation  
distance

Generally, the reverberation distance is defined as the distance  $r$  where the level of the direct sound field equals the level of the reverberated sound field. However, using a directional receiver we will generalize this definition: the reverberation distance is defined as the distance  $r_{cd}$  where the direct energy received from a source equals the energy *received* from all other directions:

$$p_{dir,eff}^2 = Q_r p_{rev,eff}^2 \quad (5.14)$$

with  $Q_r$  the directivity factor of the receiver.

This results in a generalized reverberation distance (with 5.10 and 5.13):

$$r_{rd} = \frac{1}{4} \sqrt{\frac{Q_s Q_r A}{\pi (1 - \alpha_s)}} = \frac{1}{4} \sqrt{\frac{Q_s Q_r R}{\pi}} \quad (5.15)$$

with the *Room Constant* R being defined as:

$$R = \frac{A}{1 - \alpha_s} \quad (5.16)$$

Frequently, the *reverberation distance of a room* is used for a source freely placed in the centre of a room with  $Q_s = 1$  and  $Q_r = 1$ . The reverberation distance of a room is also known as critical distance or diffuse field distance.

### EXPERIMENTAL SET-UP

As mentioned before, the experimental set-up consists of 9 loudspeakers and is placed in the sound insulated room (figure 5.1). Figure 5.2 gives a sketch of the experimental set-up. One loudspeaker (Celestion CL3) is positioned at a height of 1.25 meter in front of the listener and simulates the partner in a discussion during the listening test. The artificial diffuse sound field is realized with 8 small loudspeakers (Philips Matchline CE-75 series). The loudspeakers are positioned at the boundaries of an imaginary rectangular box inside the room.

5.2

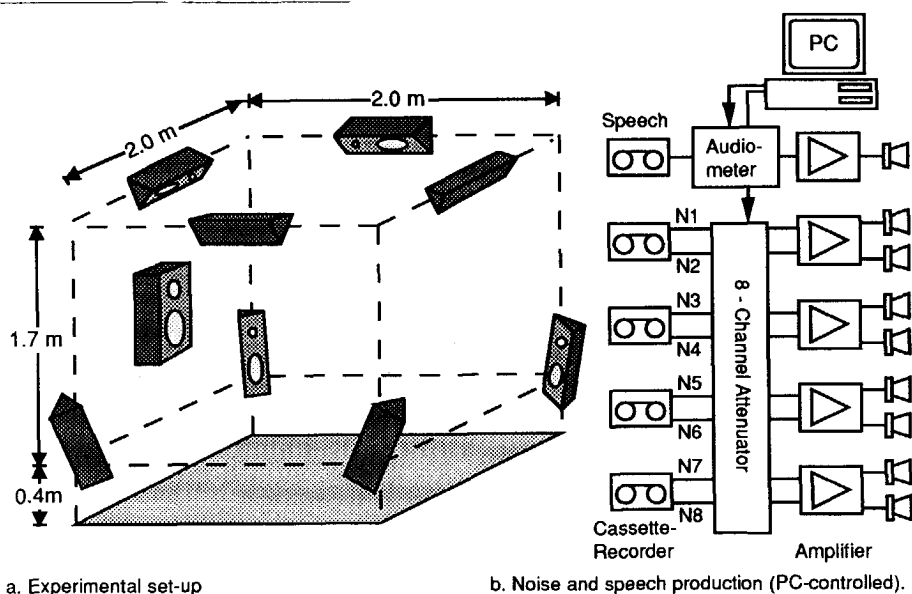
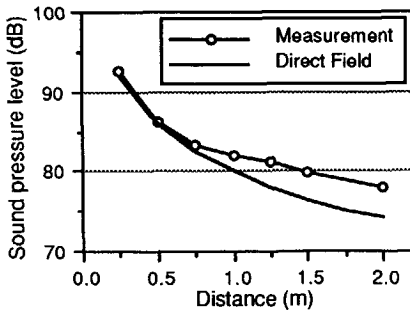


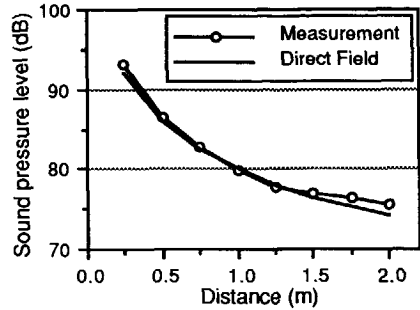
Figure 5.2 Sketch of the experimental set-up in the sound insulated room of the ENT-department of the Erasmus University Dijkzigt Hospital.

The dimensions of the box (2.0 x 2.0 meters and height 1.70 meters) are mainly determined by the boundaries of the room and are chosen in such a way that the head of a seated subject would be in the centre of the box. Four loudspeakers are placed near the ceiling of the room at the edges of the rectangular box and the other ones are placed vertically (height 40 cm) at the corners of the box.

Independent Noise	The 8 loudspeakers are fed from 4 stereo-cassette recorders (Technics RSB-105) and 4 stereo amplifiers (Akai AMA-202b) (figure 5.2b). Thus, 8 independent noise sources are obtained using 4 cassette-tapes with noise recorded on each channel. The use of independent noise sources is important to avoid undesired interference effects of the radiated sound waves. The sound levels of the speech and the noise field can be varied with an audiometer and an in-house developed 8-channel attenuator respectively; both being controlled by a personal computer.
Reverberation	Because the experimental set-up is realized in the sound insulated room, the sound of each loudspeaker will also contribute to the reverberated sound field in the room. The influence of the reverberated sound field in the centre of the imaginary box depends on the specific reverberation distance of each loudspeaker and is mainly determined by the room parameters and the directivity factor of the loudspeakers. The room parameters are given in table 5.1 and the directivity factor of the loudspeakers was measured in the anechoic room (see section 4.2): $Q_s(\text{Celestion}) = 3.7$ and $Q_s(\text{Philips}) = 3.4$ . We can now estimate the reverberation distance using equation (5.15). This results in $r_{rd} = 1.50$ m for the speech loudspeaker and $r_{rd} = 1.45$ m for the noise loudspeakers. We can verify this estimation with the measurement of the sound pressure level as a function of the distance to the loudspeaker. Figure 5.3 gives the measured sound pressure level in the experimental set-up as a function of the distance to the speech loudspeaker and one noise loudspeaker. The level of a theoretical direct sound field is also given (1/r-law). The measurements of the sound pressure level are carried out on a horizontal and diagonal line through the centre of the experimental set-up being the axes of the speech loudspeaker and one of the noise loudspeakers at the ceiling respectively. Figure 5.3a shows that at the centre of the box (distance 1 m) the sound level of the speech loudspeaker is increased with 1.4 dB due to the reverberated sound of the speech loudspeaker. The reverberation distance equals 1.60 m and corresponds reasonably well with the estimated critical distance.
Distance	



a. Speech loudspeaker (Celestion).



b. Noise loudspeaker ceiling (Philips).

Figure 5.3 Measured sound pressure level as a function of the distance between the loudspeaker and a sound level meter with an omni directional microphone.

However, figure 5.3b shows that the reverberation distance of the noise loudspeakers at the ceiling is considerably larger than the estimated value of 1.45 m. An explanation can be found in the position of the noise loudspeakers near the ceiling and floor. The noise loudspeakers will have a mirror-source due to the lower sound absorption of the ceiling and floor, giving a hard boundary. This results in a higher direct sound field and, equivalently, a higher directivity factor and thus a reverberation distance larger than 2 m (Beranek, 1954).

Summarizing, the sound level of the front loudspeaker (which will be used for speech reproduction) will be increased in the centre of the box with 1.4 dB due to reverberation.

#### DIFFUSIVITY MEASUREMENTS

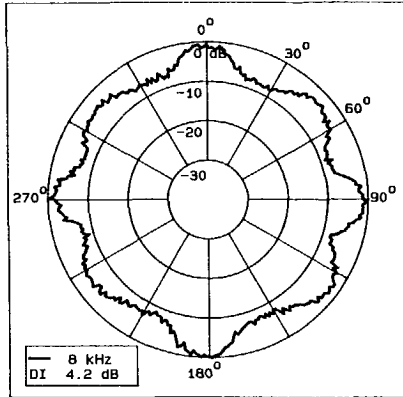
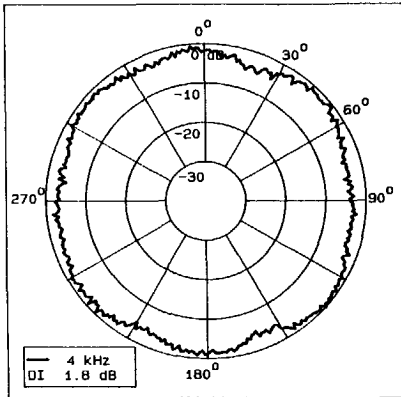
The determination of the degree of diffusion, i.e. the diffusivity, of the artificial noise field can be done in three ways.

##### Intensity Meter

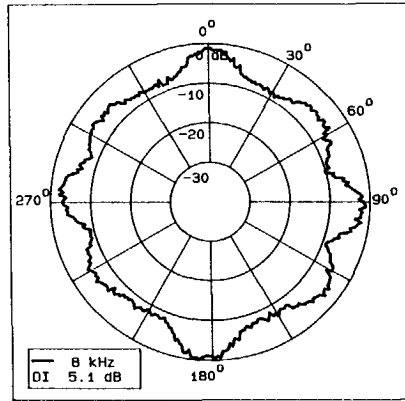
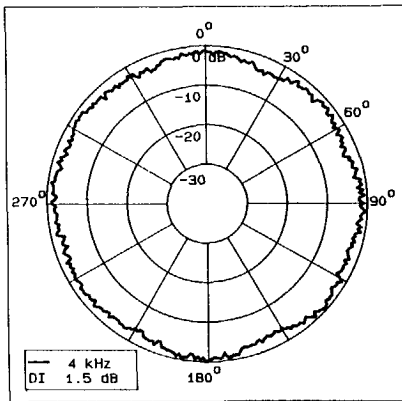
The spatial distribution of the sound pressure and, in addition, the sound intensity with a modern *intensity meter* is determined using a two-microphone technique. Although this method was used by Veit to determine the diffusivity of the 8 loudspeakers on the edges of a cube, it has the disadvantage of a low angular resolution. The two-microphone intensity probe of the modern intensity meter has the property of a dipole (figure 2.16) and thus a low directivity (<4.8 dB) and a large main beam with a (-6 dB) beam width >130°.



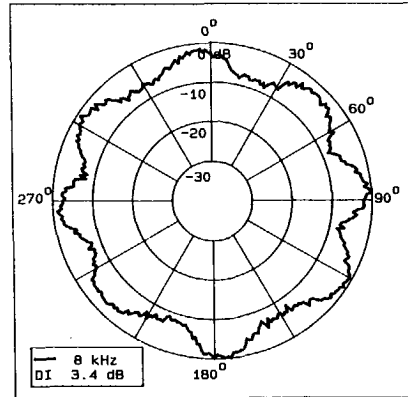
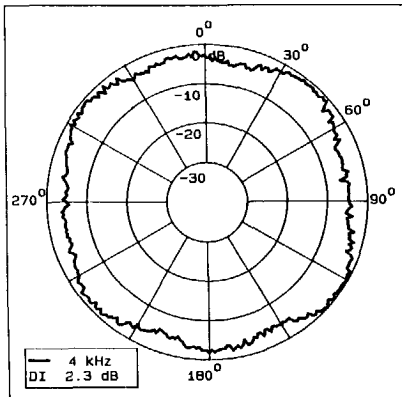
Highly Directional Microphone	<p>Other methods, also mentioned by Veit, are the determination of the diffusivity using <i>cross-correlation techniques</i> and the determination of the sound intensity coming from different directions to a given point in a room with a <i>highly directional microphone</i>. It is clear that the last measurement method can easily be carried out using one of the microphone arrays!</p> <p>In the following measurements we have used the broadside array because we expected that diffusivity deviations could better be discriminated with the very narrow horizontal main beam (figure 4.24). The diffusivity variations were determined by using the 'Polaris' system (section 4.2) with the broadside microphone placed on the turntable. The eight loudspeakers radiated wide band noise and the microphone signal was filtered with a 1/1 octave band-pass filter. The diffusivity is measured on a sphere with radius 10 cm in the centre of the imaginary box.</p>
Results	<p>Figure 5.4 gives the polar diagrams for the 4 and 8 kHz octave band with the array, at the fixed radius <math>r = 10</math> cm, horizontally (<math>0^\circ</math>) and the array 'looking' up and down <math>40^\circ</math>. The <math>0^\circ</math>-direction in the polar diagrams equals one of the corners of the box (with a loudspeaker on the ground). The intensity measurements show that we have obtained an acceptable artificial diffuse noise field on a sphere with radius 10 cm. In the 4 kHz octave band the variation in the output signal of the microphone array equals <math>\pm 2.5</math> dB. For the lower frequencies (not presented) this was, as we can expect, even better. The measurements for the 8 kHz octave band show the limitation of the artificial diffuse noise field. The variation in the output signal equals <math>\pm 4</math> dB, but with this set-up we have 8 noise sources (<math>d\phi = 45^\circ</math>).</p>
Conclusion	<p>Summarizing, we may conclude that in a sphere with radius 10 cm in the centre of the box an acceptable artificial diffuse noise field can be made with 8 loudspeakers. The diffusivity measurements with the broadside microphone array show that up to the 4 kHz octave band (2800-5600 Hz) a maximum deviation of the output signal of <math>\pm 2.5</math> dB can be reached. This is sufficient for the simulation of a practical cocktailparty situation and our speech intelligibility test.</p>



a. Broadside microphone horizontally 0°.



b. Broadside microphone 'looking' down -40°.



c. Broadside microphone 'looking' up 40°.

Figure 5.4 Diffusivity on a sphere with  $r=10$  cm in the centre of the experimental set-up with 8 loudspeakers. Measurements carried out with 'Polaris' and a broadside microphone array (viz. section 4.2 and figure 4.24 resp.).

5.3KEMAR Measurements in Artificial Diffuse Noise Field

In section 4.4 directivity measurements were done in the anechoic room with microphones connected to the head of a KEMAR manikin. It was stated that the real value of the directivity index could only be determined when either the full three dimensional directivity pattern could be measured, or when measurements could be carried out in a *diffuse noise field*. The directivity index can be determined from the measured ratio between the sensitivity of the microphone in the *main* direction relative to all other directions.

Front-Random

These measurements can be easily done with the experimental set-up using the 9 loudspeakers (figure 5.2); we are mainly interested in the attenuation of background noise relative to the desired speech signal in the *front* direction. Two spectra, i.e. transfer functions, of the microphone must be measured: the *front* spectrum with noise coming from the front loudspeaker and the *random* spectrum with the artificial noise field of all eight noise loudspeakers. After correction of the spectra for small spectral differences between the front and diffuse field by the use of spectrum measurements with a standard omni-directional microphone, the ratio of the sensitivity in the *front* direction relative to all other directions is given by the difference of the two spectra (figure 5.5).

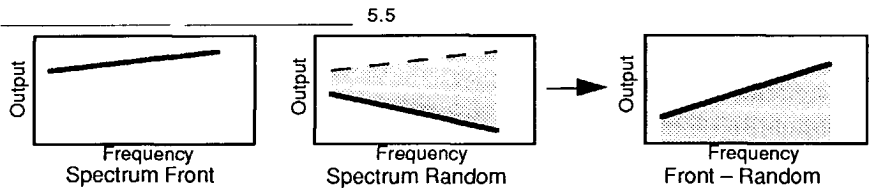


Figure 5.5 The ratio of the sensitivity in the *front* direction relative to the mean of other directions is determined by the measurement of two spectra: the *front* spectrum with noise coming from the front and the *random* spectrum in the artificial diffuse noise field.

Actually, the ratio of the sensitivity in the *front* direction relative to the mean of other directions, will give us the *Front-Random* index and not the directivity index because it is defined for the *main* direction. The value of the front-random index may become negative when the highest sensitivity deviates from the *front* direction but, in case of a positive front-random index, the indices are equal.

Measurement Set-up

The speech loudspeaker was fed with noise having the same spectrum as the other 8 loudspeakers. First, the resulting spectrum of the loudspeaker

and the spectrum of the diffuse noise field were measured with an omni directional B&K4134 1/2 inch pressure microphone and a B&K2133 spectrum analyzer in order to correct the actual measurements for the differences between the spectra of the front loudspeaker and the artificial diffuse noise.

Then, the actual measurements were carried out with the KEMAR manikin placed in the centre of the experimental set-up facing towards the front loudspeaker (distance 1 meter). The KEMAR measurements were first carried out with two behind the ear hearing aids: one with an omni directional microphone and one with a cardioid microphone and, secondly, with the portable broadside and endfire microphone arrays. The hearing aids were connected to the right ear of KEMAR with an earmould (Libby-horn with foam-plug). The signals of the microphone arrays were measured via the behind the ear hearing aid using an induction-loop and the induction coil of the hearing aid. (This equals the listening test set-up, s. section 7.2)

Results The results of the measurements are given in figure 5.6. The measured attenuation of the diffuse noise field relative to the noise coming from the front direction is given as a function of the frequency in 1/3 octave bands (400-5000 Hz). The mean level is computed from the 1/3 octave bands with equal weights.

Discussion The measurement with the hearing aid containing a normal omni directional microphone shows that the diffuse sound field is *not* attenuated. The mean value of -1 dB means an amplification of the diffuse sound field relative to a signal coming from the front. The hearing aid with one cardioid microphone attenuates the diffuse sound field for the lower frequencies with a mean of +1.5 dB. An improvement of +2.5 dB compared with the omni-directional hearing aid and corresponding with every-day practice (Mueller, 1981 and Hillman, 1981). The measurements with the broadside and endfire microphone arrays show a strong attenuation, especially for the high frequencies, with mean values of +6.0 dB and 5.8 dB respectively, in comparison with the omni directional hearing aid an improvement of 7.0 dB (broadside) and 6.8 dB (Endfire)!

Reverberation These results are about 1 dB lower in comparison with the directivity indices estimated from the measured KEMAR directivity patterns in section 4.4. An explanation can be found in the contribution of the reverberated sound of the front loudspeaker. Figure 5.3 shows that the actual sound pressure of the front loudspeaker in the centre of the cube (1.0 meter) is 1.4 dB above the theoretical direct sound pressure level due to the reverberated sound field.

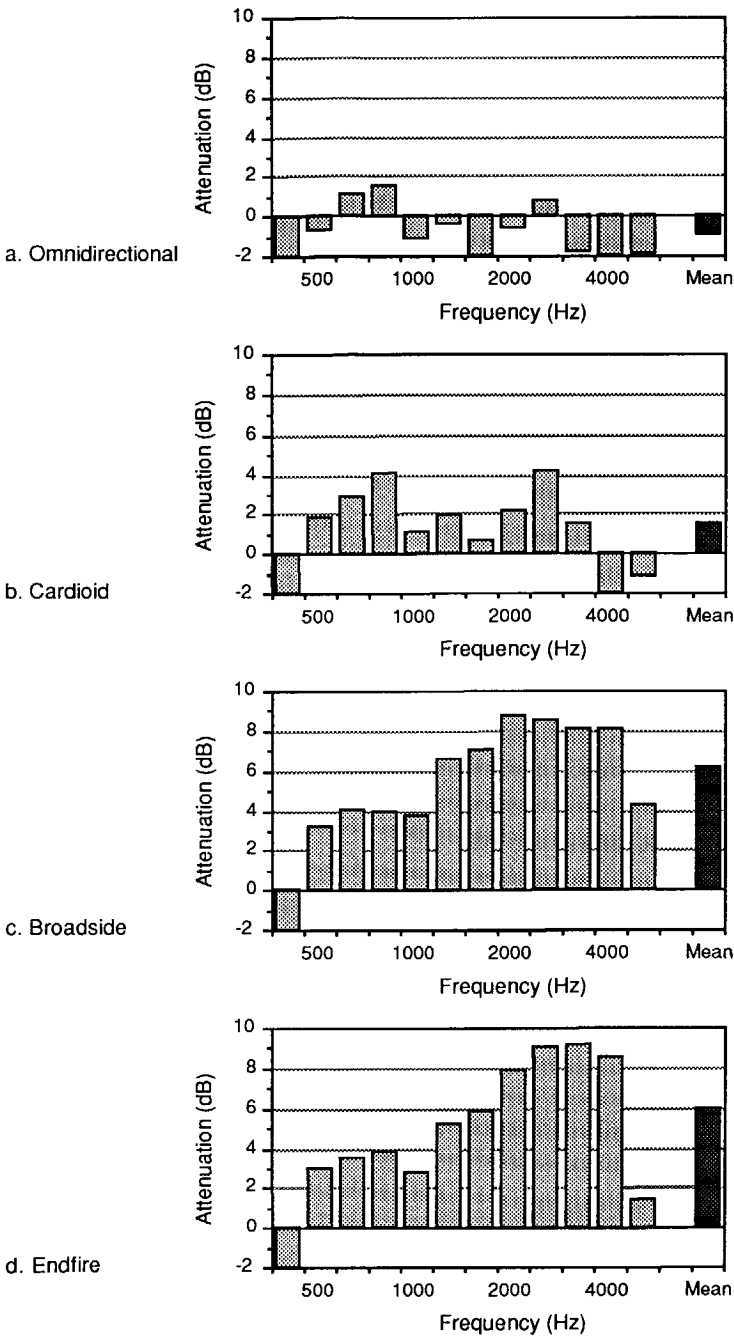


Figure 5.6 Attenuation of a diffuse sound field measured with KEMAR in the experimental set-up. Mean level computed from 1/3 octave bands with equal weights.

The reverberated sound of the front loudspeaker is incorporated in the omni-directional B&K measurements being used for correction. This is especially disadvantageous for the microphone arrays because they are corrected with the omni-directional measurements while the reverberated sound field of the front loudspeaker was already attenuated by the microphone arrays.

#### Conclusions

Summarizing, we may conclude from the KEMAR measurements that a standard behind the ear hearing aid with an omni directional microphone will *not* attenuate a diffuse noise field relative to sound coming from the front of a listener. A hearing aid with a directional microphone gives a small improvement of +2.5 dB in comparison with a normal hearing aid. The broadside array and endfire microphone arrays give an improvement of 7.0 and 6.8 dB respectively. In a truly anechoic situation the improvement of the microphones arrays will be about 1 dB higher.

### 5.4 Free Field Measurement in Natural Diffuse Noise Field

#### Influence of Reverberation

In section 1.4 we summarized research on other solutions. Peterson (1987) and Weiss (1987) reported on improved speech intelligibility in anechoic situations but on moderate results for conditions with a small amount of reverberation (reverberation times 480 and 380 ms respectively). Based on these results and discussions with other research-workers and audiologists, the following question came up:

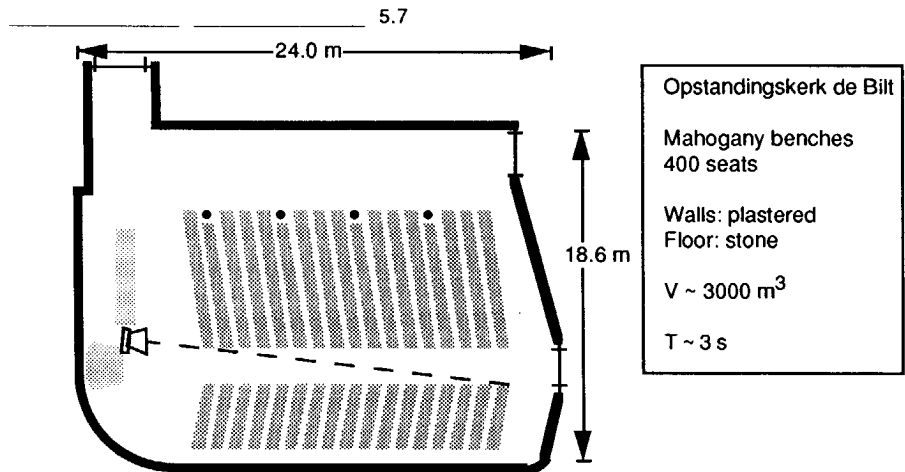


Figure 5.7 Measurement setup in large church-hall.

What is the influence of reverberation and the reverberation distance of a room on the expected improvement of the speech intelligibility when we use a microphone array? In order to answer this question, we determined the influence of the microphones on the reverberation distance using measurements carried out in a large church-hall (figure 5.7).

Reverberation  
distance

Assuming  $(1-\overline{\alpha_s}) \sim 1$ , the reverberation distance for this situation can be computed by substitution of the well-known reverberation equation of Sabine,

$$T \approx \frac{1}{6} \frac{V}{A} \quad (5.17)$$

where  $T$  represents the reverberation time,  $V$  the volume of a room and  $A$  the total absorption, in the generalized equation for the critical distance (5.15):

$$r_{rd} = \frac{1}{4} \sqrt{\frac{V Q_s Q_r}{6\pi T}} \quad (5.17)$$

For our situation  $V = 3000 \text{ m}^3$ ,  $T = 3 \text{ s}$  and a loudspeaker with  $Q_s = 3.4$  the estimated reverberation distance for an omni-directional microphone ( $Q_r = 1$ ) will be 3.4 meters. Using the measurements of the preceding section we can expect that the microphone arrays suppress the reverberated field by 6 dB being equivalent with a directivity factor  $Q_r = 4$  and thus a reverberation distance of 6.8 meters.

Measurement

A loudspeaker was placed in front of the benches at a height of 2 meters and fed with noise having a spectrum of the long time average of speech. First, the sound pressure level was measured as a function of the distance to the loudspeaker with a B&K sound level meter and an omni-directional 1-inch microphone. Afterwards, the same measurement was carried out with the broadside and endfire microphone arrays connected to the sound level meter keeping the main beam in the direction of the loudspeaker.

Figure 5.8 gives the results of the sound level measurements as a function of the distance carried out in the church-hall. The theoretical direct sound pressure level of a point source and the levels of the reverberated sound field are added to the figure.

Discussion

The measurement with the omni directional microphone shows that at a large distance from the source the reverberated sound pressure level equals 79 dB. The reverberation distance is given by the crossing of the reverberated pressure level with the direct sound pressure level and is equal to 3.3 meters being comparable with the estimated value. For the broadside and endfire microphone arrays the resulting reverberated sound pressure level equals 73 dB and the new reverberation distance 6.7 m.

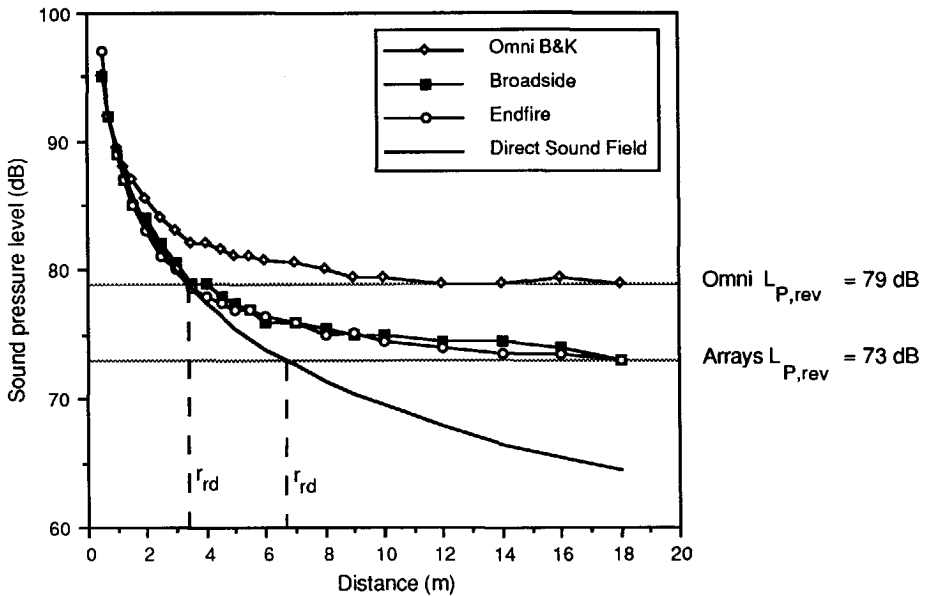


Figure 5.8 Sound pressure level as a function of the distance of a source in a church-hall.

As expected, the microphone arrays have doubled the reverberation distance of the hall.

**Speech Intelligibility** The measurements show that the microphone arrays will attenuate a diffuse reverberated sound in every place in a room. However, an improvement of the speech intelligibility will only be obtained when the distance of speaker to listener does not get too large. When we assume a *critical listening* distance of a person being the maximum distance between listener and speaker for satisfactorily speech intelligibility, it can be expected that this distance will be doubled. Outside this doubled critical listening distance the diffuse sound field will be attenuated but the direct sound level of speech is still too low.

**Conclusion** Summarizing, we may conclude that our microphone arrays will attenuate a diffuse sound field in a room with 6 dB and double the reverberation distance.



---

# LISTENING TESTS

## Chapter 6

### 6.1 Introduction

Speech-Reception  
Threshold (SRT)

In this chapter the results of listening tests for the assessment of the microphone arrays developed will be presented. The listening tests were carried out in the experimental set-up in the Erasmus University Dijkzigt Hospital (section 5.2) with 75 subjects: 30 young normal-hearing subjects and 45 hearing impaired subjects. The listening test set-up is described in section 6.2: speech-reception thresholds in noise will be determined with and without the microphone arrays using lists of short sentences, presented according to a simple up-down procedure that estimates the 50% intelligibility level: the so-called *Speech-Reception Threshold* (SRT). Section 6.3 gives the results of monaural listening tests. The monaural improvement of the SRT in noise for the microphone arrays is determined using one broadside or one endfire microphone array. Finally, section 6.4 gives the results of binaural listening tests. The binaural improvement of the S/N ratio is determined using two endfire microphone arrays.

## 6.2 Description of the Listening Test

The following description of the listening test is divided into three parts:

- Listening test procedure.
- The actual experimental listening test set-up
- Listening via induction and telecoil.

### LISTENING TEST PROCEDURE

SRT in noise

The listening test procedure is based on a model for the SRT of hearing impaired people developed by Plomp and the results of a series of investigations on the SRT in noise (Duquesnoy, 1983 and Plomp, 1986). The model and investigations show that a hearing loss for speech can be interpreted as a combination of two classes: the first class, an elevation of the SRT in quiet, and the second class, manifesting itself in a higher speech-to-noise ratio required for speech intelligibility. Figure 6.1 gives a compilation of the results for the SRT for sentences in a typical every day listening situation as a function of noise level. The SRT is given for normal-hearing young persons (20–29), normal-hearing elder persons (60–69) and a hearing-impaired person with perceptive hearing loss with and without hearing aid. A normal-hearing young person will have an SRT in quiet of  $L_0 = 16 \text{ dB(A)}$  and an SRT in noise rising linearly with the noise level.

S/N ratio

The difference between the SRT in noise and the noise level is defined as the **Critical Speech-to-Noise Ratio** (S/N-ratio). This means that the normal-hearing young person will have a *constant* S/N ratio of  $-8 \text{ dB}$  for noise levels being  $+10 \text{ dB}$  above the SRT in quiet. The curve for elderly persons shows not only an elevation of the SRT in quiet ( $L_0 = 28 \text{ dB(A)}$ ) but also a constant relative elevation of the SRT, i.e. a hearing loss for speech in noise, giving a S/N ratio of  $-5 \text{ dB}$ . The hearing-impaired person in figure 6.1b without hearing aid has also elevated thresholds for speech in quiet and noise ( $L_0 = 44 \text{ dB(A)}$ ) and a S/N ratio of  $-2 \text{ dB}$ . The use of the hearing aid improves the SRT in quiet but the S/N ratio is raised by another  $2 \text{ dB}$ .

Based on these results we can expect a constant S/N ratio for normal-hearing young listeners of  $\sim -8 \text{ dB}$  (binaural with headphones) and for hearing impaired listeners with a hearing aid a S/N ratio of  $\sim 0 \text{ dB}$ . The S/N ratio will be *constant* for sound levels being  $+10 \text{ dB}$  higher than the SRT in quiet.

Therefore, we decided to determine the SRT at two noise levels:  $+20$  and  $+30 \text{ dB}$  above the SRT in quiet. The determination of the SRT at two noise levels can be used for averaging and verification.

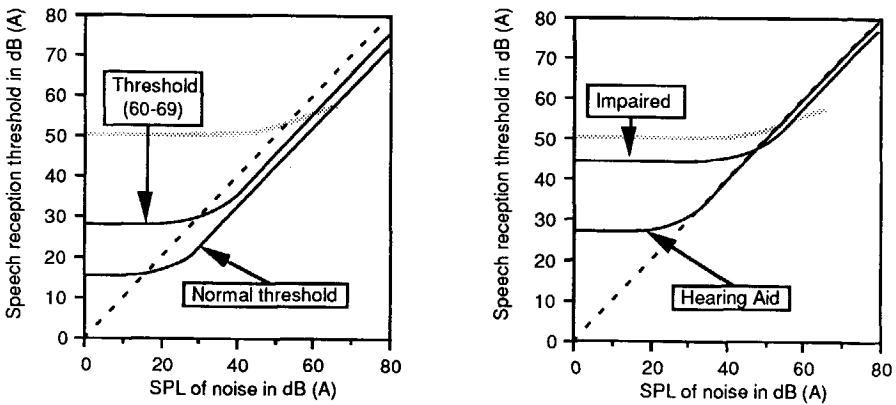


Figure 6.1 Compilation of speech-reception threshold (SRT) for sentences in a typical everyday listening situation as a function of noise level (data and functions from Plomp (1986)). The gray curve is the average sound pressure level of speech in a face-to-face conversation at a distance of 1 m (with increasing level due to interfering noise).

Listening test  
procedure

This results in the following listening test procedure:

1. Determine the SRT in quiet.
2. Determine the SRT in noise with the noise level +20 dB above the SRT in quiet giving the speech-to-noise ratio at +20 dB.
3. Determine the SRT in noise with the noise level +30 dB above the SRT in quiet giving the speech-to-noise ratio at +30 dB.
4. The final speech-to-noise ratio is the mean of the speech-to-noise ratios of 2 and 3.

Speech material

The speech material used consisted of 10 lists of 13 short Dutch sentences, representative of everyday conversation. The recorded sentences had all been read by the same female speaker and adjusted in level for equal intelligibility (Plomp and Mimpen, 1979a). With these lists of sentences a very accurate SRT in quiet and in noise can be determined with a standard deviation of 1 dB. Figure 6.2 gives the intelligibility score, found by Plomp and Mimpen, as a function of presentation level relative to SRT. The slope of the curve around the 50% intelligibility score equals 20%/dB and enables the determination of the 50% SRT with a simple up-and-down procedure.

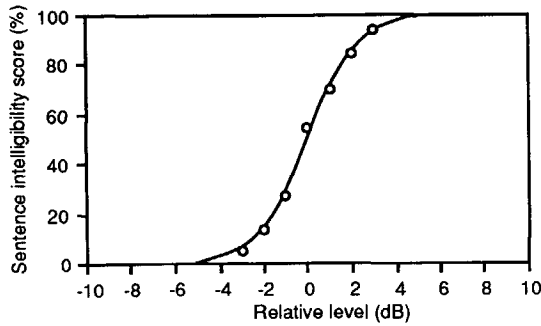


Figure 6.2 Intelligibility score as a function of presentation level relative to SRT (level for 50%) (from Plomp and Mimpen 1979a).

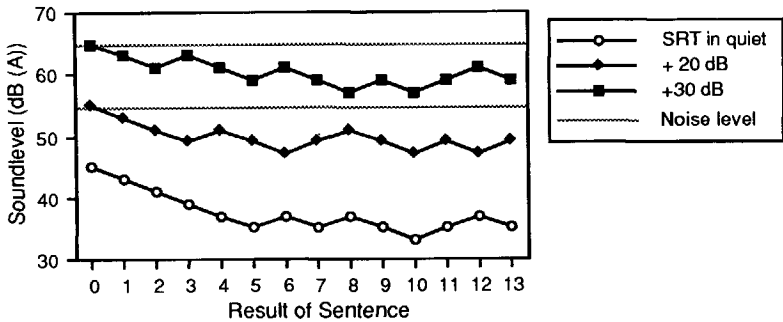


Figure 6.3 Example of a typical listening test run for determination of the SRTs in quiet and in noise.

Up-and-down  
procedure

Figure 6.3 gives an example of a typical listening test run for the determination of the 50% SRT with the Plomp-Mimpen sentences and an up-down procedure. The determination of the SRT in quiet (Step 1) starts with the speech sound level above the SRT. If the listener is able to repeat the sentence correctly, the level is decreased by 2 dB, if he is not, the level is increased by 2 dB. The average level of the last 9 points gives an SRT with a sufficiently low standard deviation. The SRT in noise (Step 2 and 3) is determined in the same way and the run starts at a S/N ratio of 0 dB.

#### EXPERIMENTAL LISTENING TEST SET-UP

The listening tests are carried out in the experimental set-up with the artificial diffuse noise field (section 5.2). One loudspeaker in front of the listener is positioned at 1 m from the centre of the imaginary rectangular box and simulates the partner in a discussion. A Celestion CL3 loudspeaker

was used to obtain an undistorted speech reproduction at high sound levels. The speech and noise sound levels are varied with an audiometer and the 8-channel attenuator respectively; both being controlled by a Personal Computer.

Speech Noise

For the simulation of the background noise at a typical cocktail party we used the speech noise made by Plomp and Mimpen having a spectrum equal to the long-term average spectrum of the sentences. The speech noise may be considered representative of the main source of interference in everyday listening situations: more competing speakers. Because we needed 8 independent noise sources, four stereo cassette tapes were made with the use of a digital signal processor. We recorded 10 seconds of the original speech noise from a Compact Disc (IZF, 1988) with the signal processor. Next, the noise was recorded on the tapes with the signal processor in recycling mode.

Figure 6.4 gives the spectrum of the original noise and the spectra of the artificial diffuse noise field and the speech loudspeaker as measured in the centre of the experimental set-up. The spectra have an equal sound pressure level (A-weighted) and are similar to the original noise on the Compact Disc.

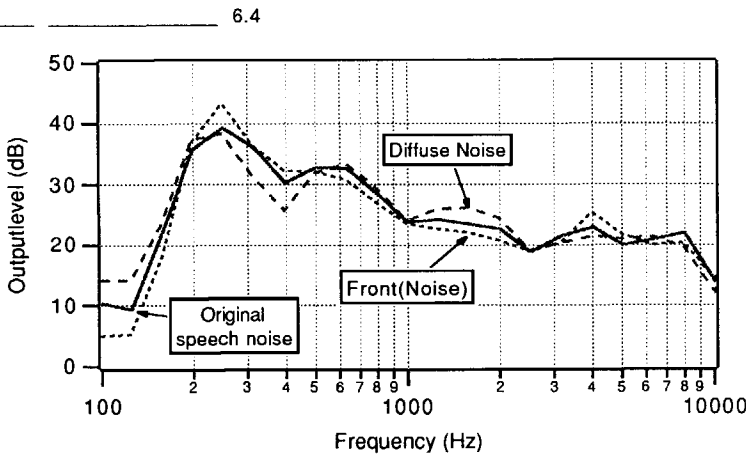


Figure 6.4 Spectrum of original speech noise (Compact Disc) and spectra speech of loudspeaker and artificial diffuse noise field measured in the experimental set-up.

LISTENING VIA INDUCTION AND TELECOIL

For the assessment of the microphone arrays with hearing impaired subjects we decided to use an induction loop and compare the SRTs obtained with an external omni-directional hearing aid microphone and one of the microphone arrays (figure 6.5).

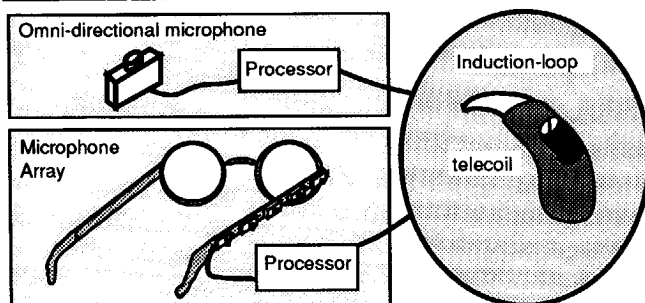


Figure 6.5 The SRTs are determined using an induction loop and the hearing aid of the hearing impaired subject.

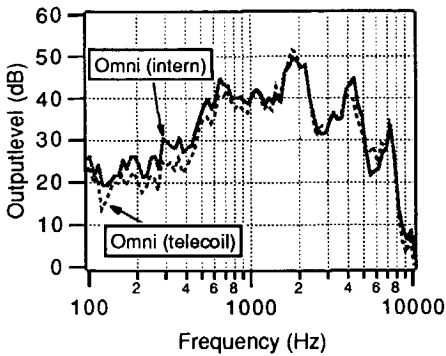
With this method the hearing impaired subject can use his own individually fitted hearing aid.

Insertion Gain  
measurements

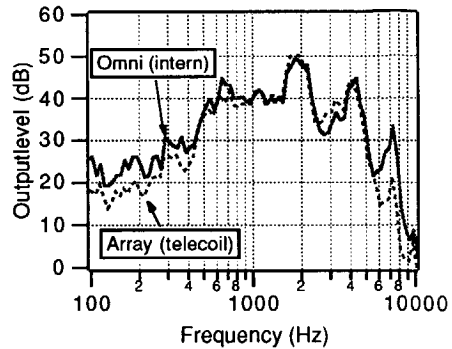
However, for a correct comparison, the resulting transfer functions of the external microphones via induction loop and hearing aid telecoil must be equal to each other and these transfer functions must be comparable with the transfer function of the hearing aid with internal microphone. Therefore, the transfer functions, i.e. the insertion gains, were measured using KEMAR. The output signal of a hearing aid with internal microphone or external microphone via telecoil was measured with the internal KEMAR microphone. Next, the transfer function of the unaided open ear of KEMAR was measured and subtracted from the hearing aid measurements giving the insertion gain. Figure 6.6 gives the results of measurements carried out with three different hearing aids, an omni-directional hearing aid microphone (Knowles EA1842) and the endfire microphone array; a Sennheiser EZI 110 induction-plate was used as induction loop. The insertion gain of the endfire array was measured because we expected a significant difference above 3500 Hz in comparison with the omni-directional microphone due to the transfer function of the endfire microphone (see figure 4.26).

Discussion

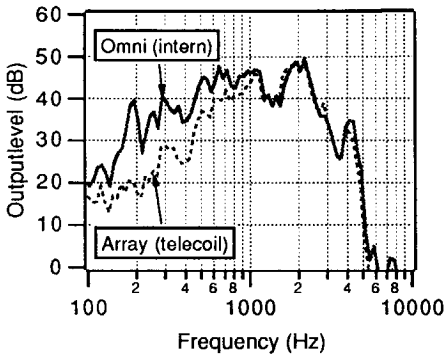
The measurements show that the insertion gain is mainly determined by the hearing aid itself. The peaks are the well-known  $1/4\lambda$  resonances of an open canal formed by the connection tube (Libby-horn with foam-plug) and ear canal. (In view of the insertion gain curve and the position of the peaks, sound has leaked out between the removable 'KEMAR-ear' and the internal ear canal-simulator being comparable with a Y-vented earmould. Therefore, we can only use these measurements for mutual comparison of the curves.)



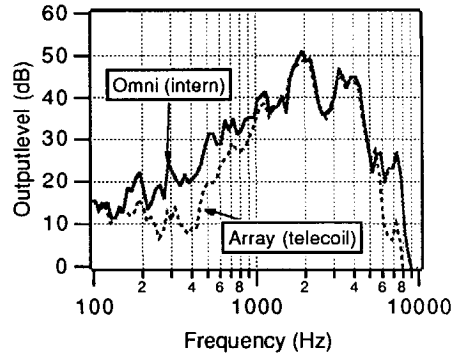
a. Internal and external omni with Philips M47



b. Internal and array with Philips M47



c. Internal and array with Widex ES1



d. Internal and array with Phonak pico-forte

Figure 6.6 Insertion gains of three different hearing aids, an external omni-directional hearing aid microphone and endfire microphone array (flattened spectrum). Measurements carried out with KEMAR.

The insertion gains of the internal microphone and the external omni-directional microphone are equal above 1000 Hz (figure 6.6a). Below 1000 Hz the insertion gain is influenced by the lower sensitivity of the hearing aid telecoil. The insertion gains measured with the three hearing aids and the endfire microphone array show the same characteristics up to 5000 Hz. Above 5000 Hz the output level decreases due to the transfer function of the endfire microphone array. However, this is not detrimental to speech intelligibility.

#### Conclusion

Summarizing, we may conclude that the method of listening via the induction plate and hearing aid telecoil will result in very similar insertion gains up to 5000 Hz for both an external omni-directional hearing aid microphone and a microphone array.

### 6.3 Monaural Listening Tests

- Subjects** The monaural listening tests were carried out with 30 normal-hearing subjects and 45 hearing-impaired subjects. The group of 30 normal-hearing listeners, equally divided in male and female, were mainly physics and medicine students with ages ranging from 19 to 37 and a median age of 26.4 years. The hearing impaired group consisted of 23 male and 22 female subjects, aged 36-90 years and a median age of 68.8. The hearing impaired listeners were asked for their co-operation while visiting the Audiological Centre of the University hospital for hearing-aid inspection. Co-operation was asked after the hearing-aid fitting received its final approval and when a discrimination score of at least 80% for monosyllables presented in quiet was found.
- Monaural tests** The monaural listening tests were all carried out in the experimental set-up according the listening test procedure as described in section 6.2. Each listening test took about 15 minutes. If necessary, the other ear was occluded with a foam plug. Because most subjects did listening tests for two conditions, the order of conditions (e.g. with and without microphone array) was varied to avoid effects of habituation and fatigue, and, moreover, to equalize small differences between the 10 lists of sentences.
- Listening conditions** Table 6.1 gives a review of the various listening conditions for the normal-hearing and hearing-impaired groups. The microphone arrays were connected to a pair of spectacles. The number of listening tests (n) is added per condition. For the group of normal-hearing subjects the listening tests were carried out with changing subgroups for the 4 conditions, as can be concluded from the number of listening tests per condition. Because we were primarily interested in the *comparison* of the omni-directional hearing aid microphone and the microphone arrays, most hearing-impaired subjects did two listening tests for two conditions: hearing aid in combination with the external omni-directional microphone and hearing aid with endfire *or* broadside microphone array.

Table 6.1 Review of **monaural** listening conditions.

Normal-hearing subjects		Hearing-impaired subjects	
Listening conditions	n	Listening Conditions	n
1. Own ear	16	1. External omni microphone via own HA	45
2. Hearing aid* (Philips M47)	14	2. Broadside microphone via own HA	26**
3. Broadside microphone array via hearing aid*	7	3. Endfire microphone array via own HA	27**
4. Endfire microphone array via hearing aid*	6		

\* Via Libby-horn with foam-plug

\*\* All three conditions for 8 listeners

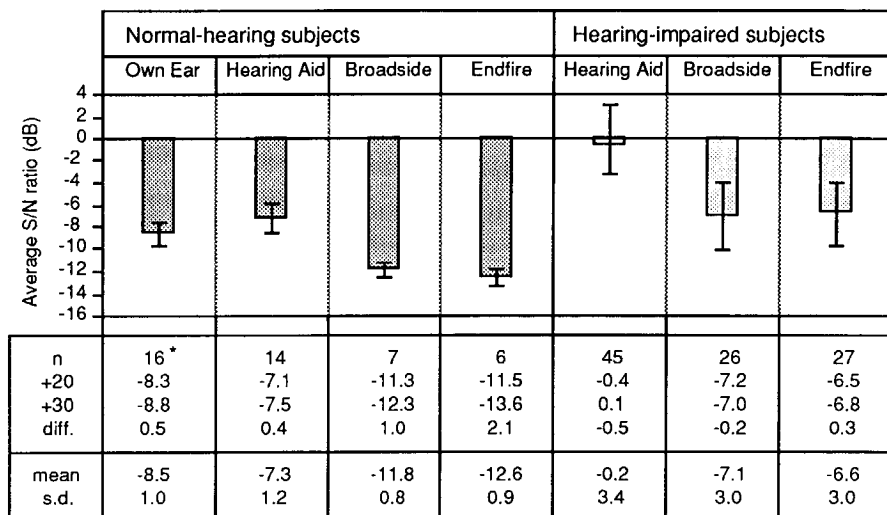


A subgroup of 8 hearing-impaired listeners was willing to do the listening tests for all three conditions. This results in three different subgroups of hearing-impaired listeners: omni and broadside (18); omni and endfire (19); omni, broadside and endfire (8).

SRT in noise

Figure 6.7 presents the averaged S/N ratios and inter-subject standard deviation for the listening conditions given in table 6.1 as a result of the listening tests for the normal-hearing group as well as the hearing-impaired group. In addition, the values of the S/N ratios at +20 and +30 dB and the difference between these values are given.

6.7



\* 10 listening tests added for fixed noise levels of 55 and 65 dB.

Figure 6.7 S/N-ratios as a result of listening tests carried out with normal-hearing and hearing-impaired subjects for different listening conditions.

Reliability

The difference between the values of the S/N ratios at +20 and +30 dB confirms the linearity of the SRTs as found by Plomp (figure 6.2) and the reliability of the mean S/N ratios for most conditions. However, two conditions of the normal-hearing group show a large difference viz. for broadside and endfire microphone arrays. In both cases the +30 dB S/N ratio is expected to be a better estimator of the S/N ratio. The explanation can be found in the sound level of the sentences. In the previous section it was concluded that the S/N ratio would be *constant* for sound levels being +10 dB higher than the SRT in quiet, but using the microphone arrays appears to give such a low SRT for the +20 dB test that the sound level of the sentences becomes only ~8.5 dB above the SRT in quiet. For the normal hearing conditions the standard deviations are less than 1.2 dB.

The standard deviation for the hearing impaired conditions is about 3 dB due to difference in impairment of the subjects.

#### Comparison

A comparison of the S/N ratios shows the following points:

1. The monaural S/N ratio of the normal-hearing group (listening with one good ear) equals -8.5 dB, being better than the values found by Plomp. This difference originates most probably from head-shadow masking in our diffuse noise field.
2. A hearing aid decreases the S/N ratio of the normal-hearing listeners by 1.2 dB.
3. The S/N ratio of the normal-hearing group can be improved using a microphone array.
4. The hearing-impaired group listening with the omni-directional microphone has a S/N ratio of only -0.2 dB with a large standard deviation of 3.4 dB.
5. The microphone arrays give a significant improvement of the S/N ratios for the hearing-impaired group. The absolute values of the average S/N ratio obtained with the microphone arrays is comparable with the S/N ratio of the normal-hearing group listening with one good ear!

#### Improvement

##### S/N ratio

Because we are mainly interested in the *comparison* of the S/N ratio of the omni-directional microphone and the microphone arrays of the hearing-impaired listeners, figure 6.8 gives the histograms of the improvement of the S/N ratio. The histograms give the combined results of the three different subgroups of hearing-impaired listeners classified with respect to

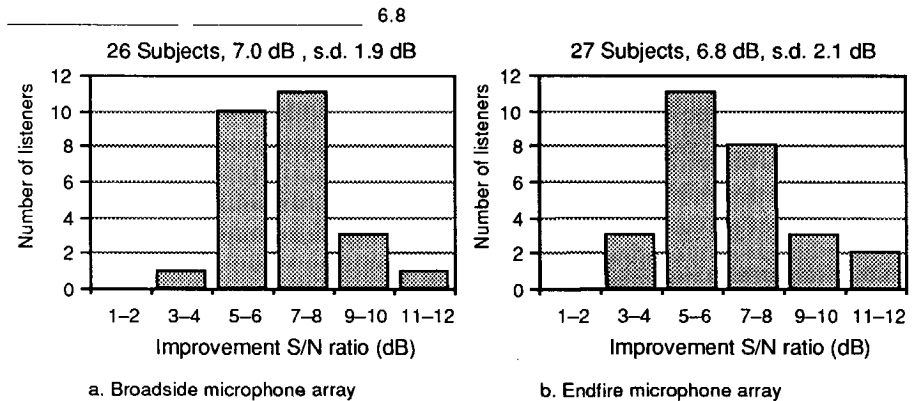


Figure 6.8 Number of patients classified with respect to the improvement of the S/N ratio as a result of comparative listening tests with an omni-directional microphone and a broadside or endfire microphone array. Combined results of three different groups of listeners (45): omni and broadside (18); omni and endfire (19); omni, broadside and endfire (8).

the improvement of the S/N ratio being obtained by using a broadside or an endfire microphone array. The broadside microphone array gives an improvement of 7.0 dB with a standard deviation of 1.9 dB and the endfire microphone array an improvement of 6.8 dB with a standard deviation of 2.1 dB. Most hearing-impaired listeners (41 of 45) obtain an improvement of at least 5 dB! The difference of 0.2 dB between the broadside and endfire microphone arrays is also found for the subgroup of 8 subjects listening to both microphone arrays. Examination of the pure tone and speech (syllable) audiograms of the listeners with an improvement less than 5 dB showed severe recruitment for 3 subjects. The listeners with a relatively high improvement showed to have a relatively flat pure tone audiogram and/or a conductive hearing loss.

Regression analysis Finally, the audiograms of all hearing-impaired subjects were examined (by eye) to find any relation between the type of hearing loss and the improvement obtained with the microphone arrays. Because no significant categories could be distinguished we decided to use regression analysis and examined the relation of the improvement with the Fletcher Index (The averaging hearing loss at 500, 1000 and 2000 Hz; the Fletcher Index is a good predictor of the SRT in quiet) and also with the average hearing loss at 2 and 4 kHz. We used as dependent variables the S/N ratios of the 45 hearing-impaired subjects obtained with the omni-directional microphones and one of the microphone arrays. The analysis revealed a very low dependence on the Fletcher Index (FI), a nearly horizontal regression line with a very low correlation coefficient  $r$ :

Fletcher Index

$$S/N_{\text{omni}} = -1.2 + 0.02FI \quad \text{with } r = 0.09$$

(6.1a)

$$S/N_{\text{array}} = -6.4 - 0.01FI \quad \text{with } r = 0.06$$

(6.1b)

However, the regression analysis for the dependence of the S/N ratios on the average hearing loss at 2 and 4 kHz ( $HL_{2,4}$ ) revealed a more significant dependence due to a higher correlation coefficient:

Average hearing

$$S/N_{\text{omni}} = -8.2 + 0.14HL_{2,4} \quad \text{with } r = 0.55$$

(6.2a)

loss 2 and 4 kHz

$$S/N_{\text{array}} = -12.8 + 0.10HL_{2,4} \quad \text{with } r = 0.45$$

(6.2b)

Figure 6.9 gives the scatter diagram with the derived regression lines for the SRTs in noise as a function of the average hearing loss at 2 and 4 kHz; the average loss equals 57 dB.

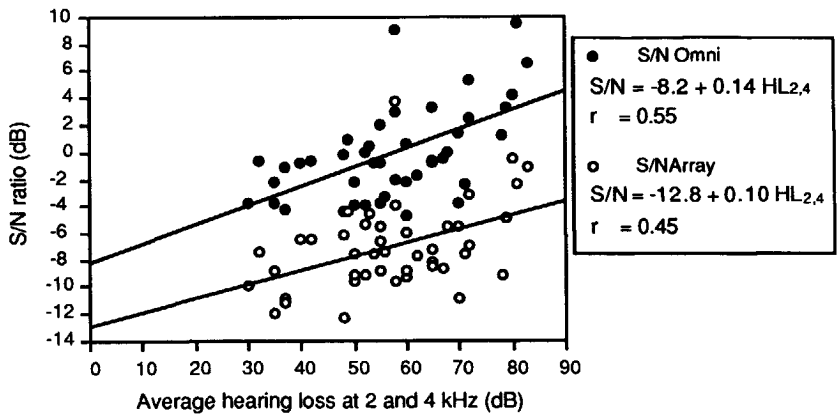


Figure 6.9 Scatter diagram showing the S/N ratios for the listening condition with an omni-directional microphone and one of the microphone arrays as a function of the average hearing loss at 2 and 4 kHz, and the derived regression lines.

The derived regression lines have three interesting properties:

1. The S/N ratio increases for a larger loss at 2 and 4 kHz which is also found by other authors (Bronkhorst 1990 and Smoorenburg 1989).
2. The derived regression lines have different regression coefficients: the microphone arrays appear to give a *higher* improvement of the S/N ratio for larger losses. A simple explanation can be found in the high directivity of the arrays at the higher frequencies: a hearing-impaired listener with a high frequency loss can use this property for a better speech intelligibility.
3. The derived constants in the equations of the regression lines appear to be supported by the results of the listening tests with the normal-hearing subjects! The SRTs obtained with the normal-hearing subjects correspond very well with the derived regression coefficients: -8.5 (own ear) against -8.2 (equation 6.2a) and -12.2 (mean of arrays) against -12.8 (equation (6.2b)).

#### Conclusion

Summarizing, we may conclude that both microphone arrays will give a significant improvement of the S/N ratio for hearing impaired listeners: the mean improvement equals 7.0 dB for the broadside array and 6.8 dB for the endfire array. This improvement will give a monaural S/N ratio comparable with (monaural) normal-hearing young listeners.

From the measured S/N ratios of the normal-hearing group and using the regression analysis of the hearing-impaired group we may conclude that with the microphone arrays an improvement can be expected of:

$$\Delta S/N = 4.6 + 0.04HL_{2,4} \quad (6.3)$$

where equation 6.3 is obtained from the subtraction of equations 6.2b and 6.2a,  $\Delta S/N$  denotes the improvement of the 'un-aided' listener and  $HL_{2,4}$  the average hearing loss at 2 and 4 kHz. This equation may be considered to be valid for normal-hearing people ( $HL_{2,4}=0$  dB) as well as hearing-impaired people (mean of our group  $HL_{2,4}=57$  dB).

## 6.4 Binaural Listening Tests

**Subjects** Binaural listening tests were carried out with only 16 subjects: 10 normal-hearing listeners, 7 male and 3 female, aged 22 to 37 and 6 female hearing-impaired listeners with ages ranging from 47 to 65. Cooperation of the hearing-impaired subjects was asked when a discrimination score of 80% for monosyllables presented in quiet was reached for both ears and hearing aids were fitted to both ears.

**Binaural test** The binaural listening tests were carried out to find an answer to the following questions: Can we find any binaural improvement using two endfire microphone arrays and is this binaural improvement comparable with the binaural improvement found for listening with both ears or two conventional (omni directional) hearing aids? Based on these questions and because only 10 lists of sentences were available, we decided to do four listening tests with each subject seated in the experimental set-up and two endfire microphone arrays connected to a pair of spectacles. The listening conditions are given in table 6.2. The normal-hearing subjects listened to the endfire array with headphones. Headphones (Sennheiser HD230) were used to obtain a relatively high and broadband sound quality and relatively good shielding of the ears for direct sound.

Table 6.2 Listening conditions for monaural and binaural listening tests.

Normal-hearing subjects (n=10) Listening conditions	Hearing-impaired subjects (n=6) Listening Conditions
1. Own ear (monaural) 2. Two ears 3. Endfire array via headphones (monaural) 4. Two Endfire arrays via headphones	1. External microphone via own HA (monaural) 2. Two external microphones with own HAs 3. One endfire via own HA (monaural) 4. Two endfire arrays via HAs

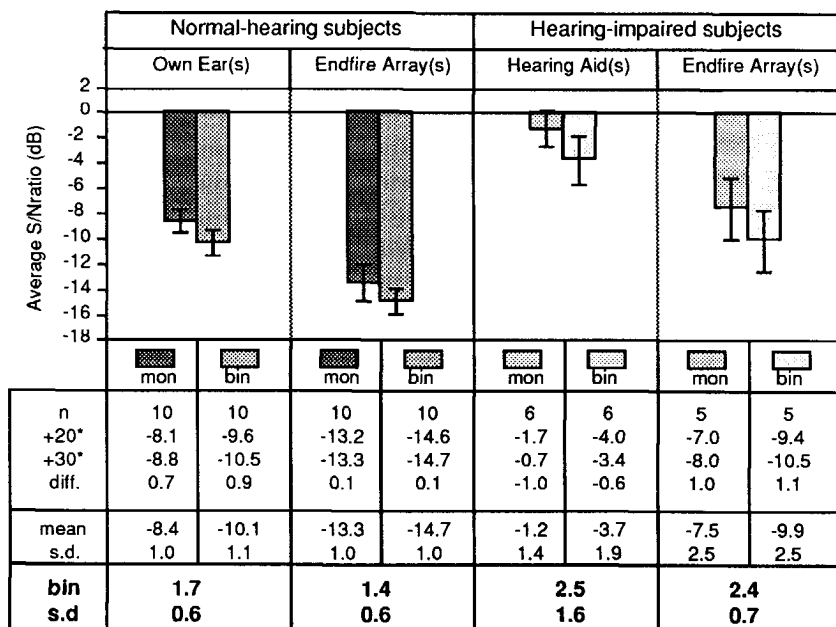
6.2

The hearing-impaired subjects listened with their own hearing aids to two external omni-directional microphones or endfire microphone arrays via the internal telecoil and two induction plates (Sennheiser EZI 110).

**Procedure** The listening tests for the different listening conditions were carried out following the procedure given in section 6.2 with the following adaptation. For the normal-hearing group the SRTs were determined at fixed noise levels of 55 dB and 65 dB.

**Results** Figure 6.10 presents the S/N-ratios for the listening conditions given in table 6.2. In addition, the values of the S/N ratios at +20 and +30 dB, the difference between the levels and the binaural improvement obtained are given.

6.10



\* For normal hearing fixed noise levels of 55 and 65 dB.

Figure 6.10 Results of binaural listening tests.

For the normal-hearing subjects we have obtained S/N ratios with low standard deviations and the maximum difference between the values of the S/N ratios at two different noise levels equals 0.9 dB. The hearing-impaired subjects have a higher standard deviation due to the degree of hearing-impairment but the maximum difference between the values of the S/N ratios at +20 and +30 dB is 1.1 dB.

**Conclusion** The binaural improvement of the normal-hearing subjects equals 1.7 dB using their own ears and 1.4 dB using the two microphone arrays. For both

conditions a small binaural improvement is found. However, the hearing-impaired listeners reach higher values of the binaural improvement: 2.5 dB for the omni-directional microphones and 2.4 dB using the endfire microphone arrays. Besides, the hearing-impaired subjects reach S/N ratios with nearly the same value as the normal-hearing subjects. Based on these results with only small groups of normal-hearing and hearing-impaired subjects we may conclude that using two endfire microphone arrays will give an improvement of the S/N ratio due to binaural interaction.





---

## CONCLUSIONS AND EVALUATION

### Chapter 7

#### INTRODUCTION

Improvement of speech intelligibility

Objective

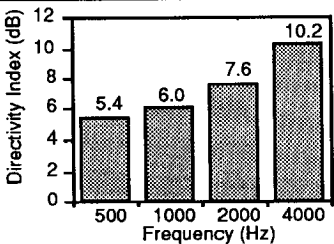
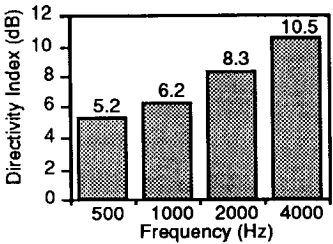
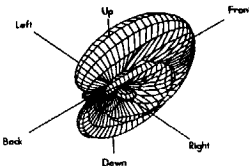
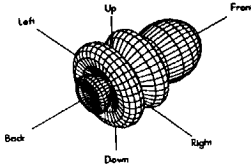
A significant number of people have difficulty in understanding speech in surroundings with background noise and/or reverberation. This is particularly true for an increasing number of elderly people. Up to now no hearing aids have been available that solve this problem satisfactorily. For that reason, we made the improvement of speech intelligibility in a diffuse background noise the objective of our research project and planned to develop a special microphone that would solve the related signal to noise problem under practical conditions. We decided to use a microphone array technique with highly directional characteristics and aimed at an improvement of the signal to noise ratio of at least 5 dB. This was based on several previous investigations on speech intelligibility in noise, which demonstrated that subjects with sensorineural hearing loss may need 5 to 15 dB higher signal to noise ratios than normal-hearing subjects (Bronkhorst, 1990 and Plomp 1986). In this chapter we will summarize the main conclusions from the research project and discuss the potential of the microphone arrays for actual use in real life.

CONCLUSIONS

The results of the research presented in this thesis can be divided into two parts: the actual development of the microphone arrays and the assessment of the proto-types.

**Development** We have used a stationary microphone array approach because it was considered to be *robust* and *simple*. We developed two array types: a *broadside* array and an *endfire* array. The characteristics of the microphones developed are given in table 7.1.

Table 7.1 Characteristics of the microphone arrays developed.

	Broadside Array	Endfire Array
Length	14 cm	10 cm
Microphones	5	5
Output level	very high	high
Stability	very high	high
Electrical Circuit	pre-amplification summation	pre-amplification/delay summation
Directivity		
Directivity Pattern		

7.1

From the simulations and measurements we may conclude:

Broadside

1. A high and very stable directivity can be reached with a *broadside* microphone array consisting of 5 directional cardioid miniature electret microphones over a length of 14 cm. The electrical circuit is surprisingly simple: pre-amplification and (weighted) summation of the microphone signals. The directivity pattern is disk-like with a very narrow beam width in the horizontal plane. This is advantageous in many practical situations

with diffuse noise in the horizontal plane. Moreover, the beam width can be widened, while the side lobes are lowered, with an amplitude weighting of the microphone signals.

Endfire 2. A stable directivity can be achieved with an *endfire* microphone array consisting of 5 directional cardioid miniature electret microphones and a length of 10 cm. The electrical circuit consists of pre-amplification, time delaying and summation. It can be manufactured using standard analogue electronics.

Influence head 3. Measurements with a KEMAR manikin show that the array effect is only slightly influenced ( $< 1$  dB) by diffraction or reflections of the head.

**Assessment** The microphone arrays were tested in a noise field having a diffuse character (a typical cocktailparty situation). Measurements with KEMAR in this noise field showed the following:

4. A normal behind-the-ear hearing aid with an omni-directional microphone will *not* attenuate a diffuse sound field relative to sound coming from the front of a listener (signal to noise ratio: -1 dB). A hearing aid with one cardioid microphone gives a small improvement of 2.5 dB in comparison with a normal hearing aid.
5. The broadside microphone array and the endfire microphone array will attenuate a diffuse sound field (speech noise) relative to sound coming from the front of a listener (frontal sound) and give an improvement of 7.0 dB and 6.8 dB respectively.

From measurements with the developed microphone arrays freely positioned in a large church-hall ( $T_{60} = 3$  s) we may conclude:

6. The microphone arrays are stable in a reverberant sound field giving a mean attenuation of the reverberated sound field of 6 dB and a doubling of the reverberation distance (distance where direct sound field equals reverberated sound field).

Listening tests Listening tests in an experimental set-up with an artificial diffuse noise field with 75 subjects, consisting of 30 young normal-hearing subjects and 45 hearing-impaired subjects, were carried out. Using short Dutch sentences the *critical speech-to-noise ratio* (critical S/N ratio) was determined this being the difference between the speech reception threshold in noise (50% intelligibility) and the noise level. The listening tests showed:

S/N ratio 7. The microphone arrays improve the critical S/N ratio of a hearing-impaired listener significantly: in comparison with an omni-directional hearing aid microphone, broadside and endfire microphone array give a mean improvement of 7.0 dB (26 subjects) and 6.8 dB (27 subjects) respectively. The results are equal to the KEMAR-measurements (5.)

8. The mean monaural critical S/N ratio of the hearing-impaired listeners, using one of the microphone arrays, is nearly equal to the mean monaural critical S/N ratio of a normal-hearing young listener under the same sound field conditions.
9. From the measured critical S/N ratios of the normal-hearing group and regression analysis for the hearing-impaired group we may conclude that an improvement with the microphone arrays can be expected of:
 
$$\Delta S/N = 4.6 + 0.04 HL_{2,4} \quad (7.1)$$
 where  $\Delta S/N$  denotes the S/N ratio improvement for the listener using a microphone array and  $HL_{2,4}$  the individual average hearing loss at 2 and 4 kHz. This equation may be considered to be valid for normal-hearing people as well as hearing-impaired people.
10. Listening with two endfire microphone arrays gives a binaural improvement of the monaural critical S/N ratio: 1.4 dB for normal-hearing subjects (10 subjects) and 2.4 dB for hearing-impaired subjects (6 subjects). This improvement is comparable with the binaural improvement obtained by listening with two normal ears or two conventional hearing aids.

## EVALUATION

### Benefits

To evaluate the benefits of the microphone arrays we can raise the following fundamental question: How important is the attenuation of diffuse background noise and/or reverberation in practical situations? For speech intelligibility in noise the ratio between the sound level of the speech relative to the background noise is an essential quantity. Figure 7.1 gives the speech intelligibility of sentences as a function of the ratio between speech and noise. The two areas give the mean and variance of the speech intelligibility of normal-hearing and a group of hearing-impaired people.

When the sound level of speech has a level being +10 dB higher than the noise, normal-hearing as well as hearing-impaired people will have a speech intelligibility score of more than 90%. However, when the level of speech equals the level of noise this will not yet influence the intelligibility of normal-hearing people but most hearing-impaired listeners will have a mean intelligibility score of only 50%!

### Cocktailparty

This low intelligibility score denotes the problem of most hearing-impaired listeners: *in many practical situations the speech-to-noise ratio is too low for satisfactory speech intelligibility.*

7.1

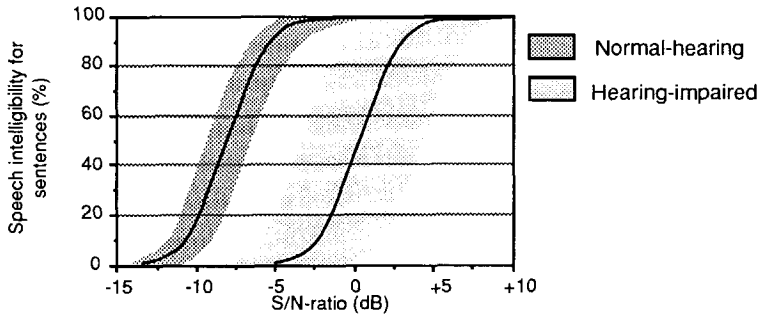


Figure 7.1 The speech intelligibility score for sentences as a function of the S/N-ratio (Noise having the mean spectrum of speech) (according to Plomp 1979a). The position of the two curves (50% level) and the variance around the curves are given as a result of our listening tests with normal-hearing and hearing-impaired people.

7.2

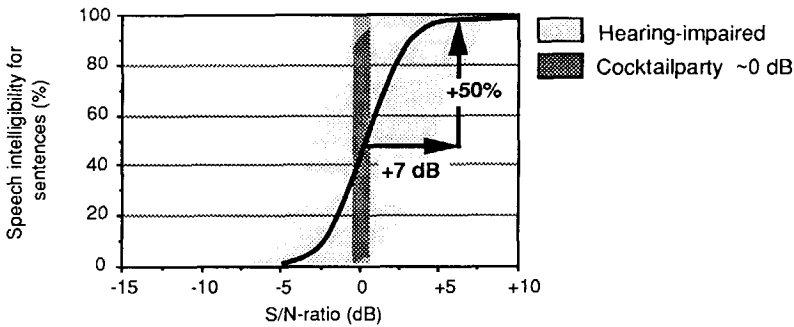


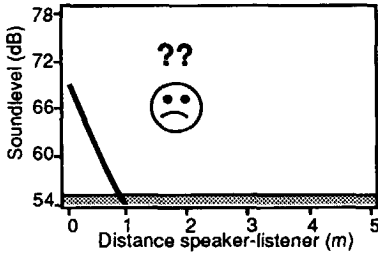
Figure 7.2. A hearing-impaired listener can increase its intelligibility from 50 to 100% using our microphone array.

Figure 7.2 gives an example of a typical cocktailparty situation where the speech-to-noise ratio will be 0 dB (Plomp,1977). The use of our directional microphone array results in an attenuation of the noise level with about 7 dB and a significant improvement of the speech-to-noise ratio. The speech intelligibility score rises by 50% resulting in a recovered communication for a large number of individuals.

Everywhere?

In a practical situation the S/N-ratio depends on the distance between the listener and the desired sound source (speaker), the noise level and the (electro) acoustical measures. This is illustrated in figure 7.3. The speech sound level decreases as a function of the distance resulting in an insufficient speech intelligibility for distances larger than 1 m (figure 7.3a).

a. Listener without hearing aid



b. Listener with ordinary hearing aid

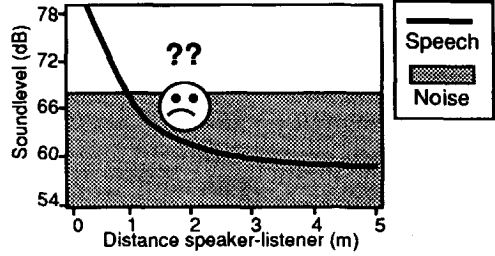


Figure 7.3 The speech intelligibility in an enclosed space depends on the distance between speaker and listener (a). Amplification with an ordinary hearing aid does not change the S/N ratio (b).

a. Lower noise level due to sound absorption

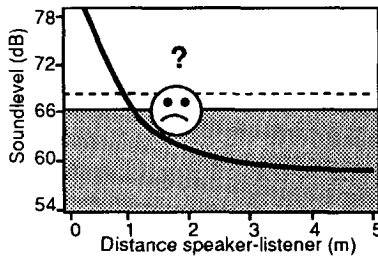
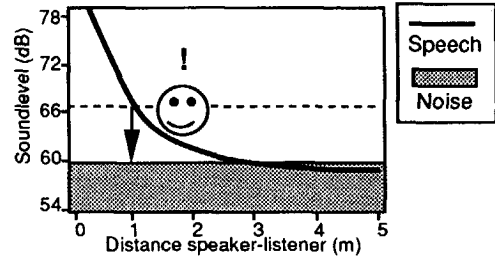
b. Listener with new microphone array ( $Q_r$ )

Figure 7.4 Sound absorption may attenuate the noise level and improve speech intelligibility (a). A microphone array gives a significant improvement of speech intelligibility when the distance to the source is not too large (b).

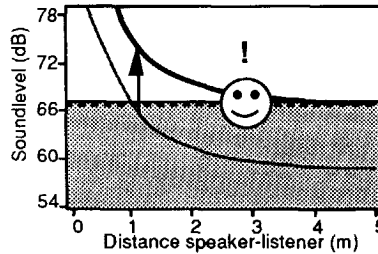
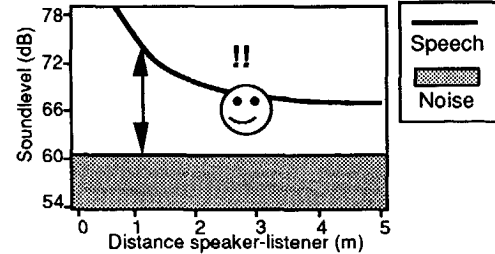
a. Speech amplification system ( $Q_s$ )b. Combination of speech system and array ( $Q_s Q_r$ )

Figure 7.5 The speech intelligibility in an enclosed space can be improved using a sound amplification system with a proper directivity (a). A microphone array attenuates the noise level and gives a further improvement of the speech intelligibility (b).

Sound amplification by an ordinary hearing aid will not only amplify the desired speech sound but also the noise level which normally has two components: the direct field of noise sources in the room (competing talkers) and the reverberated sound in the room due to the sound of the main desired speaker as well as the other noise sources (figure 7.3b).

#### Absorption

Ideally, rooms should be highly sound absorbent in order to achieve a reverberated noise level as low and a *reverberation distance* as large as possible (figure 7.4a). However, the resulting noise level may still be too high because of practical limitations of the acoustical measures or because of the direct sound field of the noise sources in the room. A further improvement of the signal to noise ratio must be found at the receiver (listener) or the source (speaker). We can distinguish three listening situations.

#### Array Listener ( $Q_r$ )

The first situation is the cocktail party situation with reverberated sound, direct noise sources (competing talkers) and other background noise. A hearing-impaired listener will already have problems with speech intelligibility at a distance of about 1 m. The microphone array will attenuate the noise level with about 7 dB at the position of the listener and the speech intelligibility of a hearing-impaired listener will be back to normal at a distance of 1 m (figure 7.4b). Unfortunately, the direct speech sound level decreases with distance and when the distance gets too large, the relative level of the noise may be too high.

#### Speaker ( $Q_s$ )

The second situation is one speaker with listeners (without array) in a hall. The noise may consist of the reverberated speech sound and other diffuse background noise. The signal to noise ratio at the position of the listener can be improved using a sound amplification system. Improvement of speech intelligibility is only obtained when the system raises the direct frontal sound level at the position of the listener with a minimum increase of the reverberated noise level. So, loudspeakers with a high directivity factor  $Q_s$  are necessary (figure 7.5a).

#### Speaker and Array

#### Listener ( $Q_s Q_r$ )

Using a microphone array creates the third situation: one (amplified) speaker in front of the listener. A microphone array will attenuate the (reverberated) noise level by 7 dB at each position in the room (figure 7.5b). The speech intelligibility may be significantly restored by using a combination of the sound amplification system and the microphone array resulting in a total directivity  $Q_s Q_r$ .

Summarizing, we may conclude that a microphone array will give a significant improvement of speech intelligibility in many practical situations where the S/N-ratio at the (hearing-impaired) listeners location nears the limit of satisfactory speech intelligibility.

## GENERAL CONCLUSION

Using array techniques, we have developed two robust and simple microphone arrays with a high directivity. Measurements and listening tests with hearing-impaired listeners show that the microphone arrays developed give a mean improvement of the speech-to-noise ratio of 7 dB. Therefore, a significant improvement of the speech-intelligibility may be expected in many practical situations such as informal get-togethers, parties or meetings, where the S/N-ratio at the location of the listener may be below the limit for speech intelligibility. The use of a microphone array gives a hearing-impaired listener a speech intelligibility in noise comparable to that of normal-hearing people. This is particularly true of people with a perceptive hearing loss due to aging of the hearing organ, disease or excessive noise-exposure.

## POSTSCRIPT

### Manufacturing

The significant improvement of speech intelligibility in noise of hearing-impaired people justifies the development of a commercial microphone array by a manufacturer. This is even more true since this new hearing instrument will in real life, not only give be beneficial to people with hearing loss due to disease or noise-exposure but will also be beneficial to all people having problems with speech intelligibility in noise. This is particularly valuable for the increasing number of elderly people: the aforementioned listening tests and regression analysis have shown that everybody will have an improvement of at least 4.5 dB.

### Design

Because the microphones have to be placed in a spatial configuration attention has to be paid to the final design of the concept. To-day it can be expected that an aesthetical modern design, including miniature electret microphones, will result in a comfortable and elegant hearing instrument.

### Further research

The use of a microphone array should be considered as *spatial* signal pre-processing. This means that the *combination* of a microphone array with a hearing aid adds a new challenge to research for the optimization of hearing aid signal processing, attenuation of high impulsive sound levels and frequency spectrum shaping.



---

## REFERENCES

- Beranek, L.L., 1954,  
Acoustics:  
McGraw-Hill, New York, p. 91-115.
- Berkhout, A.J., 1984,  
Handbook of geophysical exploration:  
Seismic Resolution (Sect. 1, v. 12):  
Geophysical Press, London.
- Berkhout, A.J., 1987,  
Applied Seismic Wave Theory:  
Elsevier, Amsterdam.
- Bilsen, F.A., 1977,  
Pitch of noise signals: Evidence for a "central spectrum"  
J. Acoust. Soc. Am., v. 61(1), p. 150-161.
- Boone, M.M., 1987,  
Design and development of a synthetic acoustic antenna for highly  
directional sound measurements:  
Thesis, Delft University of Technology.
- Bronkhorst, A.W., 1990,  
Binaural aspects of speech perception in noise:  
Thesis, Free University Amsterdam.

- Bronkhorst, A.W., and Plomp R., 1988,  
The effect of head-induced interaural time and level differences on speech intelligibility in noise:  
J. Acoust. Soc. Am., v. 83(4), p. 1508-1516.
- Davis, H., 1970,  
Hearing and Deafness:  
Holt, Linehart and Winston, New York, p. 48.
- Dillon, H.B.E., and Macrae, J.B.A., 1986,  
Performance Requirements for Hearing Aids:  
Journal of Rehabilitation Research and Development, v. 23 No.1, pp. 1-15.
- Dreschler, W.A., 1988,  
Slechthorende en Hoortoestel:  
van Kralingen, Loenen (Utr.), p.58.
- Dreschler, W.A., Maré, M.J. and Verschuure, J., 1989,  
The effect of digitally implemented compression and expansion on speech reception:  
13th ICA Congres, Belgrado, Abstracts v.1, p. 465-468.
- Duquesnoy, A.J. and Plomp, R., 1983,  
The effect of a hearing aid on the speech-reception threshold of hearing-impaired listeners in quiet and noise:  
J. Acoust. Soc. Am., v. 73(6), p. 2166-2173.
- Festen, J.M. and Plomp, R., 1983,  
Relations between auditory functions in impaired hearing:  
J. Acoust. Soc. Am., v. 73(2), p. 652-662.
- Festen, J.M., Dijkhuizen, J.N. and Plomp, R., 1990,  
Considerations on Adaptive Gain and Frequency Response in Hearing Aids: Acta Otolaryngology, 1990.
- Gill, P.E., Murray, W. and Wright, M.H., 1981,  
Practical Optimization:  
Academic Press, London and New York, 1981.
- Groen, J.J., 1969,  
Social hearing handicap; its measurement by speech audiometry in noise:  
Internat. Audiol. 8, p. 182.
- Hansen W.W. and Woodyard, J.R., 1938  
A New Principle in Directional Antenna Design:  
Proceedings IRE, v. 26, No.3, p. 333-345.
- Harris, F.J., 1978  
On the Use of Windows for Harmonic Analysis with the Discrete Fourier Transform:  
Proceedings of the IEEE, v. 66, p. 55.
- Helle, R., 1986,  
Tentative Approaches to Future Hearing-Aid Designs Intended to Improve Speech Intelligibility with Disturbed Temporal Resolution:  
Audiologische Akustik, v. 25(5), p. 186-208.
- Hillman, N.S., 1981,  
Directional hearing aid capabilities:  
Hearing instruments, v. 32(7), p. 7-11.

- IZF, 1988,  
Compact Disc: Spraakmateriaal behorende bij de test voor het meten van  
de spraakverstaanbaarheidsdrempel voor korte zinnen in stilte en in  
stationaire of fluctuerende ruis:  
Instituut voor Zintuigfysiologie TNO, Soesterberg.
- Levitt, H., Pickett, J.M., Houade, R.A., 1980,  
Sensory Aids for the Hearing Impaired:  
Wiley, New York, 1980, p. 5.
- Libby, E.R., 1979,  
The Importance of Smoothness of the Hearing Aid Frequency Response:  
Hearing Instruments, 1979, (4), p.20.
- Lybarger, B.S., 1978,  
Earmolds:  
in: Handbook of Clinical Audiology, Katz J., editor:  
Williams & Wilkins Company Baltimore, 1978, p. 508-523.
- Möller, A. M., 1974,  
Basic mechanisms in hearing:  
Keidel.
- Ma, M.T., 1973,  
Theory and Application of Antenna Arrays:  
Wiley, New York.
- Maré, M.J., Dreschler, W.A. and Verschuure, J., 1989  
The effect of digitally implemented compression and expansion on  
phonemic confusions:  
13th ICA Congres, Belgrado, Abstracts v.1, p. 453-456.
- Markides, A., 1977,  
Binaural Hearing Aids:  
Academic Press London, 1977.
- Mueller, H., 1981,  
Directional microphone hearing aids: A 10 year report:  
Hearing Instruments, v. 32(11), pp. 18-20,66.
- Olson, H.F., 1979,  
Directional Microphones:  
in: Microphones, an anthology of articles on microphones from the pages of  
the Journal of the Audio Engineering Society:  
Audio Eng. Society, New York, pp. 190-194.
- Parsons, A.T., 1987,  
Maximum Directivity Proof for Three-dimensional Arrays:  
J. Acoust. Soc. Am., v. 82(1), p. 179-182.
- Peterson, P.M., Durlach, N.I., Rabinowitz, W.M. and Zurek, P.M., 1987,  
Multimicrophone Adaptive Beamforming for Interference Reduction in  
Hearing Aids:  
J. Rehabil. Res. Developm.,v. 24(4), p. 103-110.
- Plomp, R., 1977,  
Acoustical Aspects of Cocktail Parties:  
Acustica, v. 38, p. 186-191.

- Plomp, R. and Mimpen, A.M., 1979a,  
Improving the Reliability of Testing the Speech Reception Threshold for Sentences:  
Audiology, v. 18(1), p. 43-52.
- Plomp, R. and Mimpen, A.M., 1979b,  
Speech-reception threshold for sentences as a function of age and noise level:  
J. Acoust. Soc. Am., v. 66(5), p. 1333-1342.
- Plomp, R., 1986,  
A Signal-to-Noise Ratio Model for the Speech-Reception Threshold of the Hearing Impaired:  
Journal of Speech and Hearing Research, v. (29), pp. 146-154.
- Raatgever, J. and Bilsen, F.A., 1986,  
A central spectrum theory of binaural processing. Evidence from dichotic pitch:  
J. Acoust. Soc. Am., v. 80(2), p. 429-441.
- Salomé, A.J., Huson, A., Brouwer P.J., 1977,  
Functionele anatomie:  
Spruyt, van Mantgem & de Does B.V., Leiden, p. 393.
- Schwander, T.J. and Levitt, H., 1987,  
Effect of two-microphone noise reduction on speech recognition by normal-hearing listeners:  
J. Rehabil. Res. Developm., v. 24(4), p. 87-92.
- Sessler, G.M., and West, J.E., 1975,  
Second-order gradient unidirectional microphones utilizing an electret transducer:  
J. Acoust. Soc. Am., v. 58(1), pp. 273-278.
- Smootenburg, G.F., 1989,  
Speech reception in quiet and in noisy conditions by individuals with noise-induced hearing loss in relation to their tone audiogram:  
TNO-report, IZF 1989-11, Soesterberg.
- Türk, R., 1987,  
A new hearing aid variant:  
Scand. Audiol., 16, pp. 179-185.
- Veit, I. and Sander H., 1987,  
Production of Spatially Limited "Diffuse" Sound Field in an Anechoic Room:  
J. Audio Eng. Soc., v. 35(3), pp. 138-143.
- Weiss, M., 1987,  
Use of an adaptive noise canceller as an input preprocessor for a hearing aid:  
J. Rehabil. Res. Developm., v. 24(4), pp. 93-102.
- Weston, D.E., 1986,  
Jacobi sensor arrangement for maximum array directivity:  
J. Acoust. Soc. Am., v. 80(4), pp. 1170-1181.
- Zwicker, E., Beckenbauer T., and Beer G., 1986, 1987  
Directional microphone arrangement:  
European Patent Office 0 219 026, 1986.;  
United States Patent 4.712.244, 1987.

---

## SUMMARY

Problem	Many people have great difficulty in understanding speech in surroundings with background noise and/or reverberation. This is especially a problem for the increasing number of elderly people. It may have serious consequences as they easily get isolated by the lack of communication at social events (informal get-togethers, parties or meetings). A directional hearing aid might be beneficial in reducing background noise in relation to the desired speech signal. Conventional hearing aids with a directional cardioid microphone are insufficient because of the low directivity of cardioids.
Research	In this thesis the results are described of research done to develop a special hearing microphone array with highly directional characteristics that solves the problem of speech intelligibility in noise under practical conditions. Particular emphasis is given to optimization and stability. Free-field simulations of several robust models show that a high directivity can be achieved combined with robust properties. Simulations were verified with a laboratory model. The results of the measurements show a good agreement with the simulations.

Development	Based on the aforementioned simulations and measurements, two portable array microphones were developed: a <i>broadside</i> microphone array consisting of five miniature electret cardioid microphones with a length of 14 cm and an endfire microphone array consisting of five directional miniature electret microphones with a length of 10 cm.
Assessment	<p>For the assessment of the microphone arrays developed, an experimental set-up was made in a sound insulated listening room with one loudspeaker in front of the listener simulating the partner in a discussion and eight loudspeakers placed on the edges of a cube producing a diffuse background noise (voice babble).</p> <p>Measurements with a mannikin (KEMAR) show that the two microphone arrays give an improvement of the signal to noise ratio of 7 dB in a diffuse background noise field. For listening tests with the developed microphone arrays a subject is placed in the centre of the set-up. The speech-reception threshold in noise for simple Dutch sentences was determined with a single omni-directional microphone and with one of the microphone arrays. Listening tests with 75 subjects, 30 normal-hearing young listeners and 45 hearing impaired listeners were carried out. The results with the hearing-impaired listeners show that a large improvement of the S/N-ratio of 7 dB can be obtained using either of the microphone arrays.</p>
Conclusion	<p>Owing to background noise, speech intelligibility will be below the limit for satisfactory communication in a lot of practical, daily situations. This is especially a problem for people with a perceptive hearing loss due to disease, noise exposure and aging of the hearing organ, a common phenomenon in this age with its increasing number of elderly people. Owing to the decreased sound discrimination, speech sound of the partner in the discussion and background noise can no longer be separated.</p> <p>The results of this thesis show that for these situations a significant improvement of the speech intelligibility can be achieved by the use of a highly directional microphone array. The microphone arrays proposed in this thesis are very suitable for combining with a pair of spectacles. The spectacles with microphone array can be used in combination with a standard hearing instrument: the view direction is the listening direction. It may be expected that in the near future the spectacles with a microphone array will be a very important hearing instrument for improvement of the speech intelligibility.</p>

---

## SAMENVATTING

Probleem	<p>Veel mensen hebben grote moeite om spraak te verstaan wanneer er in hun omgeving achtergrondlawaai en/of galmgeluid aanwezig is. Deze vorm van slecht horen is in het bijzonder een probleem voor de ouderen in onze maatschappij en kan gemakkelijk tot gevolg hebben dat zij geïsoleerd raken bij sociale evenementen (recepties, verjaardagen, vergaderingen) door een gebrek aan communicatie met hun directe omgeving. Een richtinggevoelig hoortoestel kan een goed hulpmiddel zijn om achtergrond lawaai te verzwakken ten opzichte van het gewenste spraak geluid. De bestaande hoortoestellen met een richtinggevoelige microfoon helpen niet voldoende omdat de richtinggevoeligheid van de gebruikte microfoons te laag is.</p>
Onderzoek	<p>In dit proefschrift worden de resultaten beschreven van onderzoek dat is uitgevoerd om een speciale microfoon-array (<i>Eng. array</i> = rij) te ontwikkelen, met een hoge richtinggevoeligheid, die een oplossing geeft voor het probleem van spraakverstaanbaarheid bij achtergrond lawaai onder praktische omstandigheden. Er is in het bijzonder aandacht besteed aan optimalisatie en stabiliteit. Vrije veld simulaties voor verschillende numerieke modellen laten zien dat een hoge richtinggevoeligheid bereikt</p>

kan worden met stabiele microfoon arrays. De simulaties werden vervolgens gecontroleerd met een laboratoriummodel. De resultaten van de metingen laten zien dat er een zeer goede overeenkomst bestaat met de simulaties.

Ontwikkeling

Op grond van voornoemde simulaties en de metingen werden tenslotte twee typen draagbare microfoon arrays ontwikkeld: een *broadside* microfoon array bestaande uit vijf richtinggevoelige miniatuur microfoons met een lengte van 14 cm en een *endfire* microfoon array bestaande uit vijf richtinggevoelige miniatuur microfoons met een lengte van 10 cm.

Evaluatie

Voor de evaluatie van de ontwikkelde microfoon arrays werd een proefopstelling gebouwd in een geluidabsorberende kamer waarbij een luidspreker recht voor de luisteraar een gesprekspartner simuleerde en acht luidsprekers zodanig waren opgesteld dat zij tezamen een gelijkmatig verdeeld (diffuus) achtergrond lawaai genereerden.

Metingen aan een kunsthofd (KEMAR-mannequin) laten zien dat met beide microfoon arrays de verhouding tussen de spraak en het diffuse lawaai verbetert met 7 dB. Voor luisterproeven werd een proefpersoon gevraagd plaats te nemen in het centrum van de ruimte. De spraakverstaanbaarheids drempel in lawaai werd bepaald met één enkele rondomgevoelige microfoon en met één van de microfoon arrays. Er zijn luisterproeven uitgevoerd met 75 proefpersonen, 30 normaal-horende (jonge) luisteraars en 45 slechthorende luisteraars. De resultaten met de slechthorende luisteraars laten zien dat de verhouding tussen spraak en lawaai sterk verbetert (7 dB) bij gebruik van een van de microfoon arrays.

Conclusie

In veel leefsituaties zorgt achtergrondlawaai voor een aanzienlijke afname in de spraakverstaanbaarheid. Dit probleem geldt vooral voor mensen met een perceptief gehoorverlies ten gevolge van een veroudering van het gehoororgaan (een probleem voor het groeiend aantal senioren in onze maatschappij), oorziekte, blootstelling aan lawaai. Het onderscheidingsvermogen van het gehoor is afgenomen waardoor het moeilijk wordt spraak van de gesprekspartner te scheiden van het overige aanwezige geluid.

De resultaten van dit proefschrift geven aan dat voor deze situaties een significante verbetering van de spraakverstaanbaarheid kan worden bereikt bij gebruik van sterk richtende microfoon arrays. De in dit proefschrift voorgestelde arrays zijn bij uitstek geschikt om elegant in een bril te worden weggewerkt. De bril dient dan als microfoon voor een standaard hoortoestel: alleen wat men ziet wordt gehoord. Verwacht mag worden dat in de nabije toekomst de bril met microfoon array een belangrijk hulpmiddel zal worden voor verbetering van de spraakverstaanbaarheid.



---

## CURRICULUM VITAE

van Wim Soede

- 5 maart 1961 geboren te De Bilt
- 1967-1973 lager onderwijs te De Bilt
- 1973-1979 middelbare schoolopleiding aan het Christelijk Gymnasium te Utrecht, afgesloten met examen Gymnasium- $\beta$  met eindexamenvakken Nederlands, Engels, Latijn, Natuurkunde, Scheikunde en Wiskunde I en II.
- 1979-1986 studie voor natuurkundig ingenieur aan de Technische Hogeschool te Delft
- 1982 kandidaatsonderzoek op het gebied van verstemming van orgelpijpen onder invloed van temperatuurvariaties
- 1983-1984 4e-jaarswerk in de onderzoekgroep Akoestische en Seismische Technieken op het gebied van medische echo-akoestiek o.l.v. prof. dr. ir. A.J. Berkhout en ir. J. Ridder
- 1985-1986 5e-jaarswerk op het gebied van de seismische dataverwerking o.l.v. prof. dr. ir. A.J. Berkhout en dr. ir. C.P.A. Wapenaar
- 1985-1986 student-assistent in de onderzoekgroep Akoestische en Seismische Technieken
- 1979-1986 lid van christelijke studentenvereniging C.S.F.R.; lid van plaatselijk bestuur (82/83) landelijk bestuur (83/84) en lid van diverse commissies; lid van diverse commissies van nationale afdeling van internationaal christelijke studentenbeweging
- 1980-1983 oprichter en voorzitter van kerkelijke jongerengroep in de Bilt
- 1982-heden aanstelling als organist van psychiatrisch centrum Zon en Schild te Amersfoort
- 1986-1990 promotieonderzoek naar de ontwikkeling van een richtinggevoelig hoor-toestel door gebruik te maken van microfoon-arraytechnieken aan de Technische Universiteit Delft bij de vakgroep Akoestische en Seismische Technieken o.l.v. prof. dr. ir. A.J. Berkhout en de vakgroep Akoestische Perceptie o.l.v. prof. dr. ir. F.A. Bilzen
- 18 sept. 1987 getrouwd met Gea Willemse